UNIVERSITA' DEGLI STUDI DI VERONA

DIPARTIMENTO DI

NEUROSCIENZE, BIOMEDICINA E MOVIMENTO

SCUOLA DI DOTTORATO DI

SCIENZE DELLA VITA E DELLA SALUTE

DOTTORATO DI RICERCA IN

NEUROSCIENZE, SCIENZE PSICOLOGICHE E PSICHIATRICHE E SCIENZE DEL MOVIMENTO

34mo CICLO

UPPER LIMB MOTOR CONTROL IN PEOPLE WITH STROKE: EXPLORING SENSORY AND MOTOR

COMPONENTS OF FORWARD MODELS DYSFUNCTIONS

S.S.D. MED/48

Coordinatore: Prof.ssa Michela Rimondini

              Firma _____

Tutor: Prof.   Nicola Smania

              Firma _____

                              Dottorando: Dott. Nicola Valè

                              Firma _____

Upper Limb Motor Control In People With Stroke: Exploring Sensory And Motor Components Of Forward Models Dysfunctions

Nicola Valè
Tesi di Dottorato

Verona 12/08/2022

Sommario

L'apparente semplicità con cui compiamo le più diverse azioni utilizzando gli arti superiori, dall'afferrare una palla al sollevare un peso, nasconde la complessità del sistema necessario per pianificare e controllare l'azione. Un aspetto cruciale per il controllo motorio dell'arto superiore è la possibilità di prevedere le conseguenze dei nostri gesti. Sebbene questa possibilità sia stata recentemente messa in discussione, la letteratura suggerisce che il sistema nervoso centrale utilizzi un modello interno *forward* che partendo dall'informazione sul comando motorio e sullo stato iniziale dell'arto, predice il *feedback* sensoriale che verrà percepito durante lo svolgimento dell'azione.

Il cervelletto è considerato essenziale per l'implementazione di tale modello e tale idea è supportata dalle osservazioni condotte su pazienti con lesioni cerebellare, il cui comportamento atassico è stato descritto come conseguenza di una disfunzione del modello *forward*. Tuttavia, minore attenzione è stata dedicate al ruolo della propriocezione nel controllo motorio anticipatorio degli arti superiori.

L'obiettivo di questo progetto è di indagare differenti aspetti del controllo motorio anticipatorio in soggetti sani e in persone con esiti di ictus cerebrale con lesioni cerebellari e deficit somatosensoriali.

Nella prima sezione ci siamo posti l'obiettivo di fornire nuove evidenze sul ruolo del modello *forward* nella funzione sensorimotoria dell'arto superiore, con riferimento al fenomeno di attenuazione sensoriale secondo cui gli stimoli tattili generati da movimento volontari sono percepiti meno intensamente di identici stimoli generati da sorgenti esterne. Sono stati inclusi dati da 3 studi precedentemente pubblicati per un totale di 375 soggetti. In questi studi ai soggetti veniva chiesto di riprodurre in diverse condizioni con l'indice della mano destra una pressione che veniva somministrata sull'indice della mano sinistra. La nostra analisi ha riguardato il confronto tra condizioni in termini di variabilità tra una prova e l'altra. I risultati hanno mostrato che tale variabilità era associate ai livelli di attenuazione relativa tra diverse condizioni supportando indirettamente il ruolo del modello *forward* nel fenomeno di attenuazione sensoriale.

Nella seconda sezione di questo progetto si è valutato la modulazione della forza di presa durante il sollevamento bimanuale di un oggetto in soggetti con ictus cerebrale e deficit somatosensoriale. Le procedure di valutazione hanno incluso due esercizi di modulazione della forza di presa e un esercizio di sollevamento. Per queste valutazioni è stato utilizzato un dispositivo sensorizzato in grado di misurare la forza di presa e la posizione dello stesso nello spazio, consentendo di ottenere parametri cinematici della prova di sollevamento. Dopo aver validato il protocollo sperimentale, sono stati inclusi 11 soggetti sani e 9 pazienti con ictus cerebrale e deficit somatosensoriale. La nostra analisi ha mostrato alcuni segni di alterazioni della pianificazione motoria nei pazienti con ictus. Nello specifico, tali pazienti hanno mostrato alterazione nel timing di esecuzione del picco di forza di presa durante il sollevamento.

Nell'ultima sezione del presente lavoro si è valutato il controllo motorio anticipatorio durante un gesto di raggiungimento dell'arto superiore in pazienti con ictus con lesione cerebellare o con deficit somatosensoriale. Con tale fine è stato sviluppato e validato un sistema di valutazione a basso costo della cinematica del movimento indice-naso. Sono stati calcolati dei parametri del movimento relativi all'accuratezza del gesto, alla sua efficacia e alla pianificazione motoria. Inoltre è stato proposto un modello interpretativo dell'atassia cerebellare e sensoriale come conseguenze di disfunzioni del controllo motorio anticipatorio. I risultati hanno suggerito che pazienti con deficit somatosensoriale sono stati più sensibili all'assenza di informazione visiva, rallentando significativamente il movimento quando eseguito ad occhi chiusi. I parametri analizzati hanno consentito di catturare deficit di pianificazione motoria nei pazienti con lesione cerebellare.

Il presente lavoro ha evidenziato l'importanza della valutazione del controllo motorio anticipatorio in pazienti con esiti di ictus cerebrale. La ricerca futura dovrà occuparsi del ruolo del controllo motorio anticipatorio nell'apprendimento e sullo studio di strategie riabilitative specifiche per tali disfunzioni.

Abstract

A crucial feature of the upper limb motor control is the possibility of predicting the consequences of our own movements. The literature suggested that the central nervous system uses forward models that, starting from the initial position of the upper limb and from the action's motor command, predict the sensory feedback and the future limb's state during the action execution. The cerebellum is considered a crucial structure for the neural implementation of such internal model. This evidence is supported by a series of studies that described the cerebellar ataxic behavior as a forward model dysfunction. However, less attention has been dedicated to the role of somatosensory information in predictive motor control for the upper limbs.

The goal of this project was to investigate different aspects of the anticipatory motor control in healthy subjects and in people with cerebral stroke with cerebellar lesions and somatosensory impairment.

In the first section, we aimed to provide further evidence on the role of the forward model in upper limbs sensorimotor function. We focused on the sensory attenuation phenomenon, and we performed new analyses on previously recorded data on force matching tasks in healthy subjects. We collected data from three experiments including a total of 375 subjects. In these experiments a target force was delivered on the subjects' left index finger and they asked to reproduce it in different conditions. Our analysis compared the within-subject trial-to-trial variability in the matching force between conditions. The results showed that, considering the matching force exertion, the trial-to-trial variability was associated with the level of tactile perception, corroborating the hypothesis that a predictive mechanism is involved in the sensory attenuation phenomenon.

In the second section, we aimed to investigate anticipatory grip force modulation deficits during a bimanual object lifting task in patients with stroke and somatosensory deficits. The assessment procedures included two force matching tasks and a lifting task. We used a sensorized device allowing us to record the grip

force with which subjects grasped it and track its position and compute kinematics parameters of the lifting. After validating our experimental procedures in healthy controls, we included 11 healthy subjects and 9 patients with stroke and somatosensory deficits. Our analysis provided some evidence of impaired motor planning in patients with CNS stroke sequelae. Specifically, patients with stroke showed abnormal timing of maximal grip force exertion during the lifting.

In the last section, we aimed to assess predictive upper limb behavior of a fast and repetitive reaching task in patients with cerebellar lesions and patients with somatosensory deficits. We developed and validated an accurate low-cost system for the kinematic assessment of the index-to-nose task and we compared a group of young healthy subjects, and stroke patients with cerebellar lesions or proprioceptive impairment. Our analysis measured a set of reaching parameters referring to movement accuracy, efficiency and motor planning in a cohort of healthy controls and patients affected by CNS stroke. Moreover, we proposed a theoretical framework for interpreting sensory and cerebellar ataxia as different forward model's dysfunctions. Our results suggested that patients with somatosensory deficit were the most affected by the absence of visual feedback significantly reducing movement speed when performing the task with closed eyes. Moreover, we found that patients with cerebellar lesions showed signs of impaired movement planning.

This dissertation underlined the importance of assessing predictive motor control in patients affected by CNS lesions. Future research should focus on the role of anticipatory motor control in motor learning and on the design of rehabilitation treatment for forward model dysfunctions.

Background

Upper limb movement planning: the sensorimotor transformations

Almost every interaction that we have with the environment occurs by the mean of a movement. From the apparently easiest acts of reaching for a cup and drinking to the most difficult actions of a professional athlete, the precision and accurateness of our movement are of paramount importance. This is particularly relevant in the context of the Upper Limb (UL), whose mechanics is particularly complex and requires sophisticated control mechanisms. The mechanisms that set the motor commands generating our movements and control the effectiveness of those movements are complex and involve several structures and areas in the Central Nervous System (CNS). This whole chain of events originates from a need or a will that is subsequently translated into a goal. For example, being thirsty leads to the will to drink and to the aim of reaching for a cup of water. The detailed description of the processes that occur before the movement planning is beyond the scope of this work, and it will not be dealt with. In contrast, this dissertation will focus on the processes that take place from the definition of the motor command to the monitoring phase during the UL movement execution.

The first task the CNS must carry out is localizing the target of the movement. This can be an object, like the previous example on the cup of water, or a part of our body. In the context of daily life tasks, the visual system is largely responsible for target localization. Visual inspection of the environment can allow us to map abject in both egocentric and allocentric reference systems (Aagten-Murphy & Bays, 2019). Then, the position of the object needs to be integrated with the position of the upper limb. This means that the locations of the target and the UL must be defined in the same coordinates system. The initial UL position is defined by the integration of different sensory modalities, including visual feedback, sense of position and tactile sensations. Previous studies showed that the CNS uses different coordinate systems to carry out this integration process (Soechting & Flanders, 1989b, 1989a). Seminal experiments suggested that firstly, the visual inspection of

the environment leads to the mapping of the target in retinal coordinates. These coordinates are then transformed into systems based on the head and, eventually, on the shoulder (Soechting & Flanders, 1989b). Evidence of this was obtained by observing the spatial errors that subjects made in pointing to a target with their index finger and with a stick. The errors' distribution was consistent with a representation of the target in spheric coordinates centered on the shoulder (Soechting & Flanders, 1989a).

Once the coordinates of the target and the hand are defined, the CNS computes the trajectory that the hand must follow to reach the object and the corresponding motor command. A vast network of frontoparietal connections is responsible for these operations. From a general perspective, these circuits allow information on the target's and hand's position to flow in the premotor cortex, where it is integrated with the representation of the goal and is translated into a motor command. These processes are usually referred to as sensorimotor transformation (Frey et al., 2011).

The posterior parietal cortex is the primary neural underpinning for coding the target's position (Frey et al., 2011). Visual in somatosensory inputs are, in fact, integrated into parietal areas, primarily in the upper parietal lobule, where bimodal neurons responding to both visual and proprioceptive stimuli were found (Rizzolatti & Matelli, 2003). Circuits connecting this region with the dorsal premotor cortex are important for the control of goal-directed UL and are involved in visually controlled pointing and reaching-to-grasp movement. Other parallel circuits connect the inferior parietal lobule with the ventral premotor cortex. The object's shape and its association with an appropriate hand posture are coded by these circuits. The integration of the somatosensory, visual and goal-related information is then used to plan the activities and generate the motor command.

The internal models

The CNS constructs and uses parametric representations of the physical word to plan actions and to define motor commands needed to perform them. These representations are often referred to as internal models (Mcnamee & Wolpert, 2019). The expression has been widely used in the literature with different

meanings, and for the sake of clarity, it is useful to revise this concept that will be used recurrently in the following chapters. A formal classification of internal models has been recently proposed (Mcnamee & Wolpert, 2019). Accordingly, they are divided into prior models, perceptual inference models, sensory and motor noise models, forward dynamic models, and cognitive maps. Prior models describe the priors over sensory signals or the state of the world. The CNS learns during the development of several statistical regularities in terms of sensory input that are used, in integration with sensory feedback, to infer the body's or external world's state. Perceptual inference models can be considered as higher-order cognitive processes. These types of models are used, for example, to compute a property of an object given the related sensory input. On the other hand, models with such characteristics are used to compute the probabilities over a latent state that has generated a given sensory input. These models are involved in the reafference cancellation of the Sensory Attenuation phenomenon (SA), which will be explored in more detail in the following sections. Models on sensory and motor noise are crucial for the CNS to determine the level of noise (and, in a sense, reliability) of the sensory input and motor output. The forward dynamical models take a state at a time instant and predict the state of the system in the future. Lastly, the so-called cognitive maps can be thought of as a structured organization of state variables that help the CNS to deal with complex systems.

In the framework of the present work, we will refer to the internal model in the context of sensorimotor integration, motor planning and motor control. Within this framework, internal models are usually defined as systems that simulate internal (musculoskeletal) or external (environmental) dynamical processes using sensory input, motor commands or prior knowledge (Kawato et al., 1987a). Historically, in this context the internal models are divided into two groups: forward models and inverse models (M. I. Jordan, 1996a). The inverse models, compute the motor command needed for reaching a desired state. The forward models, in contrast, compute the evolution of a system in the future given the present state and the motor command (Frey et al., 2011; R. S. Johansson & Edin, 1993; Wolpert & Flanagan, 2001). After a motor command is set in the motor cortex, a copy of the command (efferent copy) serves as an input to the forward model along with the estimated

previous position of the limb. The forward model predicts the sensory feedback that should accompany the execution of the motor command and estimates changes in the limb's position across time (Wolpert & Flanagan, 2001).

The forward model in the upper limb motor control

Self-monitoring is fundamental to normal functions in planning, controlling, and anticipating the consequences of motor acts. Knowledge of the actual position of the limb usually comes from the integration of proprioceptive and visual feedback along with preliminary information. As we have already seen, a forward model is essentially a map that matches the actual state of the body and the motor command to the final state and associated sensory feedback (Mcnamee & Wolpert, 2019). In order to properly understand the benefits of this mechanism on motor control, it is relevant to mention how the CNS monitors the action's execution and corrects it in case of errors (Figure 1). The execution of the motor command gives rise to consequent sensory feedback, and this returning afferent signal is compared with the predictions of the forward model, allowing online correction of the movement. This mechanism is called feedback motor control (Frey et al., 2011).

Prediction of state estimation

Although apparently efficient, a system based only on feedback control is affected by some drawbacks. The main issue is related to the intrinsic delay in sensory information. For humans, sensory loop delays are estimated to be around 100-150ms for proprioceptive feedback. This means that at each instant, the CNS process the sensory information about the state of the system 150 ms before (Davidson, 2016) . For fast UL movements that are commonly in the order of 0.5 s, this delay can be significant. A system that relies only on feedback control would present large out-of-phase excessive oscillations in response to spatial errors. A useful and intuitive example of this behavior is thinking about trying to regulate the water temperature by having a shower with an unknown faucet (Frey et al., 2011). Typically, we would start from having too cold water (error), then we would move the faucet to a warmer temperature (correction). However, it would take a few seconds for the water to warm up (delay), and we may find the temperature now

being too hot (excessive correction). Eventually, after a few trials and errors, we may finally be able to adjust the faucet at the right temperature. In the context of UL movement control, a forward model that is able to predict the system's behavior and simulate the upcoming state of the body can, in principle, contribute to a feedback loop even before the actual feedback comes (Wolpert & Flanagan, 2001). This makes the movement robust to sensory feedback delays. Moreover, the estimate of the future sensory input can be compared and integrated with the actual sensory feedback improving its accurateness (Mcnamee & Wolpert, 2019). Another interpretation of the usefulness of a forward model in motor control came from (Tanaka et al., 2020). According to the authors, forward model uses the upcoming sensory feedback and information on the motor command to update the sensory feedback and, doing so, overcome the issue of sensory delay(Tanaka et al., 2020).

Predictive motor control is crucial to performing accurate and fast movements while holding objects. One of the most famous examples of the importance of the forward model in this context is the so-called "waiter task". Imagine a waiter holding a tray with a few glasses on it. If the waiter voluntary removes one of the glasses from the tray, he will be able to keep the tray stable. However, if someone else removes it unpredictably, the waiter will fail to keep the tray stable and may push it upward. In the former situation, the waiter reduces the force with which he was holding up the tray simultaneously to the object lifting, while in the latter, he will react after the removal of the glass as it occurs in a common feedback control mechanism. Similar behavior occurs when we move an object upward while holding it with one hand. In order to prevent the object's slippage, we must increase the grip force proportionally to the acceleration we transmit to it. Previous studies showed that the grip force increases with no delay from the movement onset (R. S. Johansson & Edin, 1993). Clearly, if this behavior was driven by tactile feedback, the grip force increase would have occurred with the known sensory delay (ca. 100ms) from the movement as a reaction to the initial slippage. This has been interpreted as strong evidence supporting the predictive nature of such a phenomenon (Birznieks et al., 1998; R. S. Johansson & Edin, 1993). According to this interpretation, the efferent copy of the motor command of lifting the object is used by the forward model to predict the consequences of that movement (i.e. the

possible object slippage), and this information is used to increase the grip force. Notably, in order for the grip force to increase simultaneously to the object's movement, these processes have to be carried out before the movement onset.
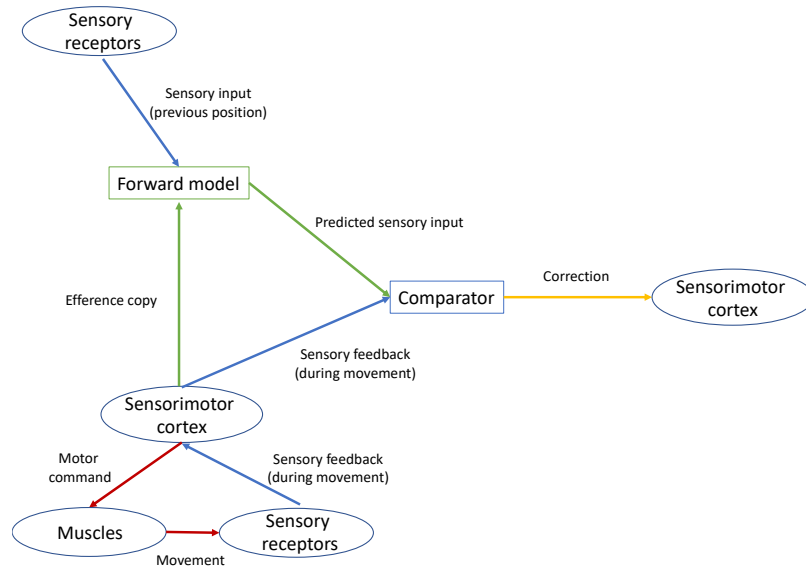
Figure 1 Schematic representation of the forward model (green) in the context of the upper limb motor control. Once the motor command is set in the motor cortex, a copy of this command (Efference Copy) is sent to the forward model that integrate it with sensory information on the current state of upper limb. The forward model generates the predicted sensory input that is then compared to the actual sensory feedback generated by the movement. The discrepancies between these two signals (yellow) allow online correction of the motor command via the so-called feedback motor control.

The attenuation of sensory re-afference

The possibility of predicting the sensory feedback from the performance of a voluntary action allows distinguishing between stimuli that are the consequence of our own actions and stimuli that are unpredictable and come from the external environment. This is possible even if, from an anatomical level, this information comes from the same receptors and is hence indistinguishable. While taking into account the predicted feedback makes the movement kinematics robust to sensory delay, this source of feedback, sometimes called re-afference, could, on the other hand, increase the overall noise of the sensory information (Bays & Wolpert, 2007b). Moreover, from a functional perspective, the unexpected and unpredictable

external stimuli are arguably the most informative source of feedback. Therefore, distinguishing between these two sources of feedback is conceivably useful to optimize movement effectiveness. Several mechanisms have been proposed to be responsible for attenuating the perception of sensations that are consequences of our own actions in order to enhance the processing of external events. However, not all these mechanisms involve a forward predictive model. For the sake of simplicity, they can be divided into unpredictive general gating mechanisms and predictive re-afference cancellation or Sensory Attenuation (SA) phenomenon. The former represents a well-known phenomenon responsible for the attenuation of all the tactile sensations perceived during a voluntary movement of the UL (Chapman et al., 1987). Recent experiments brought evidence that this attenuated perception is triggered by the motor command signal at a spinal cord level (Seki et al., 2003; Voss et al., 2006). However, this mechanism acts irrespective of the source of the sensory afference. This movement-related gating removes part of the sensations coming from voluntary generated movements along with sensations coming from external sources. In contrast, the SA phenomenon is thought to selectively attenuate only the sensation coming from the voluntary-generated actions, leaving intact the intensity of sensations coming from external sources (Figure 2). In recent years, several works provided evidence of such a mechanism in tactile sensation (Bays et al., 2005, 2006; Bays & Wolpert, 2007a; Shergill et al., 2003, 2013; Wolpe et al., 2016). In these studies, healthy subjects performed a force matching task. A motor torque attached to a lever exerted a target force on the subjects' left index finger. Then, they were asked to reproduce that force using their right index finger by either pressing directly on their left index finger (through the lever) or indirectly manipulating a slider that controlled the same lever. The former condition was called self-condition, while the latter was referred to as external condition. In other words, the subjects were asked to compare two tactile sensations: the first being the target force and the second being their matching force executed in either self- or external conditions. Consistently across different studies, the results showed that subjects were more accurate in reproducing the target force in the external condition. In contrast, they systematically exaggerated the matching force in the self-condition. In this condition, the matching force was exerted using the right

index finger right above the left index. Therefore, the forward model predicted that this voluntary action would have generated a consequent tactile stimulus on the left index. The authors proposed that this mechanism was responsible for the attenuation in the perception measured only in the self-condition. Although this hypothesis has recently been questioned and alternative explanations have been proposed (Press et al., 2020), there is compelling evidence that the SA phenomenon involves a predictive forward model (Bays et al., 2006; Kilteni et al., 2020).

From a general perspective, the ability to predict the sensory input from our own actions and its comparison with the actual sensory input can also play a role in the discrimination between self- and externally generated sensation. Famous evidence for this role was obtained decades ago by studies investigating eye movements, from the simple observation that a gentle touch of our eyeball creates the illusion that the environment is moving. In contrast, when we voluntary move our eyes to explore the environment, we perceive the environment as fixed even if the actual movement of the eyeballs is comparable in the two situations (Sperry, 1950; von Holst & Mittelstaedt, 1950). Authors were the first to suggest that a copy of the motor command of the eyes' movement (called "corollary discharge") was used for predicting eye movement and cancelled out the effect of motion on the environment. Using this mechanism, the CNS would be able to distinguish whether the same visual stimulus is generated by a voluntary movement or by an external source (the passive movement of the eyeball). This hypothesis has then been applied to other domains of sensorimotor behavior (M. Jordan & Rumelhart, 1992).
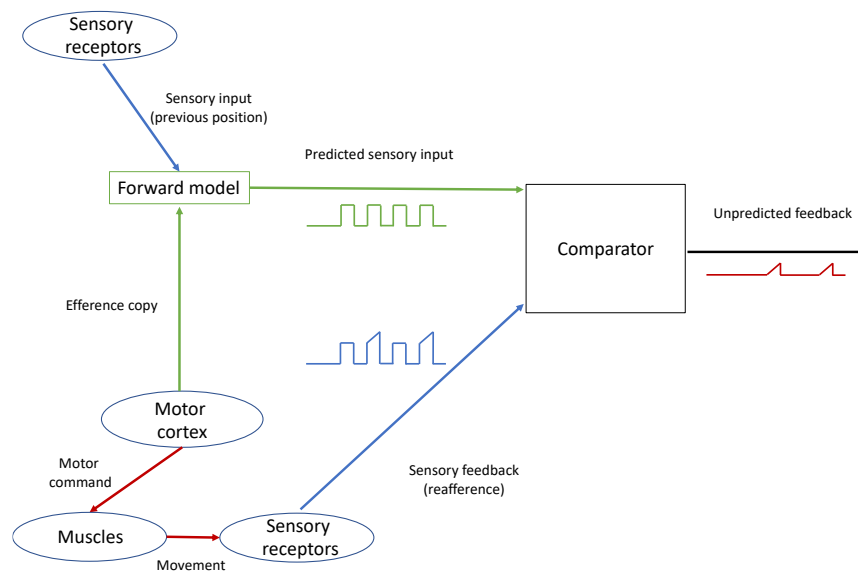
Figure 2 Schematic representation of the attenuation of the predicted sensory feedback. A motor command (red) generates a movement and, consequently, sensory feedback (reafference). In this framework, only the predicted sensory feedback is subtracted from the sensory reafference enhancing the stimuli resulting from external sources (red).

Motor learning

When the predicted and the actual sensory feedback mismatch, the motor system can correct the execution of the task and, separately, update the internal models that represent the environment's properties. Suppose, for example, that a tennis player is asked to play with a racquet heavier than the one he is used to playing with. The first hits would probably not be executed properly, but after a few trials, the player should be able to adapt to the new racquet and perform adequately. In case an error occurs (e.g. missing a target in a pointing task), the information about the sensory prediction is essential for the CNS to understand how the error was made (e.g. in which direction and how much the target was missed). This type of learning, often called error-based, has been studied in several sensorimotor domains ranging from the visual adaptation to an optical prism to reaching movement in force fields (Martin et al., 1996; Shadmehr & Mussa-Ivaldi, 1994; Thoroughman & Shadmehr, 2000). Clinical studies provided compelling evidence that the cerebellum is essential for the fast error-based learning (Smith & Shadmehr, 2005; Tseng et al., 2007). The forward model has also been linked to the learning process through observation. Studies showed that observing another person performing an action

enhances the observer's sensorimotor representation of that action (Rizzolatti et al., 2021). Interestingly, it has been shown that through observation, healthy subjects can learn to compensate for perturbation even before the actual exposition to it, showing faster adaptation than naive subjects once they face it. It has been hypothesized that this behavior involves the ability to predict the errors and their corresponding adjustments using a forward model that simulates the action performance (Mattar & Gribble, 2005).

Neural substrates

The literature on the neural substrates of forward models is wide and heterogeneous. However, there is general strong agreement that the cerebellum and the posterior parietal cortex play a crucial role in this mechanism (Mcnamee & Wolpert, 2019). Extensive evidence has been brought by lesion studies that matched damaged areas' location with motor control deficits. Generally, subjects with impairment in the forward model and in predictive motor control show a peculiar behavior. Although the specific features of motor control impairments rely on the etiology of the dysfunction, these patients show some common characteristics. Relevant evidence on patients with forward motor control impairment came from studies on cerebellar lesions. However, impairment in such a function has been showed also in psychiatric patients affected by schizophrenia, patients with UL dystonia and patients with functional motor disorders (Avanzino et al., 2018; Macerollo et al., 2015, 2016; Shergill et al., 2005).

Cerebellum

Functional anatomy

The cerebellum is a structure of the CNS located in the posterior cranial fossa, posterior to the fourth ventricle, the pons and medulla. The cerebellum is divided into two symmetrical hemispheres with a narrow midline zone called the vermis. From a functional perspective, the cerebellum can be divided in different areas in a medial-to-lateral organization. The medial section is called spino-cerebellum. It receives proprioceptive input from the spinal cord, from the dorsal columns and

from the spino-cerebellar tract and sends its output mainly via the deep cerebellar nuclei to the motor cortex. It is involved in the control of posture and limbs' movements. The lateral areas constitute the neocerebellum, which receives input from the cerebral cortex and projects through the deep nuclei to the thalamus, specifically to the ventro-lateral nuclei. The neocerebellum is thought to be involved in cognitive tasks and action planning. Lastly, the vestibulo-cerebellum lies below the cerebellar hemispheres and it is involved mainly in balance control and spatial orientation. Although representing around the 10% of the brain volume, in humans it contains more than three times the cerebrum's neurons. A layer of dura mater separates it from the cerebrum, called the tentorium cerebelli. It is connected with other regions of the CNS through the pons, by six cerebellar peduncles (three for each side): superior, middle and inferior. The superior peduncle is mainly an output pathway to the cerebral cortex via thalamic nuclei. The middle and inferior peduncles convey input fibers to the cerebellar cortex. The former collects projections from the pontine nuclei, while the latter from the spinal cord and the vestibular nucleus.

Most of the volume of the cerebellum is made of a fold layer of gray matter called cerebellar cortex. Underneath the cortex, the white matter is organized in neural streams connecting the cortex to the pons, giving rise to the so-called *arbor vitae* from its characteristic shape in cross-section. Within the white matter, lie four deep nuclei composed of gray matter: the dentate, emboliform, globose and fastigii. At a cellular level, the cerebellum shows a rather regular organization. The cerebellar cortex includes five principal cell's types: the cells of Purkinje, the granule cells, the basket cells, the Golgi cells and the stellate cells (Voogd & Koehler, 2018). The cerebellum receives input from the axons of the mossy fibers (carrying information from the cerebral cortex, the spinal cord and the vestibular system) and the climbing fibers whose cell bodies are in the inferior olive nucleus (Kelly & Shanley, 2016). The main output of the cerebellar cortex are the Purkinje cells that project to the deep cerebellar nuclei.

The cerebellar cortex is organized in three layers. From internal to external there are: the granular layer, the Purkinje layer and the molecular layer. The granular layer owes its name to the granular cells, whose bodies lie in this area. The granular

19

cells' dendrites make synapsis with the mossy fibers' axons and with the Golgi cells, in a structure called glomerulus. The axons of the granular cells extend their projections to the molecular layer originating the so-called parallel fibers. In this layer each parallel fiber makes synapsis with dozens of Purkinje cells. The Purkinje cells' body are found in the homonymous layer. Purkinje's dendrites extend externally to the molecular layer where receive input signal from the granular cells' parallel fibers and from the climbing fibers. The Purkinje's axons exert an inhibitory action on the deep cerebellar nuclei via GABAergic synapsis. In the molecular layer, along with the parallel fibers, Purkinje dendrites and climbing fibers, lie the basket and stellate cells. These cells have an inhibitory action on the cerebellar output. From a general perspective, the cerebellum receives input from the cerebral cortex through the anterior pontine nuclei, from the spinal cord via the spinocerebellar tract and from several nuclei in the brainstem including the inferior olivary nucleus. On the other hand, it emits outputs to brainstem nuclei and to the cerebral cortex via the thalamus (D'Angelo, 2018). In contrast to the cerebrum, the cerebellum control movements of the homolateral hemibody and projects to the cerebral contralateral hemisphere. The cerebellum is involved in a neural loop that include the cerebral cortex, the brainstem and the thalamus. The sensorimotor areas of the cerebral cortex project to the cerebellum through the pontine nuclei. The cerebellum integrates the input coming from the cerebral cortex with somatosensory information coming from the spinocerebellar tract and send back its output to the motor and pre-motor areas of the cerebral cortex through the ventro-lateral thalamic nuclei (D'ANGELO, 2011; D'Angelo, 2018). Moreover, the cerebellum is also provided with information about the motor error of the actions. This information is conveyed by the climbing fibers originating in the inferior olivary nucleus. When mismatch between the predicted and actual state of the body occurs, these fibers discharge through their synapses with Purkinje's cells in the molecular layer of the motor cortex, modulating their output. It is thought that this activity can modulate plasticity at the level of cerebellar cortex, allowing the cerebellum to modify and update the internal models involved in the specific action (D'Angelo, 2018). In this context, learning would be the consequence of a long-term depression caused by the climbing fibers' activity.

The cerebellum as a locus for the forward model

The position of the cerebellum with respect to the brain and the spinal cord, as well as the analysis of its sources of input and output, has suggested the hypothesis that this structure operates as a comparator between motor intention and execution (D'Angelo, 2018; Tanaka et al., 2020). These observations and emerging theories on motor controls have led to the idea that the cerebellum is indeed an ideal locus for the implementation of a forward model (Wolpert et al., 1998). According to this model, when performing a movement, the motor cortex sends a copy of the associated motor command, often called, as we have already seen, an efferent copy. The cerebellum integrates this input with information on the contextual state of the body from the spinocerebellar tract and the parietal cortex and predicts the future state of the body as well as the future sensory feedback. Finally, it integrates this predicted sensory feedback with the actual feedback generated by the action execution allowing the CNS to perform movement corrections (Wolpert et al., 1998). In order to perform this prediction, the cerebellum must also have access to internal models of the external environment (such as the internal model describing an object) and of the body (such as the internal model representing the moment of inertia of the upper limb). The cerebellum has also been shown to be crucial for adapting forward models to a changing environment (D'Angelo, 2018; Maschke et al., 2004). An example of this impaired behavior comes from studies where cerebellar patients were asked to perform planar reaching movements with a robotic arm under a periodically variable force field (Maschke et al., 2004).

Notably, the hypothesis that the cerebellum is involved in motor prediction and provides this prediction to the cerebral cortex (from which it receives input) implies that the current output of the cerebellar nuclei should predict the future input to the cerebellar cortex. In a recent electrophysiology study on a monkey, authors tested this hypothesis by analyzing the activity of some mossy fibers representing the input signal to the cerebellar cortex, some Purkinje's cells representing the output from the cerebellar cortex, and cells in the dentate nucleus, representing the cerebellar output (Tanaka et al., 2019). During the recording, the animal was performing step-tracking movements with the wrist. Authors found that the firing rate of the mossy fibers could be accurately reconstructed from the signal provided

by the dentate nucleus' cells 20-100ms before, supporting the hypothesis that a predictive forward model is implemented in the cerebro-cerebellum cortex (Tanaka et al., 2019).

The posterior parietal cortex

Functional anatomy

The parietal cortex is the mesial and lateral surface of the brain that extends in a region from the central sulcus and the lateral Sylvian fissure to the parieto-occipital sulcus and the cingulate sulcus. This broad region of the cerebral cortex can be divided into two areas: an anterior part that includes the primary and secondary somatosensory cortex within the postcentral gyrus, and the posterior part, which is divided into superior and inferior parietal lobule with respect to the intraparietal sulcus. The inferior parietal lobule involves the supramarginal and the angular gyrus and corresponds to Brodmann areas 39 and 40, while the superior parietal lobule includes a part of the lateral surface and a part of the mesial surface of the brain corresponding to Brodmann areas 5 and 7. The molecular architecture of the parietal cortex, like other areas of the neocortex, is composed of six layers: molecular, external granular, external pyramidal, internal granular, internal pyramidal and a multiform layer (Caspers & Zilles, 2018). The molecular layer is the most external and is formed mostly of dendritic tufts of the pyramidal neurons of the deeper layers and glial cells. The molecular layer receives inputs mostly from other areas of the brain cortex as well as from thalamic nuclei (Rubio-Garrido et al., 2009). The external granular layer contains stellate cells and pyramidal neurons of small dimensions, while the external pyramidal layer contains larger pyramidal neurons. This layer is considered to be the most relevant source of cortico-cortical efference. Also, stellate cells and pyramidal neurons lie in the internal granular and pyramidal layers. However, these layers receive input from thalamic nuclei and send output to the basal ganglia. The deeper layer, the multiform, is connected to the thalamus, which sends its output signals. The neocortex is functionally

organized in columns extending through the six cortical layers connecting them (Mountcastle, 1997).

The posterior parietal cortex is part of the association cortex, a region of the human brain that integrates and modulates multimodal stimuli. This cortex area is a key node in the sensorimotor network that connects prefrontal and parietal areas. Several parallel streams connect these two brain areas, each stream carrying different information to and from the prefrontal areas. One of the main paths is the superior longitudinal fascicle that connects the posterior parietal cortex extensively with the frontal cortex. It can be divided into three bundles. The most dorsal connects mesial and lateral pars of the superior parietal lobule with supplementary motor cortex and dorsolateral premotor cortex. Lastly, the middle bundle extends between the intraparietal sulcus and lateral areas of the premotor and prefrontal cortex. The ventral stream connects the inferior parietal lobule with the ventrolateral premotor and prefrontal areas (Caspers & Zilles, 2018). A second relevant stream parallel to the superior longitudinal fascicle is the so-called arcuate fascicle. The arcuate fascicle bridges the inferior parietal lobule and the superior temporal cortex with the inferior frontal gyrus. Although mainly involved in cortico-cortical connections, the posterior parietal cortex also conveys information to the basal ganglia and the thalamus, from which it receives information about the sensory state of the body (Caspers & Zilles, 2018). Both the inferior and superior parietal lobe project to the putamen and caudate nucleus (Yeterian & Pandya, 1993).

These extensive connections are involved in controlling the interaction with objects and in understanding and controlling UL actions (Binkofski & Buccino, 2018).

The posterior parietal cortex codes the upper limb's predicted sensory feedback

As mentioned in the previous sections, the posterior parietal cortex is a relevant node in the sensorimotor network responsible for sensory and motor representation in the cerebral cortex. This area is crucial for multimodal sensory integration and use this integration for guiding the ULs' movements. Patients with lesions in this area showed impairment in identifying the required motor behavior to perform an

action, along with difficulties in planning skilled movements and distinctive impairments of the UL apraxia syndrome (Goldenberg, 2013). Previous evidence suggested that also the parietal cortex plays is involved in the implementation of a forward model. The connection with motor and premotor areas candidate the posterior parietal cortex to be the ideal locus for the representation of the UL predicted sensory feedback, an essential feature of a forward model (Johnson et al., 1996). Neurons in the posterior parietal cortex, within the superior parietal lobule, showed activation consistent with a representation of future body's state (Mulliken et al., 2008). Moreover, the inhibition of these neurons via transcranial magnetic stimulation resulted in impairment in correcting reaching movement trajectories based on forward state estimation (Desmurget et al., 1999). Neurophysiological studies in monkeys found that neurons in the posterior parietal cortex showed significant activation in the planning phase of a reaching movement, an activity coherent with the idea that these neurons encode the intention to reach a target (Snyder et al., 1997). Evidence in support of this hypothesis comes from studies that found discharge in posterior parietal cortex's (Area 5 Brodmann) neurons before the movement starts (Kalaska et al., 1983). It is thought that this activity may represent the integration of information about the motor command in order to predict the consequent sensory input. Moreover, this early activation was found even in subjects with deafferentation, ruling out the possibility that it was caused by movement-related actual sensory input (Seal et al., 1982).

The posterior parietal cortex plays a role also in the mechanism of SA, or re-afference cancellation and in matching between predicted and actual sensory feedback. A functional-MRI study investigated sensorimotor Blood Oxygenation Level-Dependent (BOLD) response during finger tapping (Shergill et al., 2013). Subjects were required to tap with their right index finger a lever which transmitted the force to the left index finger synchronously, with a delay of 500 ms, or not at all. The setting was that right and left index fingers were aligned, so the subjects had the illusion that they were touching their left index with their own right index. The results showed that the activation of the SII cerebral cortex was significantly reduced when left finger sensation was perceived as a direct consequence of the right index self-generated movement. Authors suggested that SII could, therefore,

play an essential role in encoding SA using the forward-model output of sensory prediction. Moreover, the temporary inhibition of neurons in the posterior parietal cortex using transcranial magnetic stimulation was shown to affect the subjects' sense of agency during a reaching task, closely linked to the ability to predict sensory feedback (Desmurget et al., 1999). These findings suggested that the posterior parietal cortex may be responsible for maintaining a time-related representation of UL's action that relies on a forward model and not only a feedback mechanism. This representation could be used to overcome the issue of the time delay of sensory feedback during the UL movements.

Forward model dysfunctions

The crucial role of the cerebellum in implementing the forward model is suggested also by studies on patients with cerebellar lesions. These patients manifest typical UL sensorimotor symptoms that are collected under the umbrella of the cerebellar ataxia syndrome, which includes clumsiness, lacking smoothness and multi-joint coordination, spatial errors while pointing to a target (i.e. dysmetria) and irregular movements repetitions (Day et al., 1998; Lisberger & Thach, 2013; Manto et al., 2012). This can be related to both the lower limbs (gait ataxia) and the upper limbs. Multi-joint movements are usually more affected than single-joint ones. Dysmetria is the inability to accurately point to a target. Subjects affected by dysmetria make spatial errors when performing reaching movement, either overshooting or undershooting the target. Another typical UL cerebellar sign is the intentional tremor, which consists of large oscillations in the last phase of a reaching movement when approaching the target. Although a cerebellar lesion does not affect somatosensation or strength, these sensorimotor signs cause significant impairment and can have a devastating effect in terms of disability and quality of life. Some of the typical UL motor dysfunctions in patients with cerebellar lesions have been described as the consequence of an impaired forward or inverse model. On one hand spatial errors of overshooting or undershooting the target during reaching (i.e. dysmetria) was showed to be effectively modeled as an impairment of an inverse model and a miscalculation of UL's inertia (Bhanpuri et al., 2014). Interestingly, Bhanpuri et al. found that those patients who systematically overshot the target

showed kinematics parameters compatible with an underestimate of their forearm's moment of inertia. In contrast, patients that undershoot the target moved as they were overestimating their forearm's moment of inertia. Moreover, by altering the dynamic of the robot the subjects were interacting with, the authors were able to correct patients' movement accuracy (Bhanpuri et al., 2014). These results brought strong evidence that the cerebellum is crucial for maintaining accurate internal models of dynamics necessary for an inverse model.

On the other hand, the lack of smoothness, the excessive oscillations approaching the target and errors in movement planning have been interpreted as the consequence of patients' inability of anticipating the consequences of voluntary movements, consistent with an impairment of a forward model (Frey et al., 2011). Relying only on delayed somatosensory feedback for motor control, these subjects perform instable UL reaching movements with exaggerated oscillations while approaching the target (Bhanpuri et al., 2014; Cabaraux et al., 2020; Frey et al., 2011; Manto et al., 2012; Wolpert & Ghahramani, 2000). According to this idea, in these patients the cerebellum receives the efference copy based on a theoretically correct limbs' position estimation provided by the somatosensory system. However, cerebellar lesions may impair the computation of the predicted body's state, i.e., the output of the forward model. Being the information provided for internal feedback correction unreliable, the system is forced to rely mainly on delayed feedback control, using information on ULs' position provided by the dorsal columns to the somatosensory areas of the parietal cortex. This would lead to the typical excessive oscillations observed in cerebellar patients in the last phase of a reaching movement. Moreover, the inability of predicting the consequences of the voluntary movement and result in impaired movement's planning.

Recent literature suggested that, along with the cerebellum, the forward model's neural underpinning consist of a complex cerebro-cerebellar network including the sensorimotor cortex, and the Posterior Parietal Cortex (PPC). Interestingly, similar to cerebellar patients, patients with CNS lesions involving the spinothalamocortical pathway, the thalamus, the primary somatosensory cortex and other parietal areas involved in the proprioception sense, show dysmetria, lack of smoothness and

irregular movements, a syndrome often called sensory ataxia (Ghika et al., 1994; Melo & Bogousslavsky, 1992; Osumi et al., 2018, Caplan, 2012). This behavior is exacerbated when patients are prevented from using vision to compensate for proprioceptive deficits (Klingner & Witte, 2018). Although it has been previously suggested that patients with sensory ataxia due to stroke showed signs of both feedback and feedforward motor control deficits, limited attention has been paid in describing the role of somatosensory information in the forward model. (Osumi et al., 2018).

Besides brain injured patients, forward model dysfunctions have been found also in patients with functional motor disorders and with schizophrenia (Macerollo et al., 2015; Pareés et al., 2014; Shergill et al., 2005, 2014). Relevantly, the lack of attenuation of self-evoked sensory input has been related to the impairment in the sense of agency, a common deficit of both these category of patients (Shergill et al., 2014). A recent study of Macerollo et al. (Macerollo et al., 2015) investigated the inhibition of sensory evoked potentials in patients affected by functional motor disorders. The sensory evoked potentials were recorded by stimulating the right median nerve in two conditions: resting and self-paced finger movements. In the former subjects were sitting in a resting position during the stimulation, in the latter the nerve stimulation was triggered by subject's homolateral index abduction. Authors found that in the voluntary triggered condition patients showed reduced attenuation of sensory potentials compared to healthy controls suggesting impairment in the ability to predict sensory consequences of self-initiated actions (Macerollo et al., 2015). In line with these findings were the results of another recent study where patients with functional movement disorders were tested in a force matching task similar to the one performed in Shergill et al (Shergill et al., 2003). A motor torque attached to a lever exerted target force on subjects' left index finger. Then, they were asked to reproduce that force with their right hand either by directly pressing to their left index (through a force sensor) or by manipulating a robotic device that indirectly controlled the motor torque acting on the lever. In line with previous experiments, healthy controls were accurate in reproducing the force in the latter condition, while they underestimated the matching force they exerted

in the direct condition (they exerted a force greater than the target force). This behavior has been interpreted as a sign of SA phenomenon (Bays & Wolpert, 2007a; Shergill et al., 2003). In contrast, patients showed no difference in the matching force intensity between condition corroborating the hypothesis that in patients with functional motor disorders impairment in sense of agency and lack of SA may be correlated (Pareés et al., 2014). Sense of agency is also a typical impairment of patients with schizophrenia. Some of positive symptoms that affect these patients, like delusion control and sensory hallucinations, has been interpreted as a result of misattribution of voluntary actions as externally generated (Shergill et al., 2014). A previous study testing the SA phenomenon in these patients following the paradigm of Shergill et al (Shergill et al., 2003) found that patients with schizophrenia have reduce SA compared to healthy controls (Shergill et al., 2005). More recently, a functional-MRI study investigated sensorimotor Blood Oxygenation Level-Dependent (BOLD) response during a tapping task, reproducing the paradigm of Shergill et al (Shergill et al., 2013) in patients with schizophrenia. Subjects were required to tap with their right index finger a lever which transmitted the force to the left index finger synchronously, asynchronously with a delay of 500 ms, or not at all. Compared to healthy controls, patients showed lower levels of attenuation in SII activity. Moreover, the reduction on SII activity attenuation was associated with hallucinatory severity underlying the importance of this parietal area for the coding of the forward model's output (Shergill et al., 2014).

Overall, this evidence suggests that in a wide range of neurologic dysfunctions, predictive UL motor control impairments not related to primary sensorimotor deficits may play a key role in affecting patients' behavior. The investigation of such impairments could improve our understanding of these dysfunction and eventually lay the foundation for the design of specific rehabilitative trainings.

Project's aim

The aim of this project was to investigate different aspects of the anticipatory motor control in healthy subjects and forward model dysfunctions in stroke patients with cerebellar lesions and somatosensory impairment.

Firstly, we aimed to provide further evidence on the role of the forward model in sensorimotor function of the upper limb. Specifically, we aimed to perform new analysis on previously recorded data (Bays & Wolpert, 2007a; Shergill et al., 2005; Wolpe et al., 2016) on the sensory attenuation phenomenon to shed new light on the mechanism involved in such phenomenon.

Secondly, we aimed to investigate anticipatory grip force modulation deficits during the bimanual object lifting in patients with stroke and somatosensory deficits.

Lastly, we aimed to use an accurate low-cost movement analysis system to assess predictive upper limb behavior in the index-to-nose task in patients with cerebellar lesions and patients with somatosensory deficits.

These investigations would improve our understanding of predictive aspects of motor control in healthy subjects and patients with stroke and, eventually, allow us to design effective and specific rehabilitation interventions.

Predicted sensory feedback and sensory attenuation phenomenon[*]

Background

Sensory attenuation (SA) is a phenomenon associated with voluntary movement where there is a different perception of identical sensory inputs depending on whether they are self-generated or externally generated (Macerollo et al., 2015). This phenomenon has been mostly investigated using force matching tasks, since the seminal study by Shergill and colleagues (Shergill et al., 2003). In their setting, firstly a motor torque applied a constant force to the tip of the participants' resting left index finger. Then, the participants were asked to match the force with their right index finger either by pressing on themselves left index finger through a force transducer (Figure 3 top, "*self-condition*") or by moving a joystick that indirectly controlled the force output of motor torque (Figure 3 bottom "*Joysitck condition*"). Their results showed that while in the joystick condition the subjects were relatively accurate in reproducing the target force, in the self-condition they systematically overshot the target force. In other words, the self-generated matching forces were perceived as weaker than externally generated forces of the same magnitude. The authors suggested that the predictive forward model played a crucial role in this behavior (Shergill et al., 2003). Specifically, their hypothesis was that in the self-condition the forward model could predict that the force exerted with the right index finger would generate a tactile sensation on the left index fingertip. This prediction would then be used to attenuate the intensity of the actual tactile feedback. In contrast, given the artificial setting of the joystick condition, it was virtually impossible for the forward model to directly associate the movement of the right index finger with the consequent tactile sensation in the contralateral hand. Therefore, no attenuation was found in this condition.

---

[*] This section was performed during a visiting period at the Bayslab within the Department of Psychology of the University of Cambridge (UK) under the supervision of dr. Paul Bays
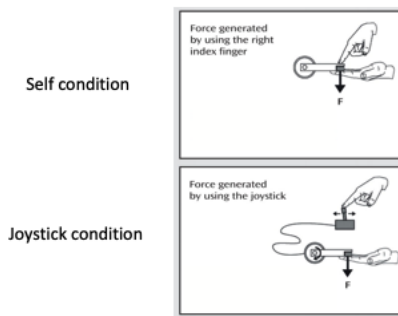
Figure 3 The bimanual task used in Shergill et al., 2003)

The hypothesis that a forward model is essential for the SA phenomenon brings some implications. Firstly, SA should be measured only in situations where the subject is able to predict the sensory feedback. Secondly, in a real-world scenario, when several different somatosensory inputs are simultaneously involved, only the predicted part of this input should be attenuated. Lastly, the presence of a prediction should be sufficient to measure an attenuation of the predicted feedback.

Only the predicted part of the sensory feedback is attenuated

A series of works in the last 15 years addressed these aspects. As previously mentioned, the results from Shergill's experiment (Shergill et al., 2003) corroborated the idea that tactile attenuation can be measured only if the sensory consequences of subject's action are predictable (self-condition) and it cannot be measured when the subject's action and the feedback are simultaneous but not directly related (joystick condition).

However, in principle it could be possible that tactile attenuation was the consequence of a general gating mechanism and not a specific predictive phenomenon. It is well known that during an arm movement the sensitivity and the ability to detect different tactile sensation is reduced (Chapman et al., 1987). This reduction of perception acuity begins prior to the movement onset and is triggered by the motor command in the motor cortex, as previous TMS studies showed, and is measured irrespective of the source of the stimulus (Voss et al., 2006). To disentangle between these hypothesis, Bays & Wolpert performed a study where

31

the subjects were asked to assess the intensity of an electrical stimulus on their left index fingertip either while resting or pressing on the same finger with their right index finger through a lever (Bays & Wolpert, 2007a). Authors found that, although they measured attenuation of tactile perception as in previous study, the perceived intensity of the electrical stimulus' intensity was not reduced by the concomitant pression exerted with their right index. This suggested that the perception of externally generated and unpredictable stimuli (like the electrical stimulus in this experiment) is not attenuated even when a simultaneous predictable stimulus (pression by the right index) is recorded. Moreover, in a similar setting another study showed that it was possible to measure tactile attenuation even if the right index does not perform any touch ruling out the hypothesis that the tactile sensation on the active finger modulate the perception of the left index finger (Bays et al., 2006). In this case, the experimental setting included a mobile lever attached to a motor torque, and a force sensor placed a few centimeters above it, vertically aligned. When the subjects tapped on the force sensor with their right index finger the lever was actioned and tapped on the left index underneath. Once again, the setting was meant to maximise the feeling that the force felt on the left index finger was a consequence of the pression exerted with the right index. Authors included a condition in which when subjects were performing the active tap, the force sensor placed above the lever shifted unexpectedly, making them fail to touch it. However, also in this condition the underneath lever exerted the tap as expected. Interestingly, even in this condition the perception of the tactile stimulus on the left index was attenuated. In these trials subjects believed they would have touched the force sensor and, therefore, the forward model based on the efferent copy of that movement was likely to predict the consequent tap perceived on the left index. In other words, this study showed that the prediction of the touch is sufficient to generate the attenuation of the tactile feedback even without the touch itself, bringing strong evidence on the predictive nature of the SA phenomenon.

Temporal and spatial coherence are necessary to measure attenuation

The influence of temporal discrepancy between the predicted and actual feedback on the tactile attenuation was corroborated by another experiment (Bays et al., 2005). Here, an experimental setting similar to the one used in (Bays et al., 2006) was used. However, in this study the temporal delay between the two taps was manipulated so the tap on the left index could occur in a range of 300ms earlier or later the active tap varying from trial to trial. Subjects were then asked to report the perceived magnitude of tactile sensation on the left index. The results showed that the attenuation was measured only when the active pression and the tactile sensation were temporally coherent, and the effect rapidly decreased with the increase of the time interval between the active force exertion and the tap perception. Specifically, the attenuation was significant when the testing tap occurred within a time interval of ±100ms from the active tap (Bays et al., 2005).

A slightly different setting was used to perform a force-matching task to test whether the level of tactile attenuation measured in the self-generated actions depends on the spatial separation between hands or on the magnitude matching force exerted and force perceived (Bays & Wolpert, 2007a). Authors used a system with two levers, one attached to a motor torque that exerted the force on the subjects' left index finger (active lever), and one that served as a force sensor, and measured the matching force the subjects applied with the right index (on the passive lever). This setting allowed to manipulate either the lateral separation between the active and the passive levers or the gain between the force measured by the passive lever and the force exerted by the active one (in this condition the levers were vertically aligned). As for the former aim, three conditions were tested. In the first one the two levers were aligned one above the other, reproducing the self-condition in (Shergill et al., 2003). In the other two conditions the levers were placed with a lateral separation of 10cm and 30cm respectively. The comparison of subjects' accuracy in reproducing the target force between conditions showed that higher level of attenuation was found in the condition where the two levers were vertically aligned while significant lower attenuation levels were measured in the other conditions. As for the second experiment, three different gain levels were

compared. In the first condition the gain was set at 1x, essentially reproducing the aligned condition of the former experiment. In a second condition the gain was set at 0.5x, so when subjects tried to match the target force exerting a force of 2N the force simultaneously exerted by the active lever was 1N. In a third condition the gain was 2x. This comparison showed no differences in terms of the magnitude of attenuation.

Patients with impaired sense of agency showed reduced attenuation

The SA phenomenon has been investigated also in patients with impairment in the sense of agency. Patients with this disturb show difficulties in discriminating between self- and external-elicited actions. It has been postulated that the sense of agency is related to the ability to predict the consequences of our own actions (Feinberg, 1978). The forward model is thought to play a crucial role in this prediction and therefore it is conceivable that these patients would present impairment in predictive motor control.

The same force-matching paradigm of the Shergill's study (Shergill et al., 2003) was used in studies that investigated this phenomenon including patients with schizophrenia (Shergill et al., 2005, 2014) and functional motor disorders (Pareés et al., 2014): patients were asked to match with their right index finger a target force presented by a lever to their left index either by pressing directly on their left finger through the lever (self-condition) or by manipulating a joystick that indirectly controlled the lever. In line with previous results, healthy controls exaggerated the matching force performed in the self-condition (that is they underestimated the tactile sensation on the left index). In contrast with patients with schizophrenia and functional motor disorders performed more accurately than healthy controls in the self-condition showing lower level of tactile attenuation. These findings were interpreted as a consequence of impairment in the forward model. Similar results suggesting a dysfunction in SA has been found using slightly different experimental procedures in other movement and psychiatric disorders like dystonia, and functional movement disorders (Macerollo et al., 2015, 2016; Pareés et al., 2014). Overall, these works suggest that the deficits in the prediction of the sensory

consequence of a movement delivered by a forward model are deeply involved in the SA reduction.

The neural underpinning of the SA phenomenon is still under debate. While, as mentioned in previous chapters, there is compelling evidence that the cerebellum plays a key role in the prediction of the consequences of voluntary movements, there is less agreement on where the output of the forward model is coded in the CNS. Some neuro-imaging studies tried to address such question focusing on the SA phenomenon. A similar apparatus than the one used in (Bays et al., 2006)was recently used in a functional-MRI study on healthy subjects (Shergill et al., 2013, 2014) to investigate sensorimotor Blood Oxygenation Level-Dependent (BOLD) response in different tasks involving touch. Subjects were required to tap with their right index finger on a lever that transmitted the force to the left index finger synchronously, asynchronously with a delay of 500 ms, or did not at all. The results showed that the activation of SII cerebral cortex was significantly reduced when left finger sensation was perceived as a direct consequence of the right index self-generated movement. Authors suggested that SII could, therefore, play an essential role in encoding SA using the forward-model output of sensory prediction.

These findings taken together suggest that when a voluntary action is performed, a forward model based on the efferent copy of the motor command predicts the sensory consequences of that action. When the movement is performed, the tactile sensory feedback that matched the predicted sensory input is perceived as attenuated. However, the comparison between the predicted and the actual feedback seems to concern general features of the tactile perception like temporal and spatial coherence rather than the intensity of the stimulus. In fact, in the aforementioned experiments, when temporal delay or spatial separation between the two hands was introduced, the attenuation was reduced (Bays et al., 2006; Bays & Wolpert, 2007a) On the other hand, when the right index action and the sensation on the left index were spatially and temporally matched, no reduction in attenuation was measured even when the force perceived was significantly more intense or weaker than the force exerted(Bays & Wolpert, 2007a).

Alternative accounts for the sensory attenuation phenomenon

Recently, this topic has gained new interest. Other research groups proposed new models for interpreting the SA phenomenon that don't involve any predictive mechanisms. Most of these claims are based on the attempt of applying the theory Bayesian inference in human perception (Press et al., 2020; Yon et al., 2018).

The theory of Bayesian inference in the context of motor control describes how the CNS deals with noisy perceptual feedback. Sensory organs in human body have indeed limited resolution and the signal they transmit is affected by intrinsic electrical noise. These limitations result in uncertainty about the true value of the stimulus. The Bayesian inference theory hypothesizes that, in order to overcome this issue, the CNS combines the noisy feedback with prior knowledge about the probability of a certain state of the body to be realistic in a specific situation (usually referred as "prior") (Bays & Wolpert, 2007b). This integration is used to improve the accurateness of the sensory estimate and can be applied both to sensory input referring to the external environment (for example the position of an object) or to internal state perception (the position of the arm). The final estimate of the sensory information obtained by the integration of noisy sensory input and the prior is called "posterior" and can be though as the probability of a specific state to be true given a sensory input. The mathematical formulation of this integration assigns to the strength of the prior belief a real number between zero and one, and computes the posterior as follows:

$$P(state|sonsory\ input) = \frac{P(sensory\ input|state)\,P(state)}{P(sensory\ input)} \qquad (1)$$

Where P(state|sensory input) is the posterior estimate of the state (e.g. the position of the subject's right hand), P(state) represents the strength of the belief of the prior (e.g. the fact that the distance between the body and the hand has to be shorter than the length of the upper limb). P(sensory input|state) is often referred to as the likelihood of the state equal to the probability of having the sensory input given the hypothesized state. This model has been proved to accurately describe the human behavior in different situations. In general, the Bayesian inference effectively

describes those situations where the sensory input is particularly noisy and subjects have to rely more on their prior beliefs, e.g. when visual feedback is perturbated or shaded. Specifically, it has been showed that in experimental setting the higher the noise applied to the visual feedback about the hand's position, the more the subjects relied on the prior and the less on the actual visual feedback (Körding & Wolpert, 2004).

Recently, it has been argued that the Bayesian theory is inconsistent with SA phenomenon as it was previously described (Press et al., 2020; Thomas et al., 2020; Yon et al., 2018). The Bayesian theory in this context is used to suggest that we are biased to perceive what we are expecting. Authors claimed that the application of the Bayesian inference to a situation where sensorimotor prediction are made (for example in the self-condition in the force-matching task in (Shergill et al., 2003), the prediction itself should sharpen the perception rather than suppress it as it was suggested. To corroborate their hypothesis, Yon et al. tested healthy subjects in a task where human participants were required to execute either index or little finger abductions while observing an avatar hand on a screen (Yon et al., 2018). The avatar hand performed finger abduction simultaneously to subjects' movement in two conditions: congruent (same finger) or incongruent (different finger). While performing the finger abduction, the subjects' neural activity was recorded using functional magnetic resonance imaging (fMRI). Participants were asked to judge about which avatar's hand finger moved. Authors found superior accuracy in those trials when the avatar's and subjects' hand were moving the same finger. Moreover, the analysis of fMRI data showed that in the congruent trials there was a reduction in activity of those voxels tuned away from the expected stimulus (Yon et al., 2018). With the aim of reconciling their results and their hypothesis with previous findings on SA phenomenon, the authors proposed a new model, called "sharpening model". According to this model, the expectation of a sensory input increases the activity of the cortical sensory units tuned to that stimulus while suppressing the activity of other units. This was intended in contrast to the cancellation model where the prediction suppresses the activity of related sensory units leading to SA. Authors concluded that previously observed attenuations of predicted tactile stimuli may

reflect a dampening of responses in units tuned to unexpected stimuli, rather than the activity suppression in expected sensory units, questioning the previous interpretation of the SA phenomenon (Yon et al., 2018). Moreover, in a more recent paper, the same authors proposed a new model called "opposing process theory" (Press et al., 2020). This theory distinguishes between two different scenarios according to whether the presented stimulus was expected or unexpected. The novelty of this proposal was that in the latter condition a biochemical process that involves catecholamine release would boost the perception of the stimulus, eventually enhancing its perception. The authors suggested that the difference between the expectation and the actual stimulus, in terms of distance between the two probability distributions, may be quantified using the Kullback-Leibler divergence. In other words, high values of Kullback-Leibler divergence may trigger the catecholamine release and modulate the subject's perception (Press et al., 2020).

Within this topic other authors proposed that the attenuation measured in (Shergill et al., 2003) may be the consequence of a mechanism of enhancement of activity of neurons that codes for the predicted stimuli rather than its suppression(Roussel et al., 2013). It has been suggested that if the baseline activity level of those neurons increases, the relative enhancement of activity due to the stimulus presentation would be relatively weaker compared to the case of an unpredicted stimulus of identical intensity. This relative reduction in increased activity could result in the subjects' attenuated perception previously found. Interestingly, Dogge et al. proposed that the prediction of the sensory consequence of our actions may relies on two distinct paths (Dogge et al., 2019). The first one is consistent with the classical idea of forward model based on an efferent copy expressed in (Wolpert & Flanagan, 2001). The second one relies on alternative prediction mechanisms that, in principle, don't need a forward model to be performed. Authors suggested that the first path may be used in overlearned and body-related predictions where the evidence for a forward model are compelling. In contrast in environment-related events, the CNS may use the latter path and the prediction may be independent to the motor system(Dogge et al., 2019).

Moreover, a recent preprint paper from Kilteni & Ehrsson aimed to disentangle the predictive SA phenomenon from an unpredictive and generic gating mechanism (Kilteni & Ehrsson, 2020). In their experiment, healthy subjects received two taps on their left index finger. The first one was a test tap of fixed intensity while the second one was a comparison tap of variable intensity. They were asked to tell which one they felt stronger. The protocol involved the manipulation of two factors: the state of the left limb (whether the left limb was resting or moving while receiving the test tap), and the origin of the tap (whether the test tap was triggered by the subject himself or by an external motor). The manipulation of these two factors led to four conditions: resting and self-tap, moving and self-tap, resting and external-tap and moving and self-tap. While the movement of the left arm attenuated the perception of both the self-tap and the external-tap (compatible with a gating mechanism), the conditions in which the tap was self-generated showed greater attenuation compared to the external-tap (suggesting a SA). Their findings suggested that gating and sensory attenuation phenomena are independent and don't interact each other, providing evidence in support of the hypothesis that a predictive forward model is essential for the SA phenomenon (Kilteni & Ehrsson, 2020).

Hypothesis and project aim

Although there is strong evidence suggesting that the SA phenomenon relies on a predictive mechanism, the recent literature has brought new interest on this topic and questioned this hypothesis. The literature on SA mainly focused on subjects' accuracy in force matching tasks, where the underestimation of the tactile stimulus in a self-like condition led to systematic errors in the matching force (Bays & Wolpert, 2007a). In contrast, according to recent papers, also a generic gating mechanism could account for those results (Press et al., 2020). Within the framework of the force matching tasks, a new perspective that could help to disentangle this issue is the analysis of the trial-to-trial variability (rather than the accuracy) of the matching forces.

Here the underlying hypothesis is that the SA phenomenon is the result of a predictive mechanism that attenuates the perception of predictable sensory stimuli. Moreover, our hypothesis is that the level of attenuation is not fixed and depends on the accuracy of the prediction. That is, the higher the congruency between the predicted and the actual tactile stimuli (in terms of spatial and temporal coherence) the higher the level of attenuation. This would mean that the level of attenuation is set on subject's estimate and is subjective to a certain amount of variability. When subjects are asked to match a target force in a self-like condition, if a forward model is involved, the incoming tactile stimulus is compared to the predicted sensory feedback leading, in case of congruence between each other, to attenuation. This comparison process along with the variability of the level of attenuation would generate some extra noise on top of the tactile stimulus' intrinsic sensory noise. Consequently, the extra noise would lead to an increase in variability of tactile perception intensity and, eventually, to an increase in variability of the matching force. Noteworthy, this process would not occur in external conditions where there is no attenuation. Therefore, if our hypothesis is true, the trial-to-trial variability of the matching forces in a self-like condition would be greater than the variability in a related external condition. Most importantly, since a generic gating mechanism would not account for this difference in trial-to-trial variability, this analysis could help to disentangle between the forward model and the gating hypothesis.

This project aimed to compare the within-subject trial-to-trial variability in the matching forces between self and external condition. For this analysis, previously collected data from different force matching tasks were used. The secondary aim was to model the subjects' behavioral responses in different force matching tasks investigating SA.

Methods

Data collection

We collected data from three previous experiments on force matching tasks (Bays & Wolpert, 2007a; Shergill et al., 2005; Wolpe et al., 2016). This project has been carried out at the Bayslab within the Department of Psychology of the University of Cambridge (UK).

- Study 1: force matching task on healthy subjects and schizophrenic patients (Shergill et al., 2005)

In this study that, for the sake of simplicity, we will call "Study 1", authors reproduced the paradigm of Shergill et al. (Shergill et al., 2003) on healthy controls and patients affected by schizophrenia. After being provided with a target force on their left index pulp, subjects were asked to reproduce that force in two conditions: a "self-condition" in which subjects matched the target force by pushing on a lever placed right above their left index, and a "joystick condition" in which subjects controlled the lever indirectly by manipulating a joystick. This study involved 19 healthy controls and 19 patients. Each subject was provided with a target force randomly varying between five levels between 0.5N and 2.75N. Each subject underwent 16 trials for each condition and force level. The authors compared the subjects' accuracy in reproducing the target force. The schizophrenic patients showed lower level of attenuation in the self-condition compared to healthy controls.

- Study 2: force matching task with gain and distance manipulation (Bays & Wolpert, 2007a)

This study, herein called "Study 2", the setting consisted of two levers, one attached to a motor torque exerted the target and the matching force on the left index finger (active lever), while another lever served as a force sensor and measured the matching force exerted with the right index (passive lever). This experiment included 12 healthy subjects. This setting allows the authors to manipulate the lateral separation between the two levers and the gain between the force measured by the passive lever and the force produced by the active lever. In the first experiment the authors compared three conditions according to the distance between the two levers: 0 cm, 10 cm, and 30 cm. In the first "direct" condition, the levers were vertically aligned reproducing the self-condition of the Study 1. This "direct" condition was used in the second experiment in all the conditions, where the authors manipulated the gain between the force exerted by the subject and the force exerted by the motor torque. Again, three conditions were compared according to the gain: 1x, 2x and 0.5x. In other words, when a subject exerted a matching force of 1N, the motor torque transmitted a force of either 0.5N, 1N, or 2N to the left index. The target force was set randomly between five level of intensity ranging from 1N to 3N. This study involved sixteen healthy subjects who performed eight trials for each target force level and each condition. The results showed that the lateral separation between the levers reduced the attenuation level. In contrast the gain manipulation did not affect the attenuation level and no difference between the conditions was found.

- Study 3: force matching task with elderly subjects (Wolpe et al., 2016)

This study reproduced the paradigm of the Study 1 (Shergill et al., 2005) comparing a self-condition and a slider (joystick) condition in a force matching task. Here, the target force level varied between four levels from 1N and 2.5N. This study included a large sample of 325 subjects of different ages, ranging from 18 to 88 years old. Each subject performed 8 trials for each target force level and condition. Subjects were grouped into three age groups: young, middle-aged, and elderly and the level of attenuation was compared between groups. The results showed that the attenuation was greater in the older subjects compared to the young group.

Aim 1: the analysis of the within-subjects trial-to-trial matching force's variability

To investigate whether the SA phenomenon found in the included studies was the result of a predictive forward model or a general gating mechanism, we analyzed the within-subjects trial-to-trial variability in the matching force comparing different conditions. We focused on the comparison between conditions that had showed different level of attenuation. Specifically, for the Studies 1 and 3 we compared variability between self and joystick conditions. For the Study 2 we firstly compared the direct condition with the 30cm condition and the 10cm condition with the 30cm conditions (for the sake of simplicity the "direct" and the 10cm conditions will be referred as "self" conditions in the comparisons). Then, we compared the direct condition with the conditions with gain 2x and 0.5x separately (the direct condition will be referred as the "self" condition). As for the Study 3, accordingly to the study of Wolpe and colleagues, we grouped the subjects into three age groups: young subjects (18-39 years old), middle-aged subjects (40-64 years old) and older subjects (age $\geq$ 65 years old) (Wolpe et al., 2016). Given the different behavior of these groups in terms of attenuation levels, the analysis was performed on the three groups separately.

Data analysis

The single-subject trial-to-trial variability in the matching force was computed as the standard deviation of the matching forces values for each target force level. Then, for each target force level the single-subject standard deviations were averaged across subjects. Analogously, the matching force values were averaged for each subject and for each target force level, and the mean across subjects was then computed for each target force level separately. From a general perspective, it is well known that the variability of a measure depends on the magnitude of the measure itself, that is the greater the value, the greater the associated variability. In our analysis it could be argued that a greater variability in the self-like conditions' matching force could be simply a consequence of the greater force exerted by

subjects in these conditions. To rule out this hypothesis, we analyzed the mean standard deviation of the matching force as a function of the target force level for conditions self and joystick separately.

Specifically, we used a linear regression model including the mean standard deviation as a dependent variable and the mean matching force for each target force level as the independent variable. Note that we assumed that between the two conditions only a change in the intercept would occur. We included the factor c representing the conditions assuming the value 0 for joystick condition and 1 for self-condition:

$$\sigma_m = \gamma_1 F_m + c \gamma_2 F_m + \beta_1 \qquad (2)$$

Where σ_m is the standard deviation of the mean matching force, F_m is the mean matching force, γ_1 and γ_2 are the coefficients so that γ_1 is the angular coefficient of the regression line for the condition joystick and $\gamma_1 + \gamma_2$ is the angular coefficient of the regression line for the condition self, c is the factor indicating the condition and β_1 represent the intercept of both the regression lines. The subject was considered as a random factor. This approach allowed us to quantify the relative variability between the two conditions as follows:

$$V = \frac{\gamma_1 + \gamma_2}{\gamma_1} \qquad (3)$$

Values greater than 1 suggest a different relation between the matching force and its variability between the two conditions.

Analogously, we used a similar model to estimate the attenuation between the conditions, with the mean matching force as the dependent variable and the target force as the independent variable:

$$F_m = \alpha_1 F_t + c \alpha_2 F_t + \beta_2 \qquad (4)$$

Where F_m and F_t are the matching and the target force respectively, c is the factor indicating the condition (c=0 for joystick condition and c=1 for self-condition), α_1

and α_2 are the estimated angular coefficients and β_2 is the intercept. The subject was considered as a random factor. Also, we estimated the relative attenuation between conditions using the coefficient A:

$$A = \frac{\alpha_1 + \alpha_2}{\alpha_1} \qquad (5)$$

Data from the included studies were analyzed. For studies 1 and 3 condition self and joystick were compared. For the study 1 healthy controls and patients were analyzed separately. When analyzing the study 3 subjects were divided into three groups based on their age. Concerning the study 2, we performed two comparisons for each experiment. Specifically, we compared the condition the condition with no distance between the levers with the 30cm condition and the 10cm condition with the 30cm. Then we compared the condition with no gain change with the 2x gain condition and the conditions with gain 0.5x and 2x.

Finally, we compared the coefficients A and V for each comparison. Given our hypothesis, we expected the coefficients to be in a direct relationship so that the greater the relative attenuation between two conditions, the greater the relative difference in matching force trial-to-trial variability.

The following plots represents the results from the three analyzed studies (Figures 4-12)

- Study 1: comparison between self and joystick conditions in healthy controls and patients with schizophrenia (Shergill et al., 2005).

Healthy controls:
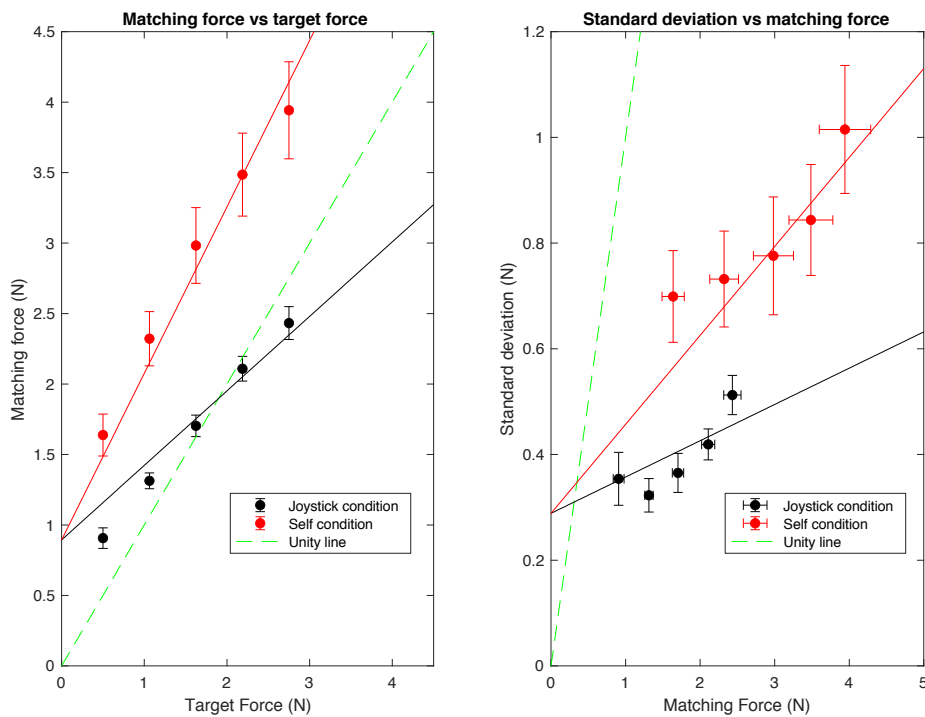
Figure 4 Study 1, healthy controls. Left: matching force in joystick (black) and self-condition (red) as a function of the target force. Right: trial-to-trial standard deviation as a function of the matching force in joystick (black) and self-condition (red). Error bars show standard error.

Fixed effects:	Variability and matching force:			Fixed effects:	Matching force and target Force:		
	Estimate	Std. Error	t value		Estimate	Std. Error	t value
β_1	0.28869	0.04888	5.906	β_2	0.89410	0.10163	8.797
γ_1	0.06866	0.02250	3.051	α_1	0.52864	0.05975	8.848
γ_2	0.09967	0.01985	5.021	α_2	0.65272	0.12775	5.109

Patients with schizophrenia
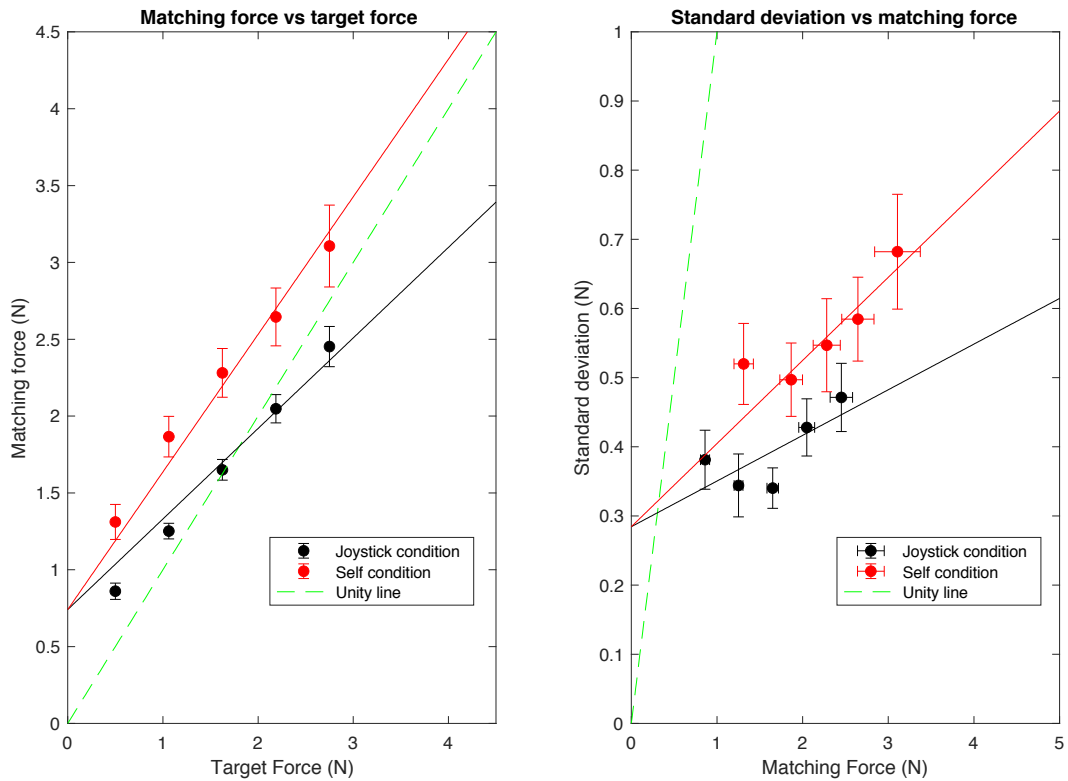
Figure 5 Study 1, patients with schizophrenia. Left: matching force in joystick (black) and self-condition (red) as a function of the target force. Right: trial-to-trial standard deviation as a function of the matching force in joystick (black) and self-condition (red). Error bars show standard error.

Fixed effects:	Variability and matching force:			Fixed effects:	Matching force and target Force:		
	Estimate	Std. Error	t value		Estimate	Std. Error	t value
β_1	0.28452	0.04433	6.418	β_2	0.74134	0.05463	13.571
γ_1	0.06601	0.02457	2.686	α_1	0.58911	0.04921	11.970
γ_2	0.05420	0.01521	3.563	α_2	0.30610	0.08268	3.702

- Study 2: comparison between condition 0cm and 30cm and between 10cm and 30cm and comparison between condition gain 1x and 0.5x (Bays & Wolpert, 2007a)

Spatial separation: comparison between condition 0 cm and condition 30 cm
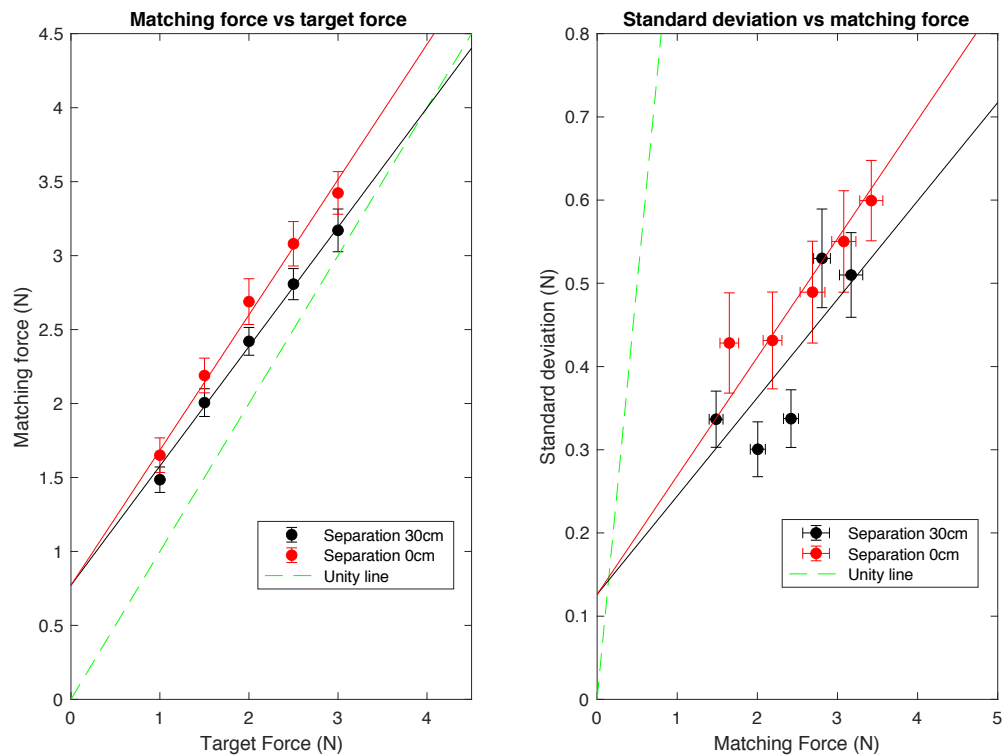
Figure 6 Study 2. Comparison between spatial separation between the levers 30cm (black) and 0cm (red). Left: matching force as a function of the target force. Right: trial-to-trial standard deviation as a function of the matching force. Error bars show standard error.

Fixed effects:	Variability and matching force:			Fixed effects:	Matching force and target Force:		
	Estimate	Std. Error	t value		Estimate	Std. Error	t value
β_1	0.12613	0.06468	1.950	β_2	0.77079	0.12085	6.378
γ_1	0.11822	0.03118	3.792	α_1	0.80695	0.05633	14.325
γ_2	0.02430	0.01420	1.712	α_2	0.10738	0.04114	2.610

Spatial separation: comparison between condition 0 cm and condition 10 cm
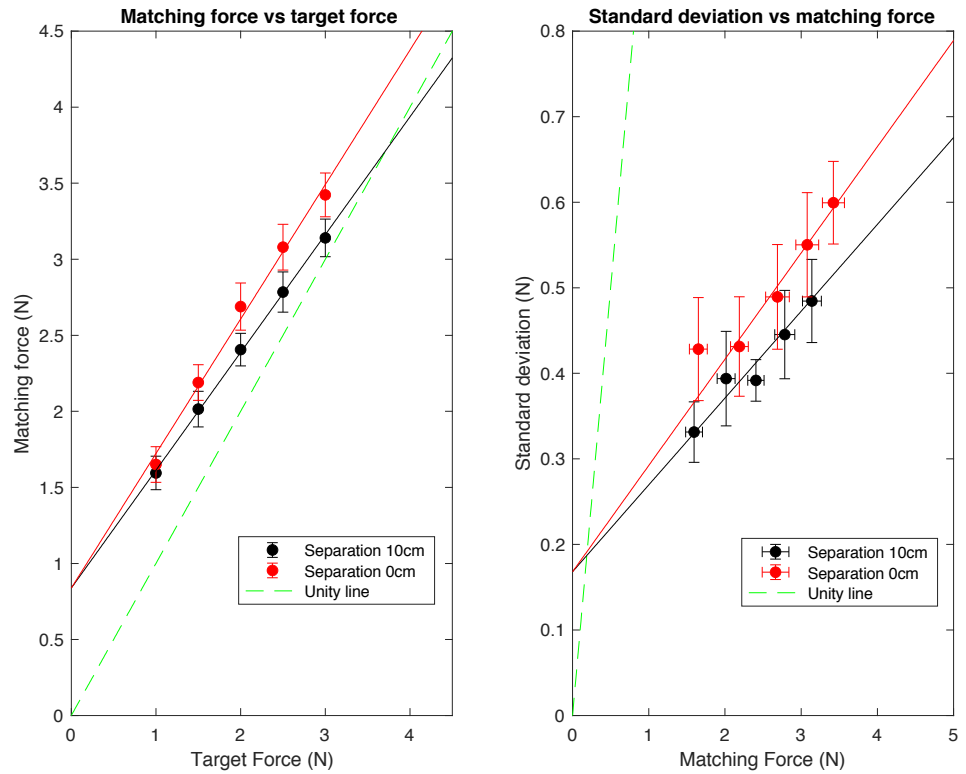
Figure 7 Study 2. Comparison between spatial separation between the levers 10cm (black) and 0cm (red). Left: matching force as a function of the target force. Right: trial-to-trial standard deviation as a function of the matching force. Error bars show standard error.

Fixed effects:	Variability and matching force:			Fixed effects:	Matching force and target Force:		
	Estimate	Std. Error	t value		Estimate	Std. Error	t value
β_1	0.16805	0.07282	2.308	β_2	0.83806	0.13202	6.348
γ_1	0.10152	0.03309	3.068	α_1	0.77469	0.05819	13.314
γ_2	0.02271	0.01473	1.542	α_2	0.10974	0.03910	2.807

Comparison between different gains: 1x and 2x
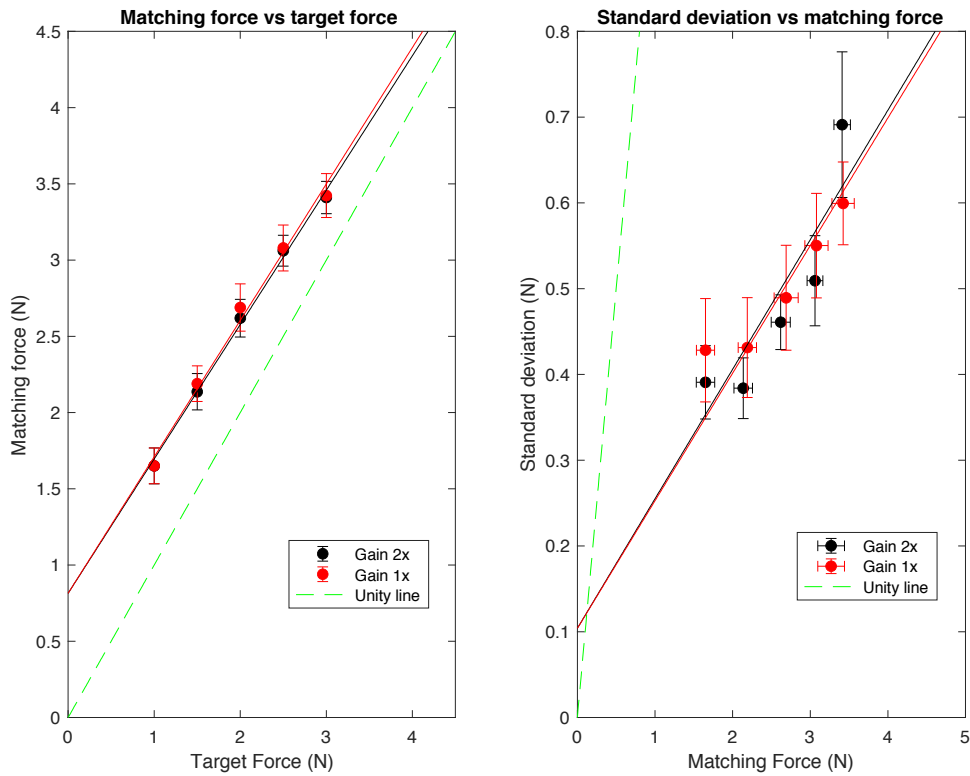
Figure 8 Study 2: comparison between different gains: 1x (red) and 2x (black). Left: matching force as a function of the target force. Right: trial-to-trial standard deviation as a function of the matching force. Error bars show standard error.

Fixed effects:	Variability and matching force:			Fixed effects:	Matching force and target Force:		
	Estimate	Std. Error	t value		Estimate	Std. Error	t value
β_1	0.104003	0.047943	2.169	β_2	0.81488	0.14947	5.452
γ_1	0.151031	0.022023	6.858	α_1	0.88128	0.06154	14.320
γ_2	-0.002263	0.018470	-0.123	α_2	0.01345	0.03856	0.349

Comparison between different gains: 1x and 0.5x
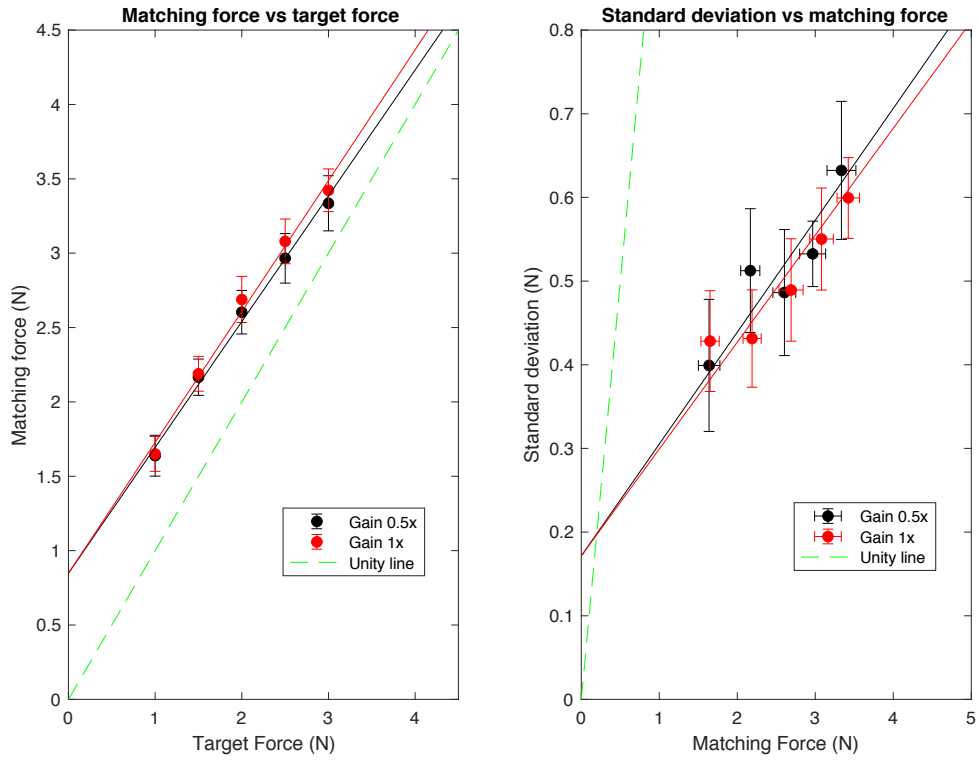
Figure 9 Study 2: comparison between different gains: 1x (red) and 0.5x (black). Left: matching force as a function of the target force. Right: trial-to-trial standard deviation as a function of the matching force. Error bars show standard error.

Fixed effects:	Variability and matching force:			Fixed effects:	Matching force and target Force:		
	Estimate	Std. Error	t value		Estimate	Std. Error	t value
β_1	0.171580	0.064614	2.655	β_2	0.84854	0.15555	5.455
γ_1	0.133734	0.026473	5.052	α_1	0.84580	0.08587	9.850
γ_2	-0.005948	0.014553	-0.409	α_2	0.03398	0.04353	0.780

- Study 3: comparison between self and joystick conditions in young subjects (18-39 years old), middle-age subjects (40-65 years old), older subjects (65+ years old) (Wolpe et al., 2016).

Young subjects:
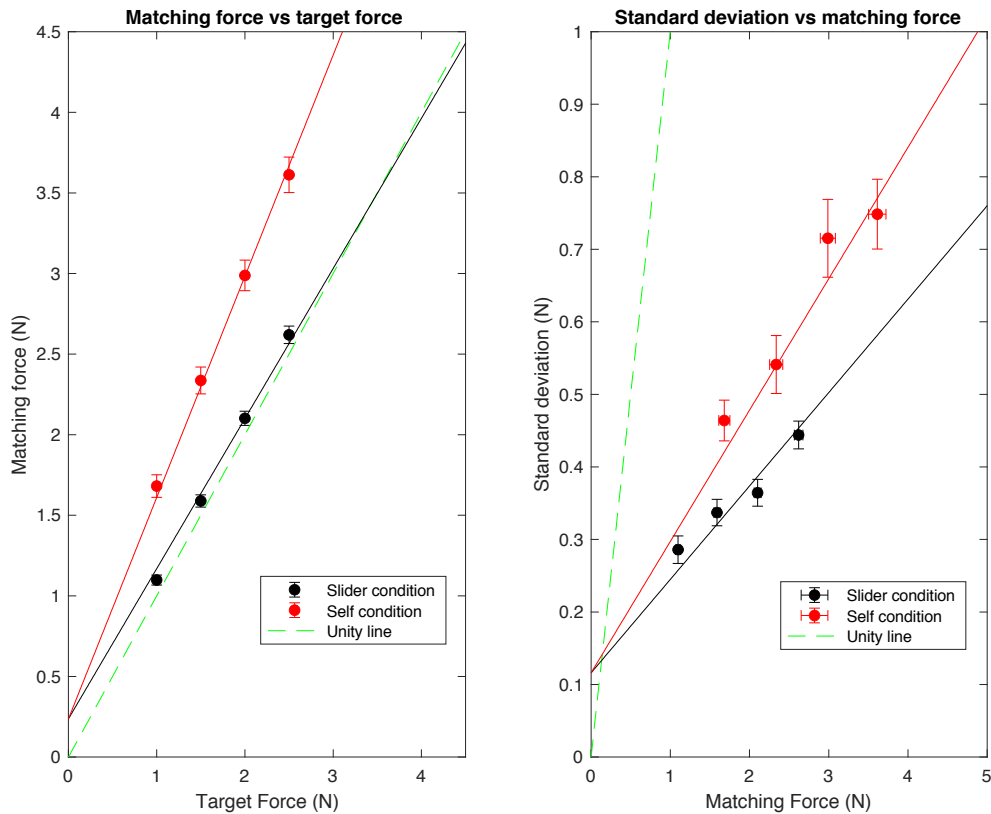
Figure 10 Study 3, young subjects. Left: matching force in slider (black) and self condition (red) as a function of the target force. Right: trial-to-trial standard deviation as a function of the matching force in slider (black) and self condition (red). Error bars show standard error.

Fixed effects:	Variability and matching force:			Fixed effects:	Matching force and target Force:		
	Estimate	Std. Error	t value		Estimate	Std. Error	t value
β_1	0.116036	0.022679	5.116	β_2	0.23727	0.05367	4.420
γ_1	0.128828	0.012835	10.037	α_1	0.93133	0.03298	28.240
γ_2	0.052319	0.008866	5.901	α_2	0.44139	0.04889	9.027

Middle-age subjects:
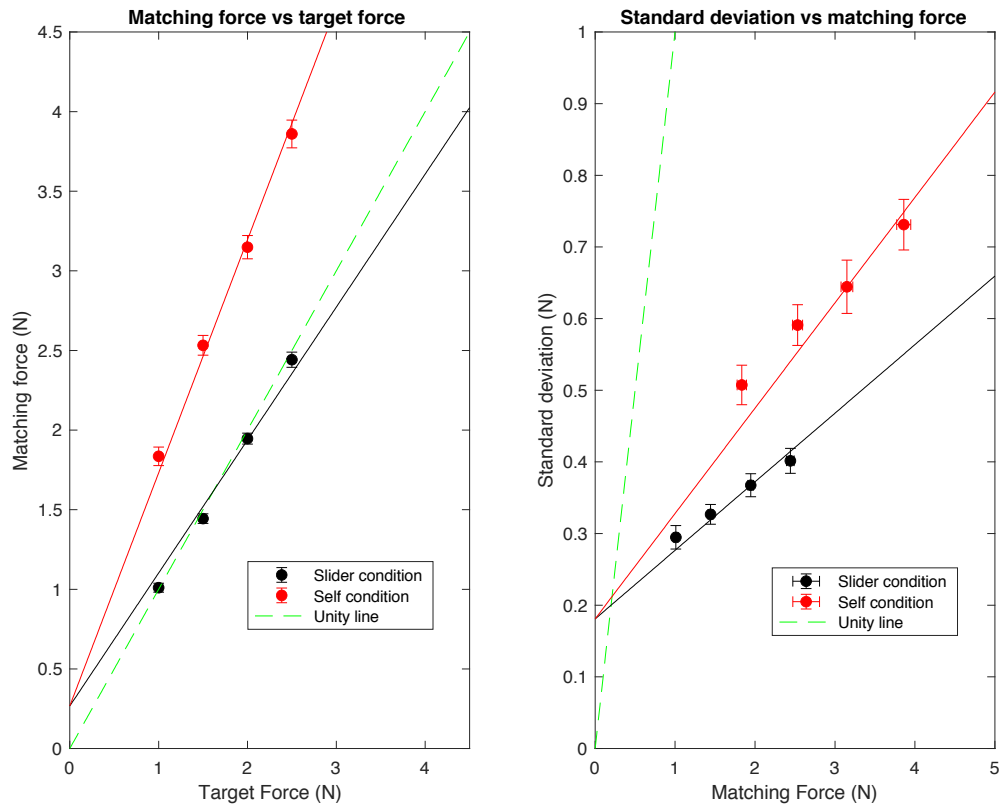
Figure 11 Study 3, middle-age subjects. Left: matching force in slider (black) and self-condition (red) as a function of the target force. Right: trial-to-trial standard deviation as a function of the matching force in slider (black) and self-condition (red). Error bars show standard error.

Fixed effects:	Variability and matching force:			Fixed effects:	Matching force and target Force:		
	Estimate	Std. Error	t value		Estimate	Std. Error	t value
β_1	0.180898	0.017473	10.353	β_2	0.26733	0.04687	5.703
γ_1	0.095702	0.011565	8.275	α_1	0.83498	0.02976	28.057
γ_2	0.051364	0.007909	6.494	α_2	0.62878	0.03989	15.763

Older subjects:
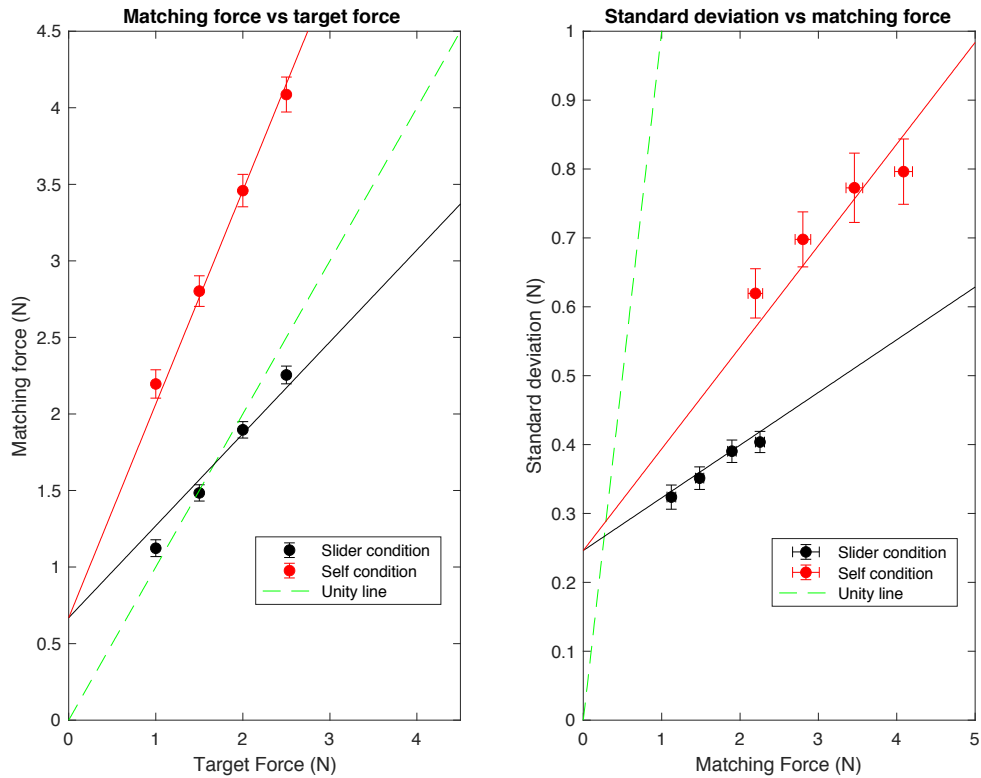
Figure 12 Study 3, older subjects. Left: matching force in slider (black) and self-condition (red) as a function of the target force. Right: trial-to-trial standard deviation as a function of the matching force in slider (black) and self-condition (red). Error bars show standard error.

Fixed effects:	Variability and matching force:			Fixed effects:	Matching force and target Force:		
	Estimate	Std. Error	t value		Estimate	Std. Error	t value
β_1	0.24629	0.02640	9.329	β_2	0.66896	0.09784	6.837
γ_1	0.07647	0.01457	5.249	α_1	0.60064	0.04543	13.221
γ_2	0.07102	0.01282	5.540	α_2	0.79433	0.04953	16.037

Then we compared the *V* and *A* coefficients for each comparison (Table 1) finding a direct relationship as showed in Figure 13.

Table 1 Attenuation factor and excess in variability for each comparison

Comparison	Attenuation factor	Excess in variability
Study 1 - healthy	2.235	2.452
Study 1 - patients	1.52	1.821
Study 2 - separation 30-0 cm	1.133	1.206
Study 2 - separation 10-0 cm	1.142	1.224
Study 2 - gain 2x-1x	1.015	0.985
Study 2 - gain 0.5x-1x	1.04	0.956
Study 3 - young	1.474	1.406
Study 3 - middle-aged	1.753	1.521
Study 3 - Elderly	2.322	1.929
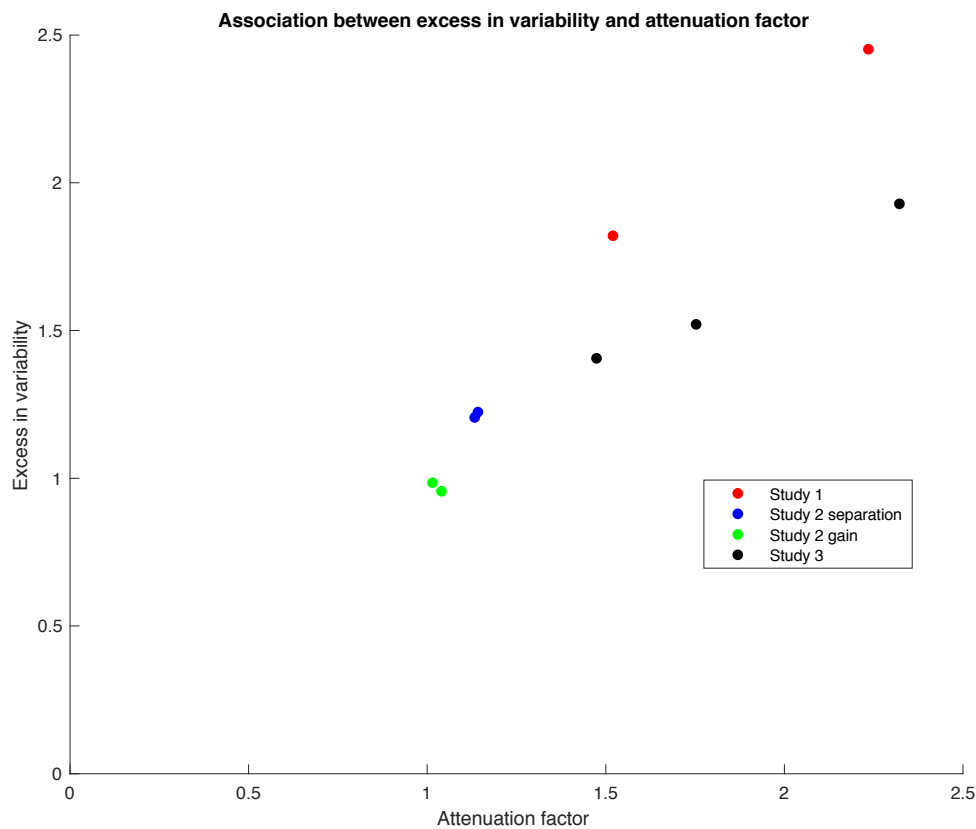
Figure 13 Association between the excess in variability and attenuation factor in different comparisons

The association between V and A was statistically significant with a Pearson's correlation coefficient $R^2=0.8$ ($p<0.001$).

Aim 2: to model the subjects' behavioral responses in different force matching tasks

In the second part of this project we modeled the subject's performance across the force matching tasks of the included studies. At a single-subject level we modeled the mean matching force in the self-condition for each target force level as a function of the mean matching force in the joystick condition. The first study on this kind of task (Shergill et al., 2003) suggested that between the matching force in the two conditions there was a linear relationship so that when plotting the mean matching force and the target force levels the two conditions were regressed with

lines with different slopes. This suggested that the amount of attenuation was proportional to the target force. In contrast, other analysis showed that plotting the mean matching force in the self-condition and the target force levels, the regression line had an intercept different from 0 but a slope not different from 1, suggesting a fixed level of attenuation irrespective to the target force levels (Bays & Wolpert, 2007a). To distinguish between these hypothesis two models were fitted to the data. The previous analysis showed that when comparing two conditions, the greater the relative attenuation coefficient V, the greater the relative difference in matching force variability A. Therefore, when building the model we assumed that the trial-to-trial matching force variability in the self-condition was greater than the variability in the joystick condition. We modeled the following comparisons: for the Studies 1 and 3 we compared variability between self and joystick conditions. For the Study 2 we firstly compared the direct condition with the 30cm condition (for the sake of simplicity the "direct" conditions will be referred as "self" conditions in the comparisons). Then, we compared the direct condition with the conditions with gain 2x (the direct condition will be referred as the "self" condition). In contrast to the previous analysis, in the Study 3 the data were not grouped for subjects' age given that the analysis was performed at a single-subject level. Given the different behavior of these groups in terms of attenuation levels, the analysis was performed on the three groups separately.

Data analysis

The distribution of the matching force trials allowed us to model the subjects' responses in the joystick condition following a normal distribution. Then, we defined two models that described the matching force in the self-condition depending on the matching force in the joystick condition and on the attenuation factor (also normally distributed). We considered the attenuation factor to be invariant to different target force levels.

Two models were fitted to the data from each subject for all the target force level:

Model 1: $$F_s = K F_j \tag{6}$$

Model 2: $$F_s = K + F_j \tag{7}$$

Where F_s is the mean matching force in the self-condition, K is the attenuation factor, F_j is the mean matching force in the joystick condition for each target force level. According to these models, the standard deviation of F_s could be estimated following the rules of the propagation of uncertainty:

Model 1: $$\sigma_{F_s} = \sqrt{\sigma_k^2 \sigma_{F_j^2} + K^2 \sigma_{F_j^2} + F_j^2 \sigma_k^2} \tag{8}$$

Model 2: $$\sigma_{F_s} = \sqrt{\sigma_k^2 + \sigma_{F_j^2}} \tag{9}$$

The two models were fitted to the data of each subject and had *2 + 2n* free parameters, *n* being the number of target force levels: two parameters referred to the mean and the standard deviation of the attenuation factor (K, σ_K), and two referred to the mean and standard deviation of the matching force in the joystick condition for each target force level (F_j, σ_{Fj}).

Notably, estimating σ_{Fs} in Model 1 we approximated F_s to follow a normal distribution. However, in principle, the product of two normally distributed variables doesn't follow a normal symmetric distribution. Therefore, we fitted a third model (Model 3) to the data that took into account this consideration and described F_s as normally distributed with a skewness different from zero. Following the description of the three moments of the product of two normally distributed variables provided by Sejias-Macìas (Seijas-Macìas & Oliveira, 2012), we were able to estimate the shape α of the skewed distribution of F_s as a function of the mean and standard deviation of the two factors' distributions K and F_j:

Model 3: $$F_s = K F_j \tag{10}$$

$$\sigma_{F_s} = \sqrt{\sigma_k^2 \sigma_{F_j^2} + K^2 \sigma_{F_j^2} + F_j^2 \sigma_k^2} \tag{11}$$

$$\alpha = \sqrt{\dfrac{\pi \cdot \dfrac{\left(6\,\dfrac{\mu_k}{\sigma_k}\,\dfrac{\mu_{F_j}}{\sigma_{F_j}}\right)^{2/3}}{1+\left(\dfrac{\mu_k}{\sigma_k}\right)^2+\left(\dfrac{\mu_{F_j}}{\sigma_{F_j}}\right)^2}}{2\cdot\left(\dfrac{\left(6\,\dfrac{\mu_k}{\sigma_k}\,\dfrac{\mu_{F_j}}{\sigma_{F_j}}\right)^{2/3}}{1+\left(\dfrac{\mu_k}{\sigma_k}\right)^2+\left(\dfrac{\mu_{F_j}}{\sigma_{F_j}}\right)^2}+\left(\dfrac{4-\pi}{2}\right)^{2/3}\right)} \Bigg/ \sqrt{1-\dfrac{\pi \cdot \dfrac{\left(6\,\dfrac{\mu_k}{\sigma_k}\,\dfrac{\mu_{F_j}}{\sigma_{F_j}}\right)^{2/3}}{1+\left(\dfrac{\mu_k}{\sigma_k}\right)^2+\left(\dfrac{\mu_{F_j}}{\sigma_{F_j}}\right)^2}}{2\cdot\left(\dfrac{\left(6\,\dfrac{\mu_k}{\sigma_k}\,\dfrac{\mu_{F_j}}{\sigma_{F_j}}\right)^{2/3}}{1+\left(\dfrac{\mu_k}{\sigma_k}\right)^2+\left(\dfrac{\mu_{F_j}}{\sigma_{F_j}}\right)^2}+\left(\dfrac{4-\pi}{2}\right)^{2/3}\right)}} \tag{12}$$

Where α is the third moment of the F_s distribution, μ_k and μ_{Fj} were the mean of the attenuation factor and the matching force in the joystick condition respectively.

To check the accuracy of the three models we compared the predicted values of the attenuation factor K and the measured attenuation for each subject. For Models 1 and 3 the measured attenuation was computed as the mean ratio between the mean matching force in the self-condition and the mean matching force in the joystick condition for each target force level. In contrast, for Model 2, the measured attenuation was estimated as the mean difference between the mean matching force in the self-condition and the mean matching force in the joystick condition for each target force level. The residuals' distribution was then inspected for each model. Finally, the models' performances were compared using a repeated-measures ANOVA between the single-subjects log-likelihood values for each model.

Results

The results of the three models' performances are reported consequently (Figures 14-18):

- Study 1: comparison between self and joystick conditions in healthy controls and patients with schizophrenia (Shergill et al., 2005).

Healthy subjects:

Figure 14 Healthy controls. Left: measured attenuation as a function of predicted attenuation for each subject, unity line in green. Right: residuals as a function of the predicted attenuation (fitted values). Top: Model 1, middle: model 2, bottom: model 3.

Single-subject log likelihood between-models comparison using repeated-measure ANOVA showed a significant effect of the model:

Within Subjects Effects

Cases	Sum of Squares	df	Mean Square	F	p
Model	201.138	2	100.569	3.378	0.048
Residuals	893.215	30	29.774		

The post-hoc analysis was performed using t-test for paired-samples and the Bonferroni's correction for multiple comparisons showed a significant difference comparing Model 2 and Model 3. Specifically, the analysis suggested that the Model 3 performed significantly better than Model 2, having greater log-likelihood values:

Post Hoc Comparisons - Model

		Mean Difference	SE	t	p bonf
Model 1	Model 2	2.897	1.929	1.502	0.431
	Model 3	-2.096	1.929	-1.086	0.858
Model 2	Model 3	-4.993	1.929	-2.588	0.044

Note. P-value adjusted for comparing a family of 3

Patients with schizophrenia:

Figure 15 Patients with schizophrenia. Left: measured attenuation as a function of predicted attenuation for each subject, unity line in green. Right: residuals as a function of the predicted attenuation (fitted values). Top: Model 1, middle: model 2, bottom: model 3.

Single-subject log likelihood between-models comparison using repeated-measure ANOVA showed no significant effect of the model.

- Study 2: comparison between condition 0cm and 30cm (Bays & Wolpert, 2007a)
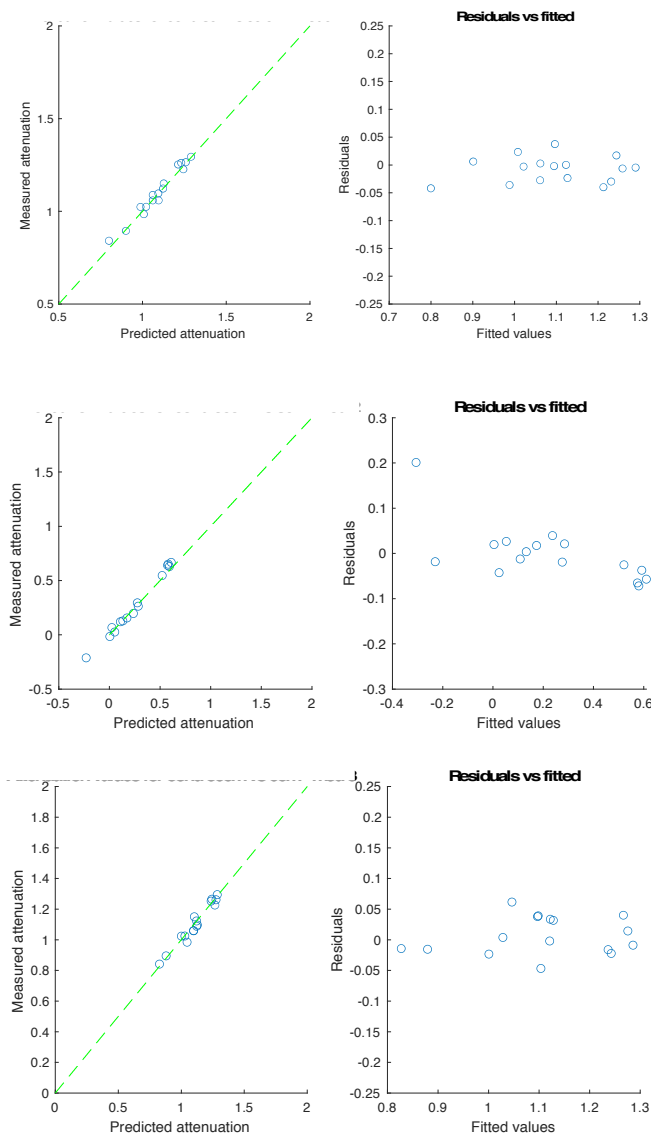
Figure 16 Comparison between levers' separation 30cm and 0cm. Left: measured attenuation as a function of predicted attenuation for each subject, unity line in green. Right: residuals as a function of the predicted attenuation (fitted values). Top: Model 1, middle: model 2, bottom: model 3.

Single-subject log likelihood between-models comparison using repeated-measure ANOVA showed no significant effect of the model.

- Study 2: comparison between condition with gain 1x and 2x (Bays & Wolpert, 2007a)
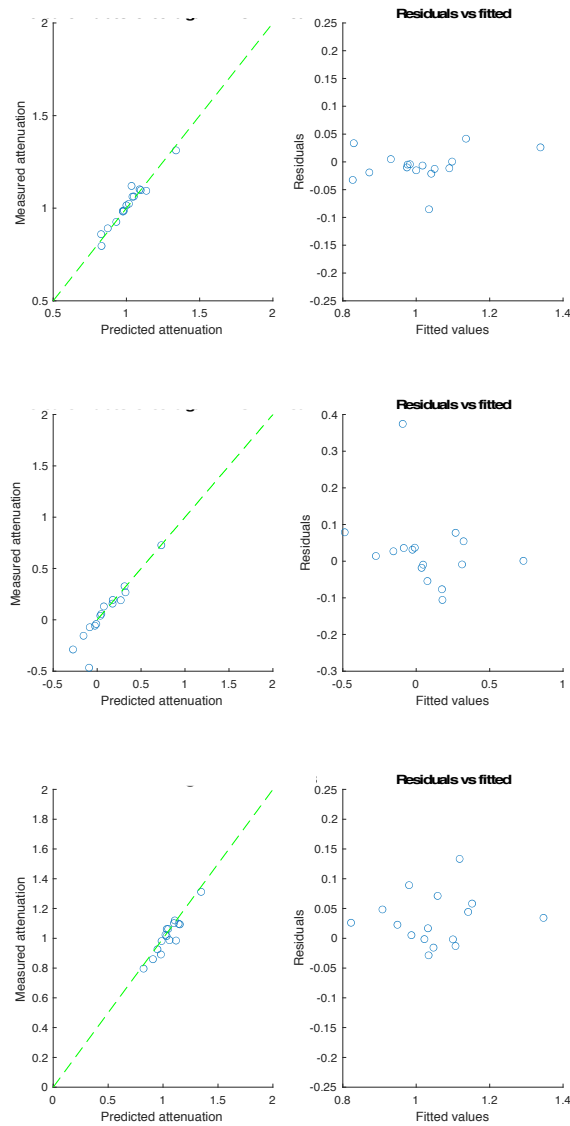
Figure 17 Comparison between gain 2x and 1x. Left: measured attenuation as a function of predicted attenuation for each subject, unity line in green. Right: residuals as a function of the predicted attenuation (fitted values). Top: Model 1, middle: model 2, bottom: model 3.

Single-subject log likelihood between-models comparison using repeated-measure ANOVA showed no significant effect of the model.

- Study 3: comparison between self and joystick conditions in 320 subjects with different ages (Wolpe et al., 2016).

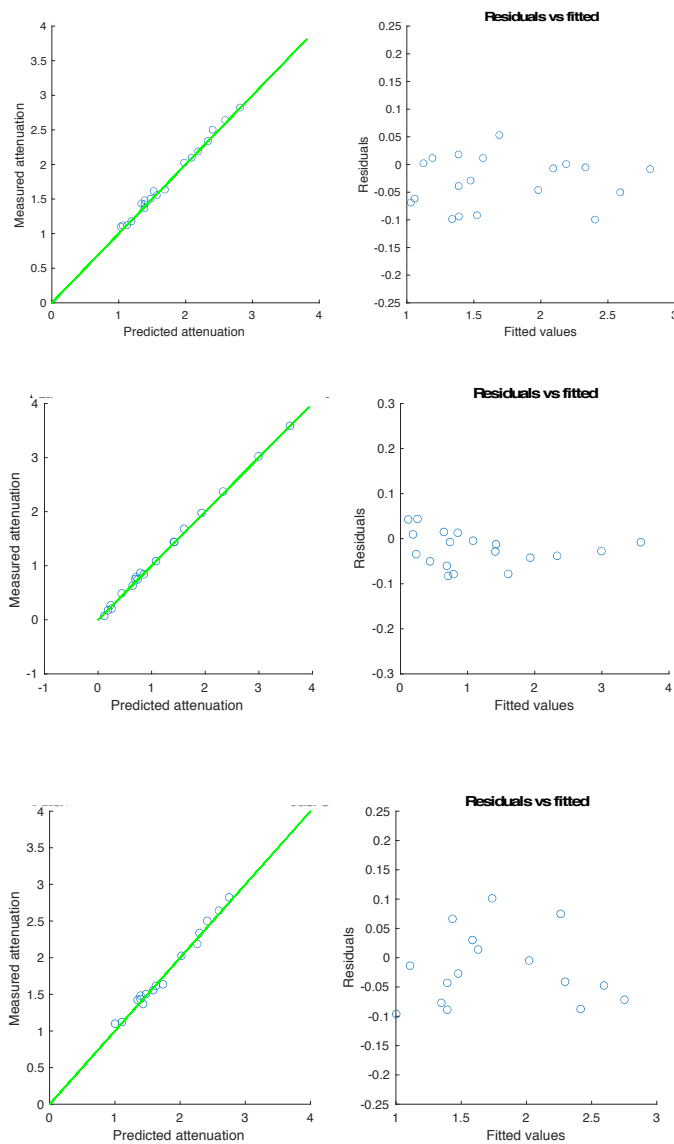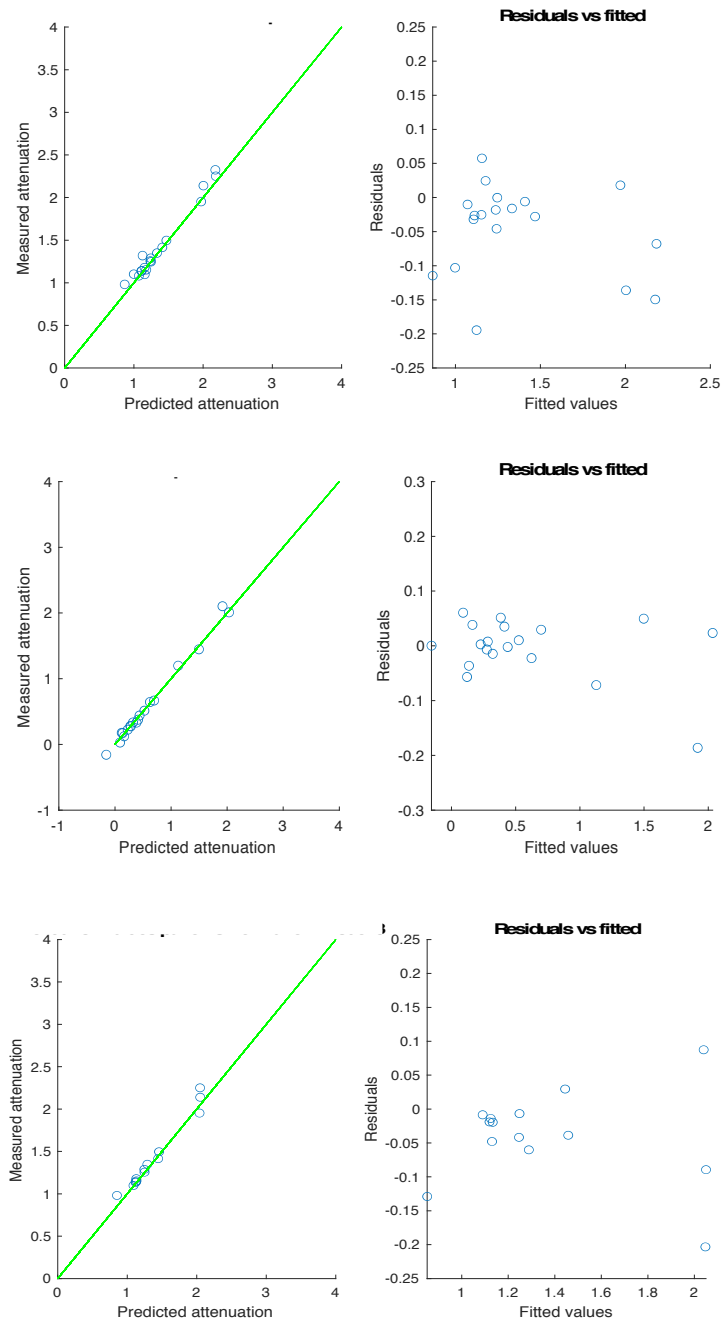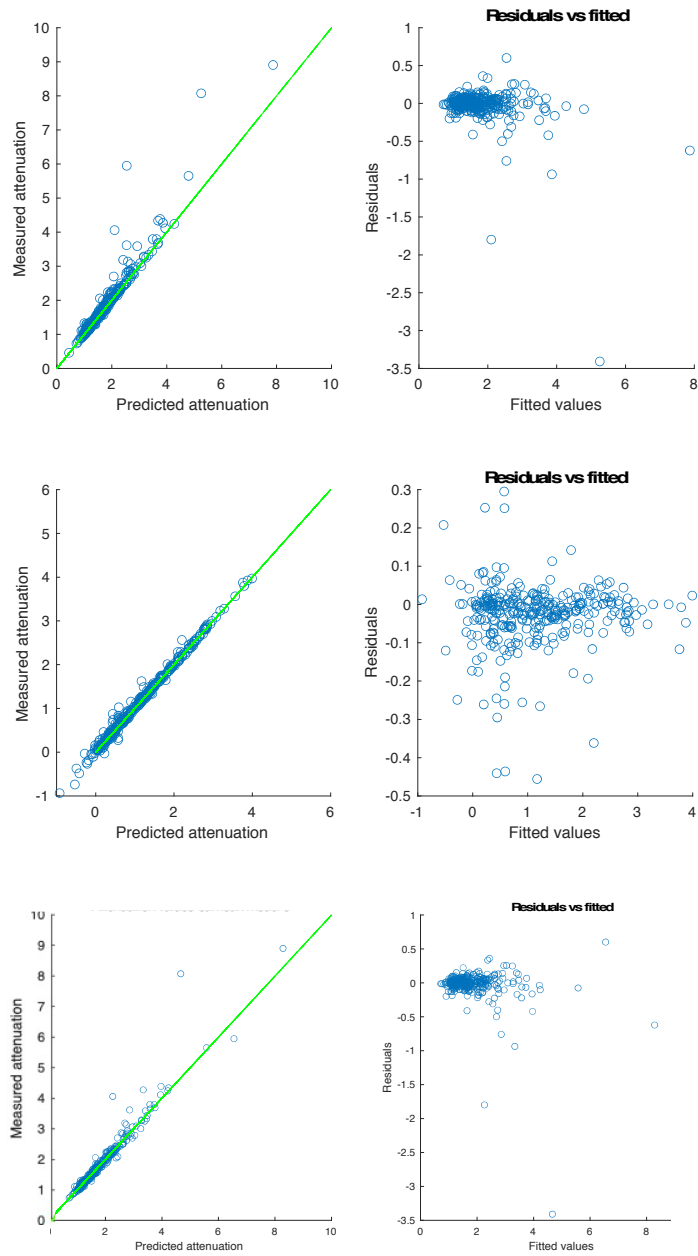Figure 18 Study 3. Left: measured attenuation as a function of predicted attenuation for each subject, unity line in green. Right: residuals as a function of the predicted attenuation (fitted values). Top: Model 1, middle: model 2, bottom: model 3.

Single-subject log likelihood between-models comparison using repeated-measure ANOVA showed a significant effect of the model:

Within Subjects Effects

Cases	Sum of Squares	df	Mean Square	F	p
Model	1257.840	2	628.920	43.559	< .001
Residuals	9009.552	624	14.438		

The post-hoc analysis was performed using t-test for paired-samples and the Bonferroni's correction for multiple comparisons showed a significant difference comparing Model 3 to both Model 1 and 2. Specifically, the analysis suggested that the Model 3 outperformed the other models, having greater log-likelihood values:

Post Hoc Comparisons - Model

		Mean Difference	SE	t	p_{holm}
Model 1	Model2	0.651	0.304	2.144	0.032
	Model 3	-2.064	0.304	-6.795	< .001
Model 2	Model 3	-2.715	0.304	-8.939	< .001

Note. P-value adjusted for comparing a family of 3

Lastly, for data from the Study 3, we analyzed the relationship between the attenuation coefficients K and subjects' age (Figure 19). This analysis aimed to corroborate the findings of the original study that suggested an increased level of attenuation with increased age (Wolpe et al., 2016). A linear regression was performed with the attenuation coefficient K as the dependent variable and the age as the independent variable. Seven subjects were excluded from this analysis after inspecting the residuals' distribution.
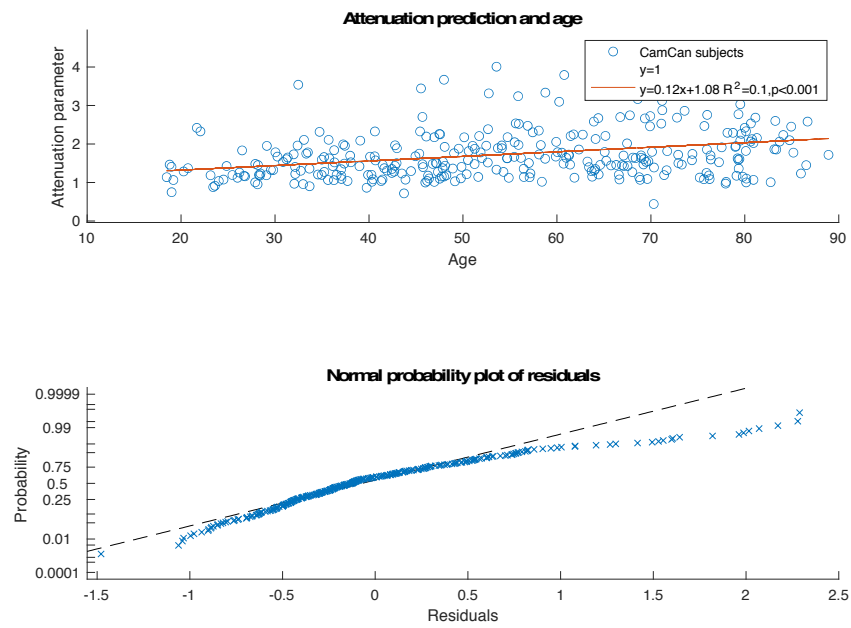
Figure 19 Top: Study 3, attenuation parameters and subjects' age. Bottom: normal probability plot of residuals for attenuation parameters and subjects' age.

The linear regression showed a weak but significant positive correlation between attenuation factor and subjects' age (R=0.32 p<0.001).

Discussion

This project aimed to analyze the within-subject trial-to-trial variability in force matching tasks in order to test the forward model hypothesis within the framework of the sensory attenuation phenomenon. Our results showed that when comparing two conditions in a force matching task, the relative level of attenuation was directly associated with the relative trial-to-trial variability. These results supported the idea that a forward model plays a key role in the SA phenomenon. According to this hypothesis, when performing a voluntary action, a copy of the motor command is sent to a forward model that predicts the tactile sensory feedback that the action performance would generate. As the movement is then executed, the comparison between the actual and the predicted tactile sensory feedback would lead to the attenuation of the predicted part of the feedback.

Recent studies argued against the forward model hypothesis (Press et al., 2020; Roussel et al., 2013; Thomas et al., 2020; Yon et al., 2020). Authors claimed that their suggestion is based on the vast literature on Bayesian inference theory of perception. According to this theory, the CNS combine the sensory feedback with prior knowledge about the probability of a certain state of the body to be realistic in a specific situation (Körding & Wolpert, 2004; Mcnamee & Wolpert, 2019). As a result, the subject's perception is biased to his/her prior and the strength of this bias depends on the stimulus' noise: the noisier the stimulus, the greater the bias. Previous studies showed that the CNS uses the Bayesian inference in a variety of behavioral tasks involving the UL including pointing to a target, and force estimation (Körding et al., 2004; Körding & Wolpert, 2004; Tassinari et al., 2006). This evidence was then interpreted in the recent literature leading to the idea that the expectation of a sensory stimulus enhances its perception rather than suppress it (Press et al., 2020). Moreover, this was considered incompatible with the SA phenomenon according to which the expected stimulus should be attenuated. A series of experiments aimed to corroborate this hypothesis. Yon et al. tested healthy subjects in a task where human participants were required to execute either index or little finger abductions while observing an avatar hand on a screen (Yon et al., 2018). The avatar hand performed finger abduction simultaneously to subjects'

movement in two conditions: congruent (same finger) or incongruent (different finger). Participants were asked to judge about which avatar's hand finger moved. Authors found superior accuracy in those trials when the avatar's and subjects' hand moved the same finger. In another recent preprint paper, authors modified the paradigm widely used in SA experiments of Shergill (Shergill et al., 2003) to test subject's perception of force intensity in different conditions (Thomas et al., 2020). In the first experiment subjects were asked to compare the intensity of two taps on their left index finger. The first one was delivered in two conditions: either triggered by a downward movement of their right index or delivered while resting. The first condition was further divided in two subconditions according to whether subject, during their right index downward movement, touched a sensor or their movement was recorded using a motion tracker. In this experiment authors found that the touch of the sensor was crucial in order to find attenuation comparing the active and the resting conditions. In a second experiment subjects were trained to expect a tap on the left index or middle finger if they moved downward or upward the right index respectively. After the training subjects underwent the experimental session in which a third of the trails did not respect the association experienced during the training, provided the subjects with a tap on the unexpected finger. In this experiment also, subjects were asked to compare the intensity this test tap with a comparison tap delivered subsequently. The results suggested that subjects perceived (relatively to the comparison tap) the tap in the expected condition as more intense compared to the unexpected condition, apparently in contrast to what previously found in similar experiments (Thomas et al., 2020). Taking together these recent studies, the authors proposed that the previous findings on sensory tactile attenuation in force matching tasks (Bays et al., 2005, 2006; Bays & Wolpert, 2007a; Shergill et al., 2003, 2005, 2013, 2014; Wolpe et al., 2016, 2018) were to be meant as the results of a general unpredictive gating mechanism and that the measured attenuation was triggered by the tactile sensation on the active finger (right index finger) rather than being the effect of a predictive cancellation (Press et al., 2020). However, a careful look at these recent experiments that tried to confute the forward model hypothesis suggests that their findings are not necessarily in contrast with the SA literature. The prediction of the action's sensory

consequences requires an internal model of that specific behavior, and therefore the association between movement and sensory feedback needs to have been experienced dozens (if not hundreds) of times throughout the subject's life. In contrast, the association, for example, between moving upward the right index finger and expecting a tap in the left index placed below it like in the study of Thomas et al. (Thomas et al., 2020), does not occur often in natural environment. In that context subjects did learn to expect a tap on their left index, but that learning may have relied on more general prediction mechanism that does not necessary involve a forward model, as suggested in a recent review on this topic (Dogge et al., 2019). Following this interpretation, when subjects moved upward their finger, a forward model may have predicted the proprioceptive feedback directly related to that movement but not the tapping on the left index finger. For this reason, it is not surprising that the authors did not find any attenuation of perception in that task. In another of these studies the authors investigated the subjects' accuracy of detecting a finger movement in an avatar's hand following their hand's movement (Yon et al., 2018). In this case as well, following the previous reasoning, it can be argued that the visual detection of a movement does not rely on a predictive process involving a forward model. Finally, in some of these studies subjects were observing avatar's hands moving while recent literature suggested that somatosensory attenuation does not occur in action observation (Kilteni et al., 2021).

In the present study, we aimed to provide further evidence for the predictive nature of the SA phenomenon. The underlying idea of our project was that the amount of attenuation depends on the accurateness of the prediction: the more it is accurate, the more the perception is attenuated. Notably, the accuracy of the prediction is herein to be intended in terms of spatial and temporal coherence rather than intensity. A variable level of attenuation and the neural process that implements the comparison between the predicted and the actual sensory signals would generate additional noise to the sensory feedback. This sensory noise would lead to an additional variability in reproducing that force in a force matching task. Moreover, this process would occur only in the conditions where attenuation is found. In

contrast, if there isn't any predictive mechanism involved in this process, no additional noise would be generated. We compared the level of relative attenuation and the trial-to-trial variability between two conditions in different force matching tasks. We found that the levels of relative attenuation were positively associated with the relative variability in reproducing the force perceived. This finding is consistent across different settings and different comparisons and provides evidence for an anticipatory mechanism responsible for the sensory attenuation phenomenon.

Previous studies attempted to quantify the amount of attenuation in force matching tasks. Some studies suggested that the amount of attenuation was proportional to the matching force intensity (Shergill et al., 2003, 2005), while later metanalysis claimed that perception of the tactile sensation was attenuated by a fixed amount irrespective to the matching force magnitude (Bays & Wolpert, 2007a). To solve this partial disagreement, we modeled the subjects' behavior in different force matching tasks that included the comparison of two conditions: one in which attenuation was found (self-condition) and one in which it wasn't (joystick/slider condition). The model that better captured the single subject' performance assumed a direct proportionality between the matching force in the self and external conditions and their ratio being the attenuation level. This model outperformed the alternative model where a constant difference between the matching forces in the two conditions was hypothesized. Notably, for the sake of simplicity, we have been referring to the compared conditions as self or joystick. However, this model captured the subjects' behavior also comparing conditions where no relative attenuation was found like in the experiment from the work from Bays and Wolpert (Bays & Wolpert, 2007a).

The physiological meaning of the SA phenomenon represents a challenging question. Previous studies suggested that the attenuation of the predictive part of sensory feedback has the scope of enhancing the salience of unexpected external stimuli (Bays & Wolpert, 2007a). Other studies highlighted the importance of such mechanism in discriminating between self-generated and externally generated

stimuli contributing to the sense of agency (Macerollo et al., 2015, 2016; Pareés et al., 2014). Our findings don't provide further evidence on the physiological purpose of the SA phenomenon. However, considering the remarkable amount of literature on this topic, some considerations can be made. Firstly, it is noteworthy that, according to our results, the comparison between the actual and predicted feedback, along with its attenuation, corrupt the sensory information with additional noise. So one could ask why the CNS should attenuate the perception of a predicted tactile stimulus. From a practical perspective, as it has previously suggested, the attenuation of the predicted part of the sensory feedback can have the final effect of enhancing the unexpected stimuli, which are the most informative part of somatosensory signals during the movement (Bays & Wolpert, 2007a). For example, during an object's manipulation the increase of a tactile stimulus' intensity can be caused either by a change in the object's shape, such as a protuberance, or by the increase of pression that we generate on it with our holding. The attenuation of the tactile sensation in the latter situation could be useful for distinguishing between the former and the latter situations, ultimately improving our knowledge on the object's shape. Moreover, imaging studies suggested that the inhibition of the activity of SII, may be associated with the phenomenon of SA. From an efficiency perspective, it could be useful for the CNS to allocate less resources for the coding of tactile perception that could be predicted. Therefore, the SA could be considered a mechanism by which the CNS optimize its activity allocating more resources to the coding of the unexpected stimuli.

To conclude, our analysis provided further evidence supporting the forward model hypothesis for the prediction of the sensory input arising from voluntary actions. These findings are in line with a recent work of Kilteni et al. that demonstrated that SA and general unpredictive gating mechanism are different and independent phenomena (Kilteni & Ehrsson, 2020), in contrast to recent literature that argued against this idea (Press et al., 2020). The study of this predictive mechanism is crucial not only for improving our understanding of the somatosensory perception in healthy individuals, but also to shed new lights on predictive motor control dysfunctions that can affect subjects with CNS lesions.

Bimanual object lifting

Predictive estimation of the consequences of upper limb's movements is essential for performing the rapid and precise movements commonly observed in object manipulation. Along with the consequences of the voluntary movement on our own upper limb, when dealing with an object the CNS must take into account the properties of the object itself. These properties include weight, surface grip, mass distribution, temperature, material, and generally all the tactile sensations that would arise after the touch. The lift of an object is indeed a complex action that involves both the control of the upper limb and the hand-object interaction. Specifically, when we move an object from position A to position B, we need to modulate the grip force accordingly to the acceleration we apply to prevent the object to slip out. That is the greater the acceleration, the greater the grip force needed. These complex actions are supported by somatosensory feedback that provide the CNS with tactile and proprioceptive information. Cutaneous mechanoreceptors respond to skin deformation and pression, while intrafusal muscle fibers along with joint capsules generate information on dynamic properties related to the UL's kinematics or the object

This behavior has been widely investigated by assessing the anticipatory grip force modulation during the lifting of an object of known properties (Flanagan et al., 2001; R. S. Johansson & Edin, 1993; Y. Li et al., 2011; Nowak et al., 2005). When moving the UL while grasping an object, predictive state estimation was usually associated with an increase of grip force before the UL movement onset. This anticipatory reaction is crucial in order to prevent the object slippage during the movement (Flanagan & Wing, 1997; Frenkel-Toledo et al., 2019). Therefore, it has been suggested that the anticipatory grip force modulation is based on an internal model of prediction of the movement consequences of the voluntary action of the object lifting, possibly representing an indirect measure of a forward model (Flanagan et al., 2001; Nowak et al., 2013). Anticipatory grip force has been investigated in people affected by central nervous system stroke sequelae. Stroke subjects presented delayed grip force onset (Blennerhassett et al., 2008; Hermsdörfer et al., 2003; Nowak et al., 2013) and, likely to compensate for these

deficits, produced exaggerate grip force (Nowak et al., 2013). Interestingly, tactile sensitivity deficits but seemed not to affect timing onset of grip forces (Hermsdörfer et al., 2003).

In contrast to the robust literature body concerning unimanual object lifting, bimanual force modulation in lifting task has not been widely investigated. Moreover, while movement prediction deficits in unimanual load lifting of the affected hand of stroke subjects are relatively well-defined, there is no clear evidence whether the coupling of ULs could improve these deficits or not. Furthermore, the question about the unilateral or bilateral nature of UL forward model is still under debate (Frey et al., 2011).

The present section aimed to investigate the anticipatory behaviour during a bimanual object lifting in people affected by stroke. The secondary aim was to investigate the bimanual force control deficit in coupled tasks in healthy young and elderly subjects. Given the central role of cerebellum and somatosensory areas in the anticipatory grip behaviour, we focused on patients with lesions to these cerebral areas.

Age related changes in bimanual force control

Several common daily activities performed with force and kinematics coupling between two hands, such as holding or moving a large box, or holding a can and simultaneously unscrewing its tap, require bimanual coordination (Krishnan & Jaric, 2010; Swinnen & Wenderoth, 2004). Although in these actions the temporal and spatial coordination between the two hands seems easy and natural, the central nervous system must deal with the complex upper limbs' mechanical properties, share control between arms, and integrate sensory feedback from both sides of the body (Córdova Bulens et al., 2018). Performing bimanual actions involves an extensive network of cortical and subcortical structures, including the primary sensorimotor, premotor, supplementary motor, parietal associative cortices, cerebellum and basal ganglia (Swinnen, 2002). During bimanual actions, the sensorimotor cortices have distinctive activity compared with unimanual tasks (Long et al., 2016; Nair et al., 2003; Serrien et al., 2003) and the corpus callosum has a crucial role in the interaction between the two hemispheres (Long et al., 2016). Neurological diseases such as stroke, Parkinson's disease and multiple sclerosis impact the ability to perform these bimanual actions (Gorniak et al., 2014; Kang and Cauraugh, 2014; Yan et al., 2015; Ballardini et al., 2019b). Also, aging affects bimanual coordination (Maes et al., 2017), both in motion (C.-H. Lin et al., 2014) and force tasks (Y. Jin, Seong, et al., 2019).

Deficits in bimanual force control tasks in older adults could be due both to central factors, as changes in the structures and the physiology of the nervous system (Fjell et al., 2014; Goble et al., 2010) and peripheral aspects, as diminished tactile sensibility and degenerative process of the neuromuscular systems (McNeil, 2005). These changes determine weaker hand-grip strength, higher variability, and lower accuracy in isometric bimanual force matching task (Hu & Newell, 2011; Y. Jin, Seong, et al., 2019; Kubota et al., 2012; C.-H. Lin et al., 2014, 2019), increased reaction time (Fozard et al., 1994), decreased bimanual (Y. Jin, Seong, et al., 2019; C.-H. Lin et al., 2014; Vieluf et al., 2015) and impaired manipulation abilities (Sebastjan et al., 2017), compared to young adults.

Here, we focus on *bimanual isometric force tasks*. The ability to produce bilaterally isometric force has been studied mainly in tasks where subjects are required to produce maximal forces or match constant and time-variant force levels (Kang & Cauraugh, 2014; C.-H. Lin et al., 2019). Most of these studies were limited to hand-grip (Jaric et al., 2005, 2006) or single-digit force (Kang & Cauraugh, 2014; C.-H. Lin et al., 2014; Long et al., 2016; Patel et al., 2019), i.e., tasks where the force is due to distal muscles. Instead, several daily living activities as holding large objects also require the control of proximal muscles, i.e., upper arm and shoulders' muscles. Different muscle districts could significantly determine force control performance in terms of accuracy, variability and bilateral asymmetries. Moreover, in several studies often the two hands are evaluated separately, under the assumption of mutual single-hand independence, while bimanual control is characterized by specific and unique features, including between-hands interaction, that are poorly investigated (Y. Jin, Kim, et al., 2019; Kennedy et al., 2016; Morrison & Newell, 1998; Serrien & Wiesendanger, 2001). Most of the studies where the two hands are evaluated together focused their analysis on the overall performance of both hands (Ferrand & Jaric, 2006; Kang & Cauraugh, 2018), while only a few works investigated the strategies of each hand and their coupling, investigating asymmetries and differences due to the specialization of each hemisphere or to handedness (Hu et al., 2011; X. Jin et al., 2011). Therefore the knowledge about bilateral asymmetry when the hands' performance are evaluated simultaneously is still limited (Takagi et al., 2020).

Force control studies in healthy right-handed subjects, where the hands are tested sequentially or separately, found that the *right-dominant hand* tends to produce more force when matching the force previously produced by the other hand. This behavior was found for hand-grip (Lafargue et al., 2003; Mitchell et al., 2017) and isometric fingers force tasks (Henningsen et al., 1995). The reason for this behavior is that the *right-dominant hand* is usually stronger (Armstrong & Oldham, 1999; Incel et al., 2002), and less noisy in several motor tasks (Kubota et al., 2012). The right hand applied more force than the other hand also in the isometric concurrent tasks proposed by (Davis, 2007), where the force was applied by the fingers, involving distal muscles. However, O'Sullivan et al. (O'Sullivan et al., 2009),

focusing on a bilateral finger force control task, demonstrated that in bimanual tasks where the two hands act concurrently, the control responsibility is shared among the two sides: the brain decides the role of each hand based on its strength and variability. This evidence was confirmed by (Salimpour & Shadmehr, 2014a), investigating a bimanual task in which people chose how much force to produce simultaneously with each arm so that their sum would equal a target. They applied forces toward eight different directions on two quasi-static handles, involving also proximal muscles. The *right-dominant hand* applied more force than the other one only in specific directions, and because it was less noisy, not stronger. If the *right-dominant hand* is generally the strongest, the hand variability, instead, depends on several factors, including the proposed task, the muscles involved, and the population age, leading to different results in lateral asymmetries (K. Li & Wei, 2014). Specifically, with age, the variability in task performance of the dominant right arm tends to increase (Vaillancourt & Newell, 2003). Several studies reported with age a loss of the advantage of this hand (e.g. (Kalisch et al., 2006; Vaillancourt & Newell, 2003)) due to its higher rate of decrease in performance. However, the literature results also provide conflicting or task-dependent evidence reporting an increase in *right-dominant hand* use (Weller & Latimer-Sayer, 1985) or not change (Cabeza, 2001; Hausmann et al., 2003).

The purpose of this study was to investigate task performance, bilateral coordination, and lateral asymmetries in *young* and *elderly healthy right-handed subjects* during *a bimanual isometric force task* requiring an essential contribution of the upper arm and shoulder muscles. Subjects were explicitly asked to simultaneously apply the same amount of isometric force pushing with the palm and fingers on two decoupled plates corresponding to a sensorized object's lateral faces. They were asked to reach, following a time variant-profile, three target forces, corresponding to 8 N, 20 N, 40 N applied by each arm.

The main hypothesis is that since in this task, subjects use three muscle groups - postural stabilizers (abdomen, pelvis and back), muscles supporting the execution of force exertion (shoulder, trunk), and the muscles responsible for the isometric force production (forearm and hand) (Sebastjan et al., 2017) - strategies and

performance in our task will differ from strategies and performance observed in power grip or the application of a force by single fingers: a higher level of proximal muscle recruitment could reflect different motor control strategies than those associated with distal muscle recruitment in fine movements.

Our results showed that older subjects had higher errors and more variable force profiles, and most of them undershoot the highest force level. They also had more asymmetric performance between the two hands, although the hand applying more forces varied across subjects and depended on the target force. Interestingly, for the lower target force when strength was less important, for our subject population the % of force applied by the *left non-dominant hand* correlated with its variability.

Methods

Assessment procedure has been carried out on a cohort of healthy subjects in order to collect normative data. Two groups were compared: sixteen young healthy subjects (YG; age = 24.65±1.32(std) years) and sixteen older subjects (OG; age = 75.25±6.6(std) years). All the subjects were right-hander. The study protocol has been approved by the ethic committee Comitato per l'Approvazione della Ricerca sull' Uomo (CARU) of the Verona University, submission number: 22/2019.

Participants

Thirty-one healthy volunteers participated in our study. The exclusion criteria were the presence of musculoskeletal injuries or any other neurological condition, history of surgery or pain affecting upper limbs, normal or corrected to normal visual and auditory abilities. To be included in the study, subjects had to be right-handed according to the Edinburgh Handedness Inventory (EHI score > 60) (Oldfield, 1971) and between 18 and 30 years old or between 65 and 85 years old. The two ranges corresponded to two different cohorts: sixteen participants (age = 24.65±1.32(std) years, 10 female, Edinburgh Test Score: 89.62±14.28) have been enrolled in the 'younger group' (YG) and the other fifteen (age = 76.66±6.61(std)

years, 7 female, Edinburgh Test Score: 96.66±8.99) in the 'older group' (OG). We verified no statistically significant difference between the two groups in terms of gender (Chi-squared test p=0.15) and hand-dominance (t-test p=0.07).

This study was conformed to the ethical standards of the 1964 Declaration of Helsinki and all the study procedures and documents, including the consent form, were approved by Verona University Institutional Review Board (CARU n. 22/2019). All participants provided written informed consent to participate in the study and publish the results in the de-identified form.

Bisbox device

The device used in this experiment, *Bisbox 2.0,* is a sensorized rectangular box, a new and lighter (0.8 kg) version of the prototype described in (Galofaro et al., 2019). The dimensions of the box were 15×35×25 cm (height × width × depth). The 35 cm length was chosen to match the participants' average inter-shoulder distance, who should hold the device with the two hands placed on the two smaller faces. These smaller faces consisted of a rigid frame connected to the box frame via three load cells (mod. CZL635, Phidgets Inc., Calgary, Canada; full-range scale of 5 kg; precision of 0.05% and linearity of 0.05% FS) for measuring the force applied during the experiment (each plate: overall accuracy after offset calibration ± 0.3N in the range 0-60 N). The sensorized box could be used stand-alone, with a memory card for data recording, or, as in this experiment, connected to a laptop via wireless communication (Wi-Fi network connection through a WIPY 3.0 microcontroller, programming language: Python). The laptop ran the software that controlled the experiment and provided instructions and feedback to the participants on a screen. The user interface was developed in Python 2.7.9 with the open source libraries OpenGl and Pygame. In this experiment, the *Bisbox* was secured to a table with a system that allowed to avoid any movement of the device and to decouple the force applied by the two hands on each of its two lateral plates.

Experimental setup

Participants sat in an armless chair in front of a 24" monitor placed ~ 0.5 m away from the subject's chest. The height of both table and chair was adjustable so that

the forearms rested on the table with shoulders in ~20 deg flexion and elbows at ~110 deg flexion. The hands were positioned fully open on the lateral sides of the device. A schematic representation of the setup is shown in Figure 20 A.

Subjects were asked to keep a cursor on top of the sides of an isosceles trapezoid, displayed on a computer screen (Figure 20 A). The cursor was programmed to move horizontally from left to right with respect to the subject, at the constant speed of 0.85cm/s, regardless of the subjects' actions. The sum of the force applied by the participants' hands on the lateral plates of *Bisbox* controlled the height (i.e., the vertical displacement) of the cursor (1 N = 0.30 cm). When no forces were applied, the center of the cursor was on the lower side of the trapezoid, corresponding to his major base. Each trial consisted of four phases of equal duration (two constant and two time-variant, Figure 20 B):

Phase 1) *Increment phase*, *I*, where the cursor should move upward and rightward along one leg of the trapezoid. In this phase, subjects had to gradually increase the applied force, starting from 0 N and reaching the maximum force level after 3.5s.

Phase 2 & 3) *Holding phases*, H_1 *and* H_2, where the cursor should stay at the same height, moving rightward along the top side, i.e., the minor base of the trapezoid. Thus, subjects had to maintain the same maximum force for 7s. H_1 accounted for the first 3.5 s, and H_2, for the last 3.5s.

Phase 4) *Decrement phase*, D, where the cursor should move downward and rightward along the other leg of the trapezoid. In this phase, subjects had to gradually decrease the force reaching the 0 level in 3.5 seconds.

A trial lasted 14 seconds, and subjects paused for 6 seconds between trials.

In each trial, subjects had to reach with the *sum of the force* applied by the two hands one of the following three maximum force levels presented in random order: low (L=16 N), medium (M=40 N) and high (H=80 N). Three minor bases of the trapezoids corresponding to these three force levels were always displayed in grey on the screen, while for each trial, the sides of the trapezoidal shape to match were highlighted with a white line (thickness 0.8 cm) against a black background. The cursor was a red square of 0.4 cm side length.

The experimental session consisted of 30 trials, i.e., ten trials for each value of the maximal target force. An initial phase of familiarization was provided to explain the task sequence and how to perform it correctly.

Data analysis

The raw force signals from the six load cells were recorded at 50 Hz and filtered using a 4th order low-pass Butterworth filter with a 10 Hz cutoff frequency before computing the performance metrics described in the following paragraph. Indicators were computed for each of the above-mentioned phases and for the entire trial. For each subject, we averaged the values obtained for the same target force.

Bimanual task performance.

We computed three parameters to evaluate the accuracy in controlling the total force applied by the two hands.

- ***Root-Mean-Squared Error (RMSE)*** measures the deviation of the participant's total force output from the target force trajectory (Lodha et al., 2010). Higher values for relative RMSE indicate less accuracy of total force output. It is defined as:

(A) **(B)**
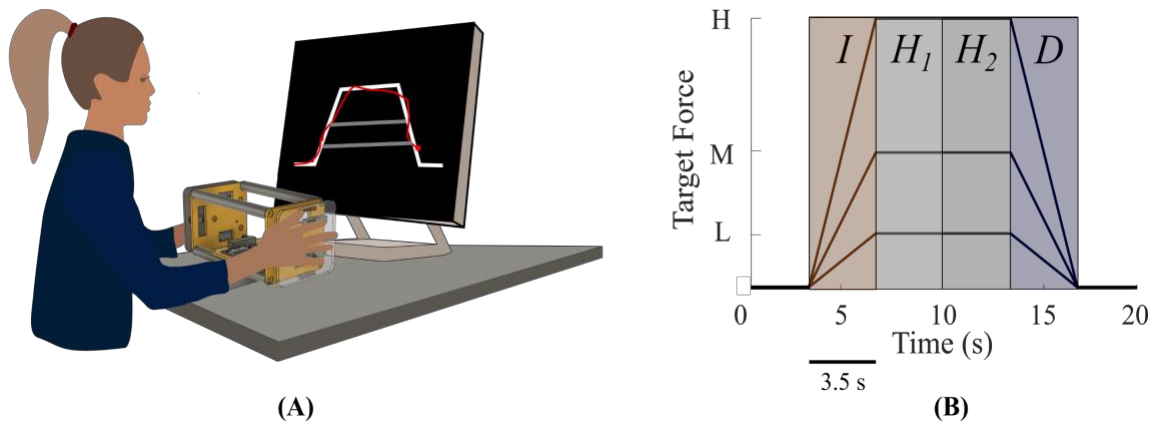
Figure 20 . **(A)** Schematic representation of the setup. Subjects sat on an armless chair and pressed laterally the fixed device (designed with Fusion 360) following the visual cue on the screen (red cursor). All three trajectories (grey lines) were depicted on the screen and for each trial one of these was evidenced (continuous white line). **(B)** Ideal trajectories (L, M and H, evidenced on y-axis) that subjects had to follow. All the phases are evidenced by shaded areas: increasing phase (I, orange), holding phase 1 (H$_1$, light grey), holding phase 2 (H$_2$, dark grey) and decreasing phase (D, blue).

$$RMSE = \sqrt{\frac{1}{N}\sum_{i=1}^{N}(F_{Mi} - F_{Di})^2} \qquad (13)$$

where F_{Mi} is the *measured* total force at the sample *i* and F_{Di} the corresponding *desired* force. N is the total number of samples considered either on a single phase or on the entire trial.

- ***Bias Error (BE)***, the systematic component of the error, computed as the signed difference between the participant's total force output and the target force:

$$BE = \frac{1}{N}\sum_{i=1}^{N}(F_{Mi} - F_{Di}) \qquad (14)$$

Positive values indicate an overshoot of the target force, negative values an undershoot (Schmidt et al., 1988; Marini et al., 2016; Ballardini et al., 2019a).

- ***Coefficient of Variation (CV)***, *a measure of* force variability (standard deviation) of the total force expressed as a percentage of the mean force output (Galganski et al., 1993):

$$CV(\%) = \frac{std\left(detrend(F_M)\right)}{|mean\ (F_M)|} * 100 \qquad (15)$$

Where F_M is the vector of the samples from force trajectory in each phase. We computed the standard deviation (std) of this signal after removing the best straight-fit line from the data (least-squares method, *Matlab* function detrend).

Differences between the force applied by each hand.

To determine the difference between the two hands while performing the bimanual task, we computed:

82

- **Symmetry Index (SI)**, a measure of force symmetry between the two hands, computed as follow:

$$SI = \frac{1}{N}\sum_{i=1}^{N}\left(1 - \frac{|F_{MLi} - F_{MRi}|}{F_{Mi}}\right) * 100 \qquad (16)$$

when the contribution % of the *right-dominant* (F_{MR}) and *left-non dominant* (F_{ML}) hands are equal, the symmetry index is 100, 0 instead indicated that the total force F_M is completely due only to one of the two hands. To remove contributions of noise, we computed this indicator on the average force profile (averaged over the 10 trial repetitions with equal target force) of each hand.

- **Left Hand Force (LHF).** This parameter indicated what % of the total force output (F_M) was applied by the *left – non dominant* hand (F_{ML})(Lodha et al., 2012):

$$SI = \frac{1}{N}\sum_{i=1}^{N}\left(1 - \frac{|F_{MLi} - F_{MRi}|}{F_{Mi}}\right) * 100 \qquad (17)$$

- **Correlation** between **right-dominant** and **left-non dominant** hand. To estimates the coordination between the two hands, we evaluated the temporal correlation between left (F_{ML})- and right-hand force (F_{MR}) outputs within each trial by cross-correlating the forces applied by the two hands:

$$R_{xy}(\tau) = \int_{-\infty}^{\infty} F_{ML}{}^{*}(t)F_{MR}(t + \tau)\,d\tau \qquad (18)$$

(* denotes complex conjugation) and we computed the maximum correlation Correlation $= \max_{\tau} R_{xy}(\tau)$ and the **Time Delay** between the two signals Lag$= \max_{\tau} R_{xy}(\tau)$.

- CV_H. This parameter assesses the force variation of each hand by considering, instead of the total force F_H, the force produced by each hand (H = L (*left-non dominant*) or R (*right-dominant*)). This outcome is similar to the CV (Equation 15) but defined for each hand force F_{MH} instead of the total one:

$$CV_H(\%) = \frac{std\ (detrend(F_H))}{|mean(F_H)|} * 100 \qquad (19)$$

To further understand these results, we modelled the relationship between the parameter LHF and the parameter CV_L by mean of simple linear regression.

Statistical analysis

Normality was assessed by the Kolmogorov-Smirnov test, and sphericity condition for repeated measures ANOVA was assessed by the Mauchly test. These conditions were always verified. For all indicators, we performed a repeated-measures ANOVA (rANOVA) with one between-subjects factor: *'Group'* (2 levels: YG and OG) and two within-subjects factors: *'Target Force'* (3 levels: L, M and H) and *'Phase'* (4 levels: I, H_1, H_2 and D), and their interaction. Moreover, for the metrics CV_H we include a further within-subjects factor: 'Side' (2 levels: 'left-non dominant' and 'right-dominant'). We also performed a post-hoc analysis (Fisher's LSD test) to investigate statistically significant main and interaction effects. The significance level was set at p<0.05. The p-values were reported with correction for multiple comparisons by the Bonferroni method (Hsu, 1996).

Results

The total force profiles applied by the two hands (Figure 21 A) highlighted that most subjects in the OG undershot the highest target level, while the two groups were more similar in terms of accuracy for the low and intermediate levels. By looking at the single force hand contribution (Figure 21 B), younger subjects applied similar forces with both hands for all target levels. Instead, for most of the older subjects, each hand's contribution to the total force was more asymmetric, and

the hand applying more force differed among subjects (high inter-subject variability) and depended on the force level. The analysis of these indicators confirmed and further extended these results.

In the following, we reported metrics computed for OG and YG groups related to each of the four phases (I, H_1, H_2, D) of the force profile separately and for the *overall* force profile (i.e., entire force profile considering all the I,H_1,H_2,D phases). In all the related figures, we evidenced only the principal statistical effect (between-subjects factor: YG versus OG). The other effects (within-subject factor, interaction and post-hoc analysis) are described in the text. All values reported in the following text and in the figures are referred to (mean±SE).

Bimanual task performance. Older and younger participants had significantly different *overall* bimanual accuracy expressed in terms of *RMSE* (Figure 22 A, '*Group*' effect: $F(1, 32) = 91.68$, $p<0.001$), i.e., the younger subjects had lower *RMSE* in all phases for all the target forces.

As expected, for both groups, the *RMSE and* the difference between the *RMSE* of the two groups increased with the target force ('*Target Force*' effect: $F(2,32)=189.48$, $p<0.001$, interaction effect: '*Group*Target Force*': $F(2,32)=6.81$, $p<0.001$).
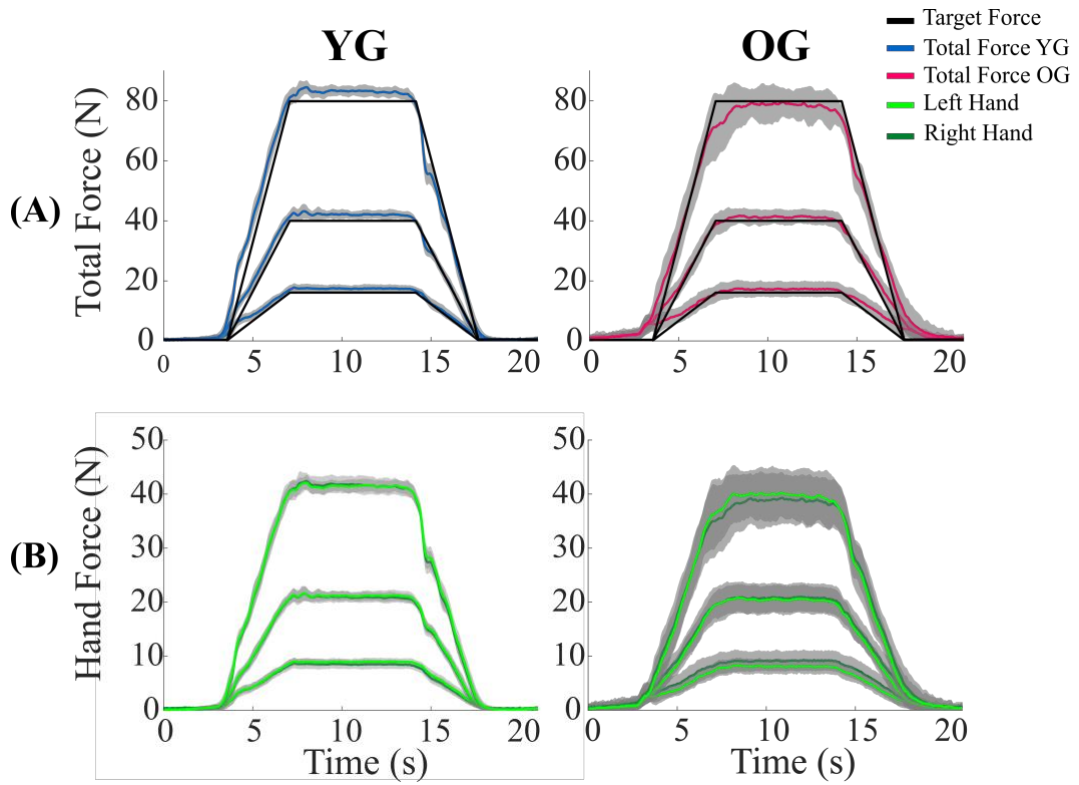
Figure 21 Trajectories (mean ± std) of each group for every target force, the first column is relative to the younger group (YG) while the second one is relative to the older group (OG). (A) Total Force: sum of the right-dominant and left-non dominant hand's forces: blue line indicates the YG while the magenta line denotes the OG. (B) Hand Force: force applied by each single hand, green lines indicate the left contribution while dark-green ones the right hand.

Finally, both groups had higher errors in the *I* and *D* phases (time-variant) than in the holding phases (*H₁* and *H₂*) and evidenced higher errors in the first holding phase compared to the second one ('*Phase*' effect $F_{(3,32)}=34.11$, $p<0.001$; '*Group*Phase*' interaction effect: $F_{(3,32)}=0.88$, $p=0.453$). The post-hoc analysis
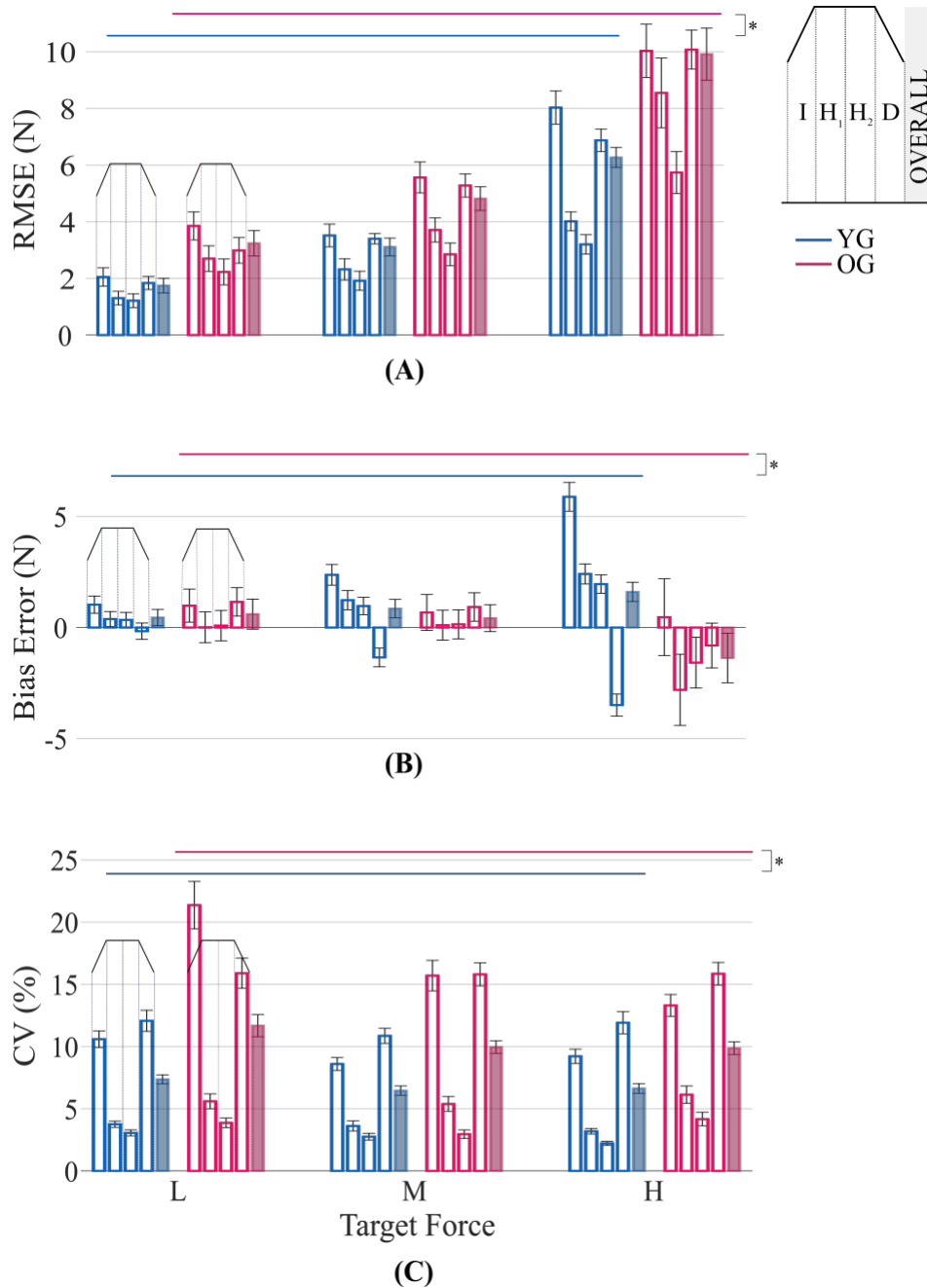
Figure 22 Bimanual performance metrics A) RMSE. B) BE. **C)** CV. Each metric is computed for the three force targets (L, M and H, as indicated in the x-axis). Blue colour denotes young adults (YG), magenta old adults (OG). As illustrated by the right-top legend, for each condition, each bar illustrates the parameter computed during one of the four phases, as indicated in the graph by the trapezoidal shape above them, while the right-ward fully coloured bar represents the metrics computed for the overall trajectory

confirmed that errors in I and D were significantly higher compared to both H_1 and H_2 (p<0.001 for all comparisons). Also, comparing the two holding phases, the *RMSE* was slightly higher in the first than in the second (p=0.01); this difference was higher for the OG. Instead, the *RMSE* was not significantly different between I and D phases (p=0.457).

To further understand these results, we investigated the presence of a bias on the *overall* force exertion by computing the *BE* parameter (Figure 22 B), whose positive and negative values indicate respectively a systematic tendency to overshoot and undershoot the required level of force.

The bias error was in general small for both groups, but the two groups were significantly different ('*Group*' effect: $F(1, 32)=11.24$, p<0.001). The difference depended on the target level and the phase of the trial (interaction effects: '*Group*Target Force*': $F(2,32)=9.56$, p<0.001 and '*Group*Phase*': $F(3,32)=12.02$, p<0.001). We also found significant main effects of the '*Phase*' factor ($F(3,32)=12.04$, p<0.001). Specifically, both groups had negligible bias errors at the lower and medium target in all phases, for the highest target force (H), the bias error magnitude increased for both groups. However, while the YG overshoot the target force in all phases except the D phase, the OG, on average, tend to undershoot the target force in all phases but in the I phase, having difficulties in reaching and maintaining the required maximum force.

As for the variability (*CV,* Figure 22 C) of the *overall* applied force, the OG force was affected by higher variability than that of the YG ('*Group*' effect: $F(1,32)=144.79$, p<0.001). Both the variability factor and the difference in variability between groups depended on the phases ('*Phase*' effect: $F(3,32)=328.27$, p<0.001; interaction effect '*Group*Phase*': $F(3,32)=20.53$, p<0.001). The *CV* was higher in the I and D phases for both groups and all target forces than in the holding phases (post-hoc: p<0.001, for all comparisons). Also, comparing the two holding phases, the *CV* was higher in the first than in the second (post-hoc: p=0.006), although this difference was higher for the OG. Instead, for both groups there was no statistical difference comparing the I and D phases (post-

hoc: p=0.523). Finally, for the OG, the *CV* was on average higher for the lowest target force than for the intermediate and the highest target force ('*Target Force*' effect $F(2,32)=7.98$, $p=0.001$, post-hoc respectively $p=0.001$ and $p=0.002$) while there was no statistically significant difference between the two other levels ($p=0.993$).

Differences between the forces applied by the two hands. We asked the subjects to control the cursor by applying the same amount of force with the two hands. OG applied forces less symmetrically than the YG (Figure 23A, '*Group*' effect: $F(1, 32) = 56.78$, $p=0.02$). The *SI* increased with the target force amplitude ('*Group*Target Force*' interaction effect: $F(2,32)=15.38$, $p=0.004$, post-hoc '*Group*' for all target force : $p<0.001$).
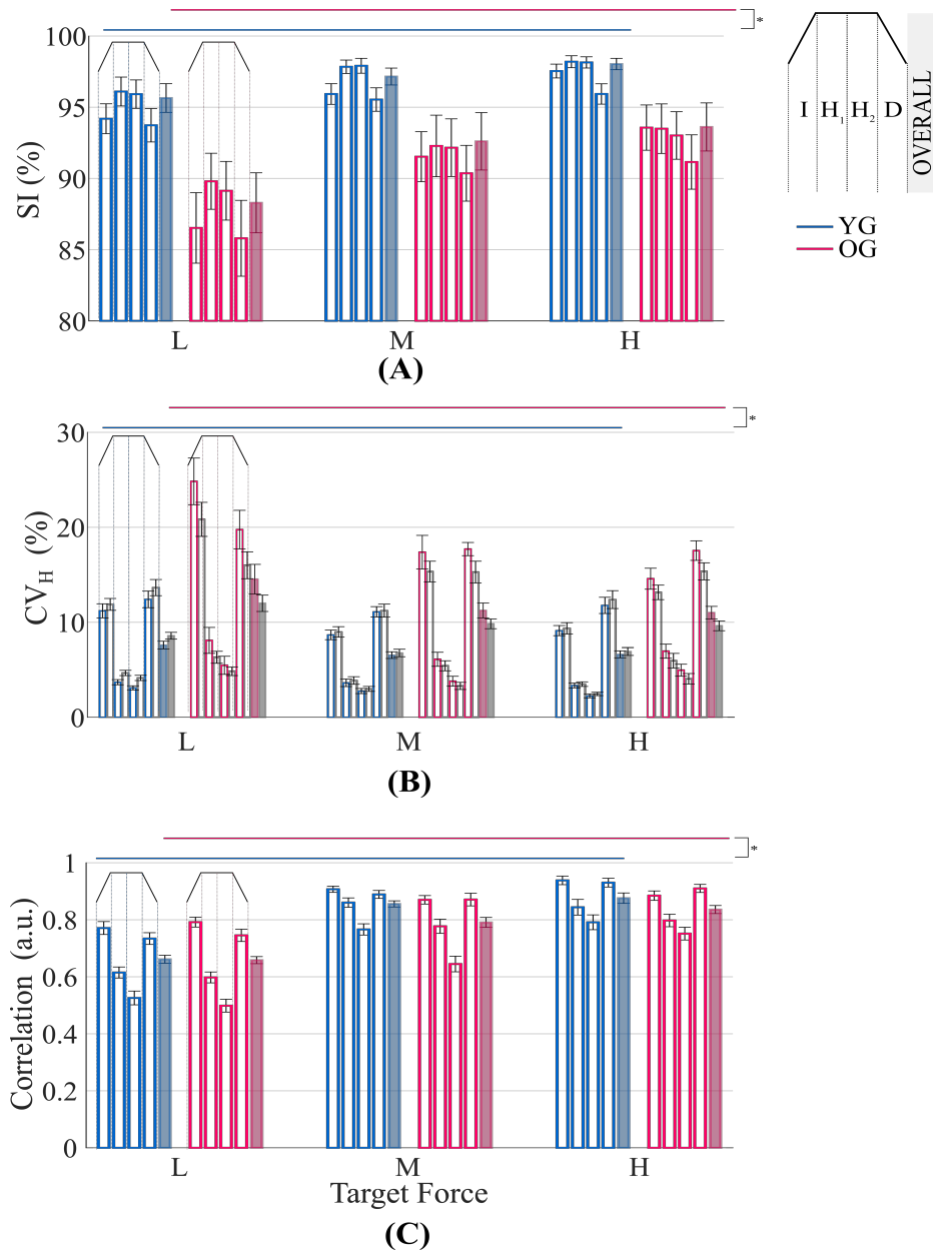
Figure 23 . Single hand performance. Blue color denotes young adults, magenta elderly adults As illustrated by the right-top legend, for each condition, each bar illustrates the parameter computed during one of the four phases, as indicated in the graph by the trapezoidal shape above them, while the right-ward fully colored bar represents the metrics computed for the overall trajectory. Each metric shows the 3 levels of force that are evidenced on the x-axis (L, M and H). A) Symmetry Index. B) CV_H – Coefficient of Variation of the force produced by each hand (the pedix H denotes that the metrics is illustrated for both the left (colored bar) and the right hand (grey bar)). C) Correlation.

While the hand applying more force varied across subjects, for the lower target force, most of the participants belonging to the OG group relied more on the *right-dominant* hand, behaviour not observed in the younger group (*LHF*: '*Group*Target Force*' interaction effect: $F(2,32)=156.78$, $p<0.001$, post-hoc between groups at the lower target force $p<0.001$).

The coefficients of variation of the *left-non dominant* and *right-dominant* hand ($CV_{H=L,R}$, Figure 23B) were similar for the YG. Instead, the OG had a higher *CV* for the *left-non dominant* than for the *right-dominant* arm ('*Group*Side*' effect: $F(1,32)=20.52$, $p<0.001$; post-hoc '*Side*' YG: $p=0.476$, OG: $p<0.001$). This effect was observable for all target forces and in all phases, although it was more marked in the *I* and *D* phases.

Interestingly, the % of force applied by the left hand (*LHF*) for the lower target force (L), where we observed the higher differences between populations, significantly correlated with its coefficient of variation CV_L ($R^{2}=0.43$, $p<0.001$): the higher CV_L, the lower the contribution of the *left-non dominant* hand. Interestingly the % of force applied by the *left-non dominant* hand had a similar correlation with CV_L /CV_R ($R^{2}=0.42$, $p<0.001$), while a lower correlation was observed when considering the CV_R ($R^{2}=0.20$, $p=0.01$). These correlations disappeared for the higher forces ($R^{2} < 0.01$ for both M and H targets force, Figure 24).

The two groups were also significantly different regarding the *Correlation* (Figure 23C) between *the left-non dominant* and the *right-dominant* hand forces profiles ('*Group*' effect: $F(1,32)=19.41$, $p<0.001$), but not in terms of *Time Delay* ('*Group*' effect: $F(1,32)=1.54$ $p=0.215$). The *Correlation* increased significantly with the increase of the target force for both groups targets ('*Target Force*' effect: $F(2,32)=220.27$, $p<0.001$), although in a different way for the two groups ('*Target Force*Group*' interaction effect: $F(2,32)=4.82$, $p=0.009$). In particular, the post-hoc analysis highlighted for the YG significant differences between the lowest level (L) and both the intermediate level (M) and the highest level (H) (post-hoc L-M and L-H: $p<0.001$ in both cases), but no difference between M and H target force levels ($p=0.689$). For the OG group, instead, we found significant differences between all levels (post-hoc: L-M and L-H $p<0.001$, M-H $p=0.02$). As expected,

both groups had higher values of *Correlation* in the *I* and *D* phases than in the holding phases ('*Phase*' effect: $F_{(3,32)}=127.81$, $p<0.001$; interaction effect '*Group*Phase*': $F_{(3,32)}=2.22$, $p=0.08$) and for the two higher target forces ('*Target Force*Phase*' interaction effect: $F_{(6,32)}=5.03$, $p<0.001$). In the latter, the difference between force levels was mainly due to the holding phases. The post-hoc analysis evidenced higher values of *Correlation* in the *I* and *D* phases compared to the holding phases ($p<0.001$ for all comparisons) and significant differences between the two holding phases ($p<0.001$).
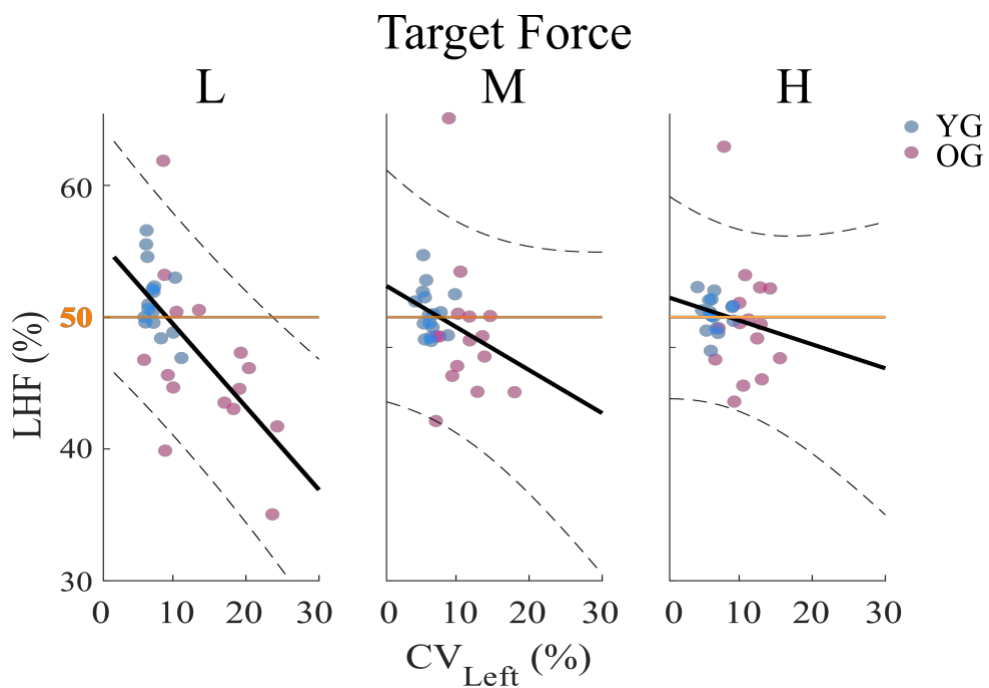
Figure 24 . LHF versus CV_L – Left Hand Force versus Coefficient of Variation of the force produced by the left-non dominant hand. The dotted lines denote the confidence interval (95%), while the continuous line represents the regression line for each target force (left: Lower target force; middle: Medium target force; right: higher target force) computed for both groups.

Discussion

From the first moment in which we are born, we interact with the outside world through touch, and haptic interactions allow us to understand the environment and to learn how planning and controlling our actions. We build and modify these abilities as we move through different stages of life, also adapting our motor skills to the changes in our brain and body.

The nerve fibers that are projected to the cerebral cortex through the corpus callosum are significantly reduced with aging, affecting the interhemispheric communication (C.-H. Lin et al., 2014; Ota et al., 2006), increasing the difficulty to perform bimanual actions (Geschwind & Kaplan, 1998; Preilowski, 1972). The bimanual force control and its changes with age is mainly studied focusing on the pressure exerted by individual fingers without considering the joints complexity presented by the arms as a whole.

In this study, we investigated the performance and lateral asymmetries of younger and older subjects in a bimanual isometric force matching task, where subjects had to control the forces exerted by their hands against a sensorized object for matching constant and time-variant force profiles. Three different levels of maximum force were required: low, medium and high. To correctly solve the task, subjects had to satisfy three specific requirements: i) using both *distal* and *proximal* upper limb muscles; ii) simultaneously controlling the two arms to achieve a shared goal; iii) both arms acting symmetrically.

The older subjects significantly had lower accuracy and higher coefficients of force variation for both hands than younger subjects in all conditions. Interesting, for most of them, the *left-non dominant* hand was noisier than the other hand. Also, in the older participants, bilateral forces were more asymmetric, but with different hand preference/dominance among subjects. This asymmetry decreased with the higher target levels. For the lower target force, where the asymmetries were more evident, subjects that exerted greater force with the *left-non dominant* hand were mainly those with lower *left-non dominant* hand variability. Conversely, subjects with higher *left-non dominant* hand variability relied more on the *right-dominant* hand to generate greater force.

As expected, we discovered significant differences concerning the different phases of the matched force profile: both groups showed lower accuracy (RMSE), higher variability (CV), and higher hands force correlation (*Correlation*) along with the *time-variant phases* compared to the *constant* ones; this result was more evident for the older group. Finally, we denoted lower accuracy, higher variability, and higher correlation, comparing the first holding phase with the second one

In the following paragraphs, we discuss these findings in detail.

Older subjects had lower accuracy and more variable performance in all conditions.

Aging is associated with a variation in the metabolic processes of the brain (Hyder & Rothman, 2012; A.-L. Lin & Rothman, 2014) and with a degenerative process of the neuromuscular systems: the muscles fibers decrease together with the motor neuron number and firing rate, resulting in a reduced number of motor units (McNeil et al., 2005). This is combined with a reduced nerve conduction velocity (Jagga et al., 2011; Norris et al., 1953; Palve & Palve, 2018).

Several studies describe lower accuracy and higher variability while controlling force by older participants (Kapur et al., 2010), (Hu & Newell, 2011), (C.-H. Lin et al., 2019), (Sosnoff & Newell, 2006), (Vaillancourt et al., 2003), (C.-H. Lin et al., 2014). In our task, the reduced muscle strength (Kubota et al., 2012; C.-H. Lin et al., 2019; Rantanen et al., 1999) and a faster fatigue onset (Hunter et al., 2016) for the older subjects could account for their undershooting the highest target force. Although we mitigated the last two factors by selecting three force levels that all our subjects were able to reach and we interspaced pauses among trials, the request of applying a force of 40 N repetitively with each hand could have been exceedingly challenging for the older subjects.

The increased variability we observed in older subjects instead could be associate with the decrease of the acuity of the somatosensory feedback and with increased widespread cortical activity and reduced functional connectivity during the execution of motor tasks characterized by reduced interhemispheric inhibition (Fujiyama et al., 2016; Goble et al., 2010; Hermans et al., 2018; Monteiro et al., 2020). This increased activity has been referred to as either a compensatory

phenomenon reflecting higher cognitive demand for the elderly to accomplish the motor tasks or a differentiation deficit reflecting an impairment in recruiting specific and segregated cortical areas (Heuninckx et al., 2005), (Heuninckx et al., 2008), and (Sala-Llonch et al., 2015). In line with this evidence, Vieluf et al. (Vieluf et al., 2018) found that during bimanual force matching tasks, a frontal activation shift compared with younger subjects, suggesting a more substantial use of cognitive resources like focused attention. This factor can account for a further increase in force variability in bimanual task with age (Rudisch et al., 2020).

Older subjects had higher asymmetry between the two body' sides: the arm applying more force varied across subjects and depended on the force target. Several studies (Mutha et al., 2013; Sainburg, 2002; Wang & Sainburg, 2007) suggested that differences in the upper limbs motor performance could be interpreted as a consequence of upper limbs specialization, rather than a mere superiority of the dominant arm. Specifically, in reaching-to-target tasks, while the dominant upper limb maximized predictive control mechanisms that accounted for high precision in movement direction and trajectory, the non-dominant hand stabilizes the arm at the desired goal position by specifying the impedance around that position. This hypothesis was tested mainly in unimanual studies and/or by looking at the two hands' independent performance. Few studies focused on bimanual tasks where the two hands were physically coupled. Recent findings shed new light on the phenomenon of hand dominance and preference, highlighting that it is significantly more complicated than it appeared. Woytowicz et al. (Woytowicz et al., 2018) found a better stabilization performance of the *left-non dominant* hand in a task where the hands were coupled together by spring and had to reach a target position, moving one while holding steady the other. Instead, Takagi et al. (Takagi et al., 2020) found a more significant contribution -in terms of co-contraction- of the *right-dominant* arm investigating a task of hold and transport of a sizeable oscillating box. These two findings support the hypothesis that the *right - dominant* hand had a leading contribution in the bimanual stabilization task, while the *left– non dominant* one is 'only' better at compensating the *right-dominant* hand's interaction forces.

In our study the task was isometric, thus not influenced by the superiority in dynamic tasks of the right hand (Blakemore et al. 1998). The two arms performed a congruent task, as in (Takagi et al., 2020), but they were visually and not physically coupled, although they had to reach the same force goal. These isometric visually coupled tasks were mainly investigated for fingers or hand-grip forces. In these cases, a higher force contribution of the strongest hand, i.e., the *right-dominant*, was found. However, the CNS is supposed to assign control authority based on each arm's strength and noise (O'Sullivan et al., 2009). While the strongest arm is usually the *right-dominant* arm, noise can depend on task requirements as the muscle districts involved or the specific target directions. In fact, in a task also involving proximal muscles (Salimpour & Shadmehr, 2014b), a higher contribution of the *right-dominant* hand was found only for specific directions. Also, our task involves proximal muscles. As for the strength factor, lateralization is preserved in older subjects, although associated with a decreased asymmetry in between-hands dexterity (Teixeira, 2008) (Sale & Semmler, 2005). As for the noise factor, the somatosensory receptors can be affected by side-asymmetric changes with age (Iandolo et al., 2019), and this would increase the sensory feedback noise on one of the two sides of the body. These two findings could suggest that the control authority might vary individually, depending on sensorimotor noise. This evidence is confirmed by our data for the lower target force, requiring finer control and lower strength: there was a significant relationship between the relative amount of force exerted by the *left-non dominant* hand and the variability of such force. This relation was not observed for the higher forces when strength became more important for solving the task.

Both groups had more difficulty matching a *time-variant* than a *constant* force profile, and this difficulty was more remarkable for the older group.
Both groups' performance was more accurate and affected by lower variability when maintaining a constant force level than when matching a *time-variant* force profile. This result was expected and supported by other literature results (Kubota et al., 2012). More interestingly, the elderly group's performance showed higher differences between *constant* and *variant - time* phases compared to young

96

participants. The previous reporting suggested that aging is associated with an impaired ability to rapidly vary the force exerted (Kubota et al., 2012). In the study by Voelcker-Rehage et al. (Voelcker-Rehage & Alberts, 2005), the older adults performed as accurately as young subjects in static grasping force matching tasks, while their performance was significantly reduced in the time-variant tasks. Also, in our task, the two populations' force profiles highlighted the older subjects' more difficulty to change the control of the force from *time-variant* to *constan*t (this reflected on the higher error o the first constant phase with respect to the second). Several factors associated with the deterioration of the sensorimotor system could account for this phenomenon. First, the cognitive demand could be more relevant when rapid changes are required (Goble et al., 2010). Second, the decline in the motor neuron firing rate and the number of motor units associated with aging could slow down the modulation rate of the force exerted (Kubota et al., 2012).

Both populations had higher hands force correlation in the *time-variant* phases compared to the *constant* ones.

The bimanual coupling was investigated by computing the force profile cross-correlation (*Correlation*) between hands. We discovered that both groups evidenced higher correlation along with the time-variant phases compared to the constant ones. Patel et al. (Patel et al., 2019) evidenced that higher correlation coefficients are associated with less accurate young and healthy adults' performances. The literature also emphasized the role of between-hands decoupling in the bimanual force control tasks as it could foster error compensation strategies (Patel et al., 2019), (Hu & Newell, 2011). Our data also support this result, finding higher hands force correlation (and lower accuracy) along with the *time-variant* phases compared to the *constant* ones.

A limitation of our work was the absence of a concurrent muscle activity assessment that we plan to address it in a future study. This will allow us quantifying the contribution and the activation timing of both proximal and distal muscles involved in the task. This will also detect possible onset of fatigue that we tried to avoid interspacing resting phases between trials. Moreover, we made two protocol choices that could have determined the present results. First, we decided to select

three-force levels equal for all subjects, not proportional to each individual's maximum force, after verifying that the highest level, 40N for each hand, was a force level reachable by all participants. Second, we explicitly asked participants to apply equal force with the two hands, not allowing them to freely choose their strategy. It would be interesting to investigate if a different instruction would lead to equal or different results.

This study aims at delivering a general view on the age-related changes in the physiological aspects influencing the modulation of bimanual isometric force, involving, at the same time, both proximal and distal muscles. The results are promising, and the device and the protocol could be integrated as assessment tool into clinical practice, while exploring its potential as rehabilitative instrument. Indeed, force modulation is crucial in multiple daily activities and the recovery of this ability is an import goal for several people suffering from different neurological diseases.

Modulation of grip force in bimanual object lifting task in patients with stroke

Introduction

Predictive estimation of the consequences of upper limb's movements is essential for the rapid movements commonly observed in object manipulation. The act of grasping and lifting an object requires a complex coordination between the force used to grasp the object (usually referred as the grip force) and the force exerted to move the object in the space (lift force). This action involves spatial exploration, motor planning, multisensory integration, and both predictive and reactive control strategies (Frey et al., 2011). Seminal works from Johannson and Westling firstly described the sophisticated system of tactile machanoreceptors responsible for conveying information about distinct mechanical events involved in object's grasping (Johansson & Flanagan, 2009; Johansson & Westling, 1984). However, tactile feedback is affected by intrinsic sensory delay and in case of unexpected perturbation, the reaction time has been estimated being 100ms or longer (R. S. Johansson & Flanagan, 2009). This is what happens, for example, when we lift an object that is heavier than expected or when an external unpredicted perturbation is exerted on the object we are holding: tactile receptors signal the initial slippage to which we react, with a certain delay, increasing the grip force to avoid the object to fall. In contrast, a series of studies showed that if the perturbation is the consequence of a voluntary action (for example when we move our upper limb while holding an object), we are able to increase the grip force synchronously or even in advance to the movement resulting in a more efficient performance (Gordon et al., 1993; R. S. Johansson & Westling, 1984). It has been proposed that this behavior is made possible by a predictive forward model that uses information about the movement's motor command and the object's properties to predict the sensorial and kinematic consequences of our action (Blakemore et al., 2001; Wolpert & Flanagan, 2001). The CNS is then able to use this prediction to modulate the grip force in order to compensate in advance the effect of the perturbation. For this reason, the behavior during objects' lifting has been widely investigated to

assess subjects' sensorimotor control strategies or impairments in predictive motor control (Flanagan & Wing, 1997; Hermsdörfer et al., 2003; R. S. Johansson & Cole, 1994; Nowak et al., 2013). Specifically, the time coherence and relative delay between lift and grip force modulation is considered to reflect crucial aspects of forward model in object lifting (Flanagan & Wing, 1995; R. S. Johansson & Flanagan, 2009). Moreover, studies on healthy subjects showed that, typically, during an object lifting the grip force increase around 200ms before the movement onset. The grip force is then modulated proportionally to the acceleration transferred to the object being usually 10% to 40% greater than the minimum required to preserve a safety margin in case of unexpected events (R. S. Johansson & Flanagan, 2009).

The neural substrates of these processes are not yet fully understood. However, there is compelling evidence that the cerebellum, the sensorimotor cortex and the posterior parietal cortex play a crucial role (Ehrsson et al., 2003, Welniarz et al., 2021, Boecker et al., 2005 Kawato et al., 2003). Specifically, a solid line of research that have identified the cerebellum as the ideal locus for a forward model coding (Mcnamee & Wolpert, 2019; Tanaka et al., 2019, 2020; Wolpert et al., 1998). Moreover, neuroimaging studies supported on healthy controls supported these findings and pointed out the involvement of the cerebellum in grip force modulation during object holding (Kawato et al., 2003). Furthermore, the posterior parietal cortex has been previously claimed to be responsible for coding predicted tactile sensory feedback (Shergill et al., 2013). Therefore, patients with lesions involving parietal cortex areas or sensory nuclei of the thalamus may show predictive motor control deficits not just because of the lack of somatosensory input (like in peripheral anesthesia) but as the result of the disruption of the forward model's neural substrate.

Several studies investigated predictive motor control in objects' lifting tasks in cerebellar patients and subjects with somatosensory impairments. It is well known that tactile somatosensory deficits have devastating effects on manipulation and their role in objects' lifting task has widely been investigated in the last decades both in patients with peripheric and central lesions (R. S. Johansson & Flanagan,

2009). The importance of tactile feedback while grasping an object is variable according to the level of predictability of the action. The time relationship between grip and load force has been showed to be relatively preserved in patients with peripheric sensory deficits (Nowak et al., 2001, 2002, 2003; Parry et al., 2021). However, other reports found impairment in predictive grip force modulation in deafferentiated patients suggesting the disruption of prediction of timing of load fluctuation (Cole et al., 2003; Monzée et al., 2003; Nowak et al., 2004). Taken together, these findings suggested that sensory information is important for maintaining a precise forward model of dynamic grip force control although some deafferentated patients may be able to use alternative cues, like visual input or previous learning to use residual internal predictive models (Hermsdörfer et al., 2008). While extensive literature investigated objects' lifting tasks in patients with peripheric somatosensory deficits, fewer studies focused on patients with sensory deficits due to CNS lesions (Cole et al., 2003; Monzée et al., 2003; Nowak et al., 2001, 2002, 2003, 2004). Some studies found that stroke subjects presented delayed grip force onset (Blennerhassett et al., 2008; Hermsdörfer et al., 2003; Nowak et al., 2013) and, likely to compensate for these deficits, produced exaggerate grip force (Nowak et al., 2013). In contrast, other reports found that tactile sensitivity deficits seemed not to affect the timing onset of grip forces in respect to the load forces (Hermsdörfer et al., 2003). Patients with lesions in the parietal cortex due to stroke present unique features that distinguish them from patients with somatosensory deficits from peripheral lesions. Firstly, although the tactile sensitivity may be severely impaired, these patients are rarely affected by complete anesthesia and some residual somatosensory perception may be preserved. Moreover, even in case of severe lesion in somatosensory areas, the parietal cortex is not the only endpoint of somatosensory input. For example, the cerebellum is provided with somatosensory input and uses this information to monitor the movements and trigger its correction in case of necessity (Tanaka et al., 2019, 2020; Wolpert et al., 1998). However, the anticipatory motor control deficits in patients with lesion in somatosensory areas have been overlooked.

Little is known on the performance of subjects with CNS lesions in bimanual object lifting tasks. Bimanual tasks are important for people with focal CNS lesion like

stroke because unilateral functional impairments may be compensated by the help of the non-affected hand. Bimanual motor control is characterized by specific and unique features, including between-hands interaction, that have been poorly investigated even in healthy controls (Y. Jin, et al., 2019; Kennedy et al., 2016; Morrison & Newell, 1998; Serrien & Wiesendanger, 2001). Most importantly, while holding an object bimanually, the two hands are coupled so that the force exerted by one hand is perceived by the other and vice versa. Previous studies on task that involved the two-hands interactions showed that the CNS is able to predict the tactile feedback on one hand originated by a force exerted by the other hand (Bays & Wolpert, 2007a). This mechanism may help patients with unilateral somatosensory impairment during bimanual object lifting. This extra source of tactile information could, in principle, improve patients' predictive behavior measured in terms of grip and lift force temporal coupling, in contrast to previous findings on unimanual lifting tasks (Cole et al., 2003; Monzée et al., 2003; Nowak et al., 2004). The investigation of bimanual objects lifting task in patients with unilateral CNS lesions may improve our knowledge on whether and how the CNS is able to exploit sensory input from the unaffected hand to improve predictive motor control deficits.

The present study aimed to investigate the anticipatory grip force behavior and bimanual force control in bimanual tasks in patients with lesion to somatosensory areas of the CNS due to stroke and mild UL functional impairment. We hypothesized that the somatosensory deficits may cause specific anticipatory behavioral deficits that alter the subjects' ability of modulate the grip force during a lifting task.

Methods

Participants

Patients with cerebral stroke and age-matched healthy volunteers were recruited. Participants were recruited from the Neuromotor and Cognitive Rehabilitation Research Centre (CRRNC) of the University of Verona, Italy. For healthy controls, the exclusion criteria were the presence of musculoskeletal injuries or any other

neurological condition, history of surgery or pain affecting upper limbs, normal or corrected to normal visual and auditory abilities. For stroke subjects (SP), the inclusion criteria were: age $\geq$ 18 year old, diagnosis of stroke confirmed by a specialist in neurology and by radiologic findings (CT or MR), lesion in somatosensory areas including thalamic somatosensory nuclei and parietal cortex, Trunk Control Test score = 100/100, strength of shoulder abductors and elbow flexors $\geq$ 3/5 MRC (Medical Research Council Scale for Muscle Strength), notable to full UL capacity (Fugle-Mayer assessment scale score (FMA) $\geq$ 48) (Hoonhorst et al., 2015).

Exclusion criteria were the presence of severe cognitive, visual or communication impairments and other concomitant neurological or orthopaedic diseases interfering with patients' capacity of providing the informed consent or performing the required task.

This study was conformed to the ethical standards of the 1964 Declaration of Helsinki and all the study procedures and documents, including the consent form, were approved by Verona University Institutional Review Board (CARU n. 22/2019). All participants provided written informed consent to participate in the study and publish the results in the de-identified form.

Clinical assessment

Strength, function, and proprioception of upper limb were assessed using a battery of clinical scales. The Motricity Index (MI) is a well-known scale for the assessment of limb strength testing shoulder abduction, elbow flexion and pinch grip (score range 0-99, greater score indicates better performance) (Collin & Wade, 1990). The Fugl-Meyer assessment scale for upper limb (FMA-UL) is a measure of UL function that includes 33 items assessing reflex, activity, muscle strength and movement control (score range 0-66, greater score indicates better performance) (Fugl-Meyer et al., 1975). The Erasmus MC modifications to the Nottingham Sensory Assessment (EmNSA) was used to assess proprioceptive deficits of patients with stroke. It includes tasks investigating light touch, pressure, pinprick,

sharp-blunt discrimination, and proprioception (score range 0-40, greater score indicates better performance)(Stolk-Hornsveld et al., 2006).

Bisbox device

The device used in this experiment, *Bisbox 2.0,* is a sensorized rectangular box, a new and lighter (0.8 kg) version of the prototype described in (Galofaro et al., 2019) showed in Figure 25. The dimensions of the box were 15×35×25 cm (height × width × depth). The 35 cm length was chosen to match the participants' average inter-shoulder distance, who should hold the device with the two hands placed on the two smaller faces. Each lateral face is composed of two rigid 3D-printed plates in PolyLactide Acid. Between these plates three load cells (Micro Load Cell CZL635; full-range scale of 5kg; precision of 0.05% and linearity of 0.05% FS) are placed in a triangular configuration so the force applied by the user on the external plate is sensed by the cells and measured by the device. At the center of the bottom part of the device there was a 3D-printed rigid plate that encloses a micro-controller (Raspberry Pi, model 3B+, CPU frequency: 1400MHz) and a tracking camera (RealSense T265, Intel), and a battery (24800mAh, output 3.1A). The micro-controller is connected via USB to both the tracking camera and the external battery.

The sensorized box was connected to a laptop via wireless communication. The laptop ran the software that controlled the experiment and provided instructions and visual feedback, according to the task executed, to the participants. The device was used being placed on a table in front of the user.

Experimental procedures

Participants sat in an armless chair in front of a 24" monitor placed ~ 0.5 m away from the subject's chest. The height of the chair was adjustable so that the forearms rested on the table with shoulders in ~20 deg flexion and elbows at ~110 deg flexion. The hands were positioned fully open on the lateral sides of the device. A schematic representation of the device is shown in Figure 25 and a representation of the experimental setting is shown in Figure 20. All subjects performed three consecutive tasks: a fixed-force matching task, time-varying force matching task

and a lifting task. At the beginning of the session, the Maximal Voluntary Isometric force (MVC) was measured. The subject was asked to squeeze the box three times with a resting period of 2 minutes after each trial. The MVC was computed as the mean of the three trials and was used to normalize the target force levels in the matching tasks. Each subject completed 21 trials for the two force matching tasks, seven trials for each target force level that was set at 10%, 25% and 50% of the MVC, presented in pseudorandom order. In the fixed-force matching task subjects were provided with visual feedback of the target force and the force they were exerting during the trial, both represented as a horizontal bar in the PC screen. After a familiarization phase, they were asked to align the bar representing the force they were exerting with the target force's bar as accurately as possible. Each trial lasted 5 seconds. Visual feedback was provided also in the time-varying force matching task. Here subjects were asked to control the height of a squared cursor of 0.5cm side by modulating the force exerted on the device's lateral plates: the greater the force, the higher the square moved. Independently of subjects' performance, in each trial the cursor moved rightward at a constant speed of 0.85cm/s. In this task subjects were asked to keep the cursor on top of the sides of an isosceles trapezoid, displayed on the computer screen. Therefore, the task was divided into four phases each lasting 3.5s: increment phase, to consecutive holding phases and a decrement phase where subjects had to gradually increase, keeping constant and decrease the force exerted respectively. The force level of the holding phases varies between trials in a pseudorandom order as in the fixed-force matching task: 10%, 25% and 50% of the MVIF. Each trial lasted 14 seconds, followed by a rest of 6 seconds. Lastly, in the lifting task, subjects were asked to grasp the device by the lateral force plates and lift it, hold it at ~30cm height for ~3s and replace it on the table. A ruler of 30cm length gave visual feedback about the ideal height to reach while holding the box.
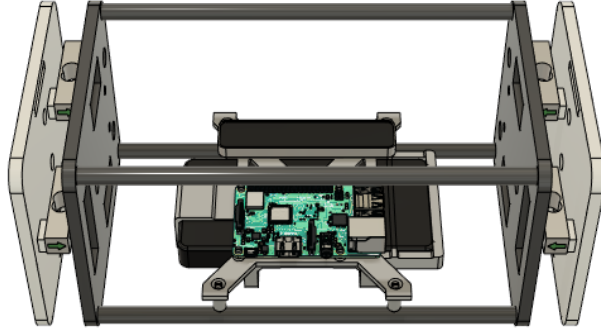
Figure 25 The customized BiSBox used in this experiment

Outcome measures

For the force matching tasks, the accuracy of the matching and the synchronization between hands were measured.

- **Root-Mean-Squared Error (RMSE)** measures the deviation of the participant's total force output from the target force trajectory (Lodha et al., 2010). Higher values for relative RMSE indicate less accuracy of total force output. It is defined as:

$$RMSE = \sqrt{\frac{1}{N}\sum_{i=1}^{N}(F_{Mi} - F_{Di})^2} \qquad (13)$$

where F_{Mi} is the *measured* total force at the sample i and F_{Di} the corresponding *desired* force. N is the total number of samples considered either on a single phase or on the entire trial.

- **Bias Error (BE)**, the systematic component of the error, computed as the signed difference between the participant's total force output and the target force:

$$BE = \frac{1}{N}\sum_{i=1}^{N}(F_{Mi} - F_{Di}) \qquad (14)$$

Positive values indicate an overshoot of the target force, negative values an undershoot (Schmidt et al., 1988; Marini et al., 2016; Ballardini et al., 2019a).

- ***Coefficient of Variation (CV)**, a measure of* force variability (standard deviation) of the total force expressed as a percentage of the mean force output (Galganski et al., 1993):

$$CV(\%) = \frac{std\big(detrend(F_M)\big)}{|mean\,(F_M)|} * 100 \tag{15}$$

Where F_M is the vector of the samples from force trajectory in each phase. We computed the standard deviation (std) of this signal after removing the best straight-fit line from the data (least-squares method, *Matlab* function detrend).

For the lifting tasks a set of behavioral features was computed, comprehending different motor control aspects as anticipatory motor control, movement planning and movement efficiency:

- Maximal total force: the peak force applied on the device in each trial during the lifting;
- Normalized maximal total force: the maximal total force divided by the MVC performed by the subject before starting the assessment procedures;
- Peak ratio between force exerted and lifting velocity;
- Absolute time when applied force reached its peak;
- The ratio between the force during the holding phase and the lifting phase;
- Time between the peak force and the starting of the holding phase (i.e. the ending of the lifting);
- Time between the force onset and the lifting movement onset;
- Coefficient of variation during the holding phase (as previously defined in Eq. 15).

Data Analysis

In the fixed-force matching tasks, only the last 2.5s of each trial were analyzed, in order to avoid the initial force increasing. Moreover, the first trial for each target force level for the matching tasks and the first three trials for the lifting task were excluded from the analysis. In the lifting task, the onset of the lifting and holding phases were identified with an automatic algorithm and visually checked by an experimenter.

Data distribution was checked using the Shapiro-Wilk test. For the analysis of the fixed-force matching task a repeated measure ANOVA was used with the force level as a within-group factor and "group" as between-group factor. For the time-varying force matching task an ANOVA was performed with two withing-group factors: force level and task phase, and one between group factor: "group". Where sphericity assumption was violated according to Mauchly's test, the Greenhouse-Geisser correction was used. Post-hoc analysis was performed using Holm-Bonferroni method. Lastly, for the analysis of the lifting task a t-test for unpaired samples or Mann-Whitney test was used according to data distribution.

Results

Eleven healthy subjects and nine patients with stroke have been included. Demographic characteristics of included subjects are listed in Table 2. Table 3 shows clinical features of SP.

Table 2 Demographic data of healthy subjects and patients with stroke

Group	Age		Sex (M/F)	Laterality (R/L)
	mean	sd		
Healthy	58,5	16,8	5/6	11/0
Patients	65,0	11,4	7/2	8/1

Table 3 Clinical data from patients with stroke

Patient	Time since stroke onset (months)	Lesion side	Lesion site	Ictus aetiology	FMA - UL	EmNSA	MI
1	2	L	Thalamus	Ischaemic	60	40	100
2	4	R	Thalamus- posterior internal capsule	Hemorragic	50	34	91
3	8	L	Caudate - lenticular nuclei - Internal capsule (posterior limb)	Ischaemic	66	40	100
4	8	R	Fronto - parietal lobe	Ischaemic	61	40	100
5	2	R	Thalamus	Ischaemic	62	40	100
6	8	L	Internal capsule (posterior limb)	Ischaemic	62	15	76
7	5	R	Parietal lobe	Hemorragic	53	29	76
8	3	L	Temporo - occipital lobes	Ischaemic	60	37	100
9	3	R	Thalamus, Internal capsule (posterior limb)	Ischaemic	54	36	100

There was no significant difference (p=0.77) between the MVC exerted by the healthy subjects (155.5 ± 30.9 N) and patients with stroke (151.3 ± 31.1 N).

The analysis of the fixed-force matching task showed an effect of force level on the RMSE (F=21.92; p<0.001; η_p^2=0.55). The post hoc analysis showed significantly greater RMSE in the high force level compared to both medium and low force levels (low vs high: t=-6.329; p<0.001 Cohen's d=-1.42; medium vs high: t=-4.85; p<0.001; Cohen's d=-1.08) (Figure 26, top left). In terms of bias error, the ANOVA showed significant effect of force level (F=47.80; p<0.001; η_p^2=0.73) and a significant interaction "force level" * "group" (F=5.52; p=0.02; η_p^2=0.24). The post-hoc analysis found significant difference between the three force levels, with the high and medium levels being negative, suggesting undershooting of the target force and the low level being positive suggesting overshooting of the target force (low vs medium: t=4.56, p<0.001, Cohen's d=1.02; low vs high: t=9.77, p<0.001, Cohen's d=2.19; medium vs high: t=5.21, p<0.001, Cohen's d=1.17). The comparison between groups within the same force level showed a significant difference in the high force level (t=3.36; p=0.013) with SP showing greater error compared to healthy controls (Figure 26, top right). Finally, the analysis of the coefficient of variation did not show any significant affect (Figure 26, bottom).

As for the time-varying force matching task, in terms of the RMSE, the ANOVA showed significant effect of the task's phase (F=65.23; p<0.001; η_p^2=0.79), force level (F=143.08; p<0.001; η_p^2=0.89), and significant interaction "phase" * "force level" (F=15.84; p<0.001; η_p^2=0.48). The post-hoc comparison between the target force levels found significant difference between the low and medium force levels (t=-6.58, p<0.001, Cohen's d=-1.51), between low and high force levels (t=-16.79, p<0.001, Cohen's d=-3.85) and between medium and high force levels (t=-10.2, p<0.001, Cohen's d=-2.34). Within the same force level, the post-hoc analysis for the effect of the task's phase found significant effect between phase 1 and phases 2 and 3 (t=7.08, p<0.001, Cohen's d=1.62 and t=9.13, p<0.001, Cohen's d=2.01 respectively) and between phase 4 and phases 1, 2 and 3 (t=2.91, p=0.01, Cohen's d=0.67; t=10.00, p<0.001, Cohen's d=2.29 and t=12.05, p<0.001, Cohen's d=2.76 respectively) (Figure 27 top left). Analogously, for the bias error significant effects were found for movement's phase (F=53.45, p<0.001; η_p^2=0.76), force level (F=5.22, p<0.019; η_p^2=0.24) and significant interaction "phase" * "force level" (F=16.08; p<0.001; η_p^2=0.49). Here the post-hoc analysis on the force levels comparisons found significant differences between the high force level and the medium (t=-2.47, p=0.037, Cohen's d=-0.57) and the low force levels (t=-3.05, p=0.014, Cohen's d=-0.70). The post-hoc comparisons between task's phases found significant difference between phase 4 and phases 1 (t=10.36, p<0.001, Cohen's d=2.38), phase 2 (t=10.60, p<0.001, Cohen's d=2.43) and phase 3 (t=10.02, p<0.001, Cohen's d=2.30) (Figure 27 top right). Lastly, also the analysis of the coefficient of variation showed significant effects of the force level (F=105.94, p<0.001; η_p^2=0.86), task's phase (F=125.70, p<0.001; η_p^2=0.88) and significant "force level" * "task's phase" interaction (F=36.54, p<0.001; η_p^2=0.68). Overall, the low force level showed greater coefficient of variation compared to the medium (t=12.73, p<0.001, Cohen's d=2.92) and high force levels (t=12.48, p<0.001, Cohen's d=2.86). In terms of between-phases comparison the phase 1 showed greater coefficient of variation than phase 2 (t=14.59, p<0.001, Cohen's d=3.35) phase 3 (t=15.33, p<0.001, Cohen's d=3.52) and phase 4 (t=2.75, p<0.001, Cohen's d=0.63). Moreover, subjects' performance in phase 4 had greater coefficient of

variation than phase 2 (t=11.84, p<0.001, Cohen's d=2.72) and phase 3 (t=12.58, p<0.001, Cohen's d=2.89) (Figure 27, bottom).

Lastly the between-group comparison of the lifting task performance showed that patients exerted a relatively grater force in respect of their MVC during the lifting of the box (t=2.35, p=0.033, Cohen's d=1.14), (Figure 28 top right and Figure 29 left). Moreover, the time interval between the peak force instant and the starting of the holding phase (i.e. the ending of the lifting phase) was significantly greater in patients compared to healthy subjects (Mann-Whitney U: 61.0, p=0.015) (Figure 28 bottom left and Figure 29 right).

The association between behavioral performance and clinical impairment assessed with clinical scales was assessed using a linear correlation analysis but did not show any statistically significant association.
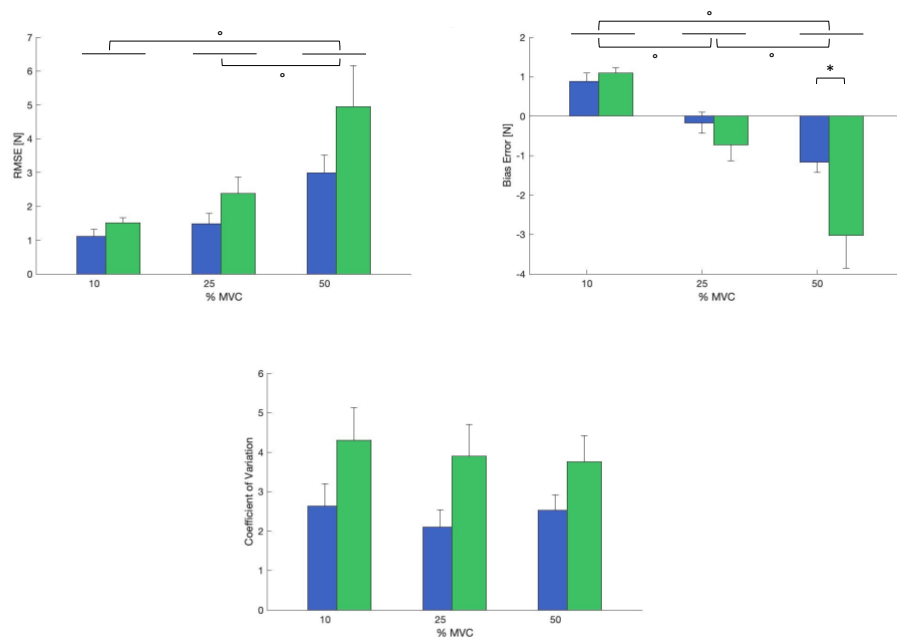
Figure 26 Results from fixed-force matching task. Green: patients with somatosensory deficits; Blue: healthy controls. Top left: RMSE, top right: Bias error, bottom: coefficient of variation. Error bars show standard errors. ° statistically significant post-hoc comparisons between different force levels (adjusted p<0.05). * statistically significant post-hoc between-groups comparisons (adjusted p<0.05).
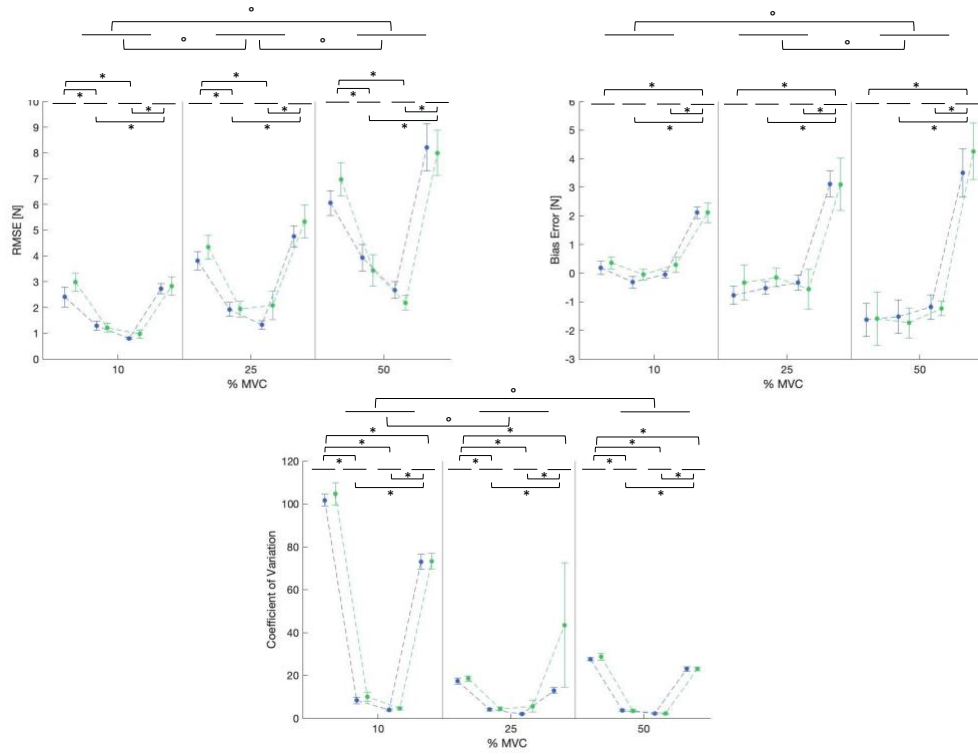
Figure 27 Results from time-varying force matching task. Green: patients with somatosensory deficits; Blue: healthy controls. Top left: RMSE, top right: Bias error, bottom: coefficient of variation. The % of MVC distinguish between low, middle and high force levels respectively. For each force level results are showed for each of the 4 task's phases. Error bars show standard errors. ° statistically significant post-hoc comparisons between different force levels (adjusted p<0.05). * statistically significant post-hoc between-phases comparisons (adjusted p<0.05).
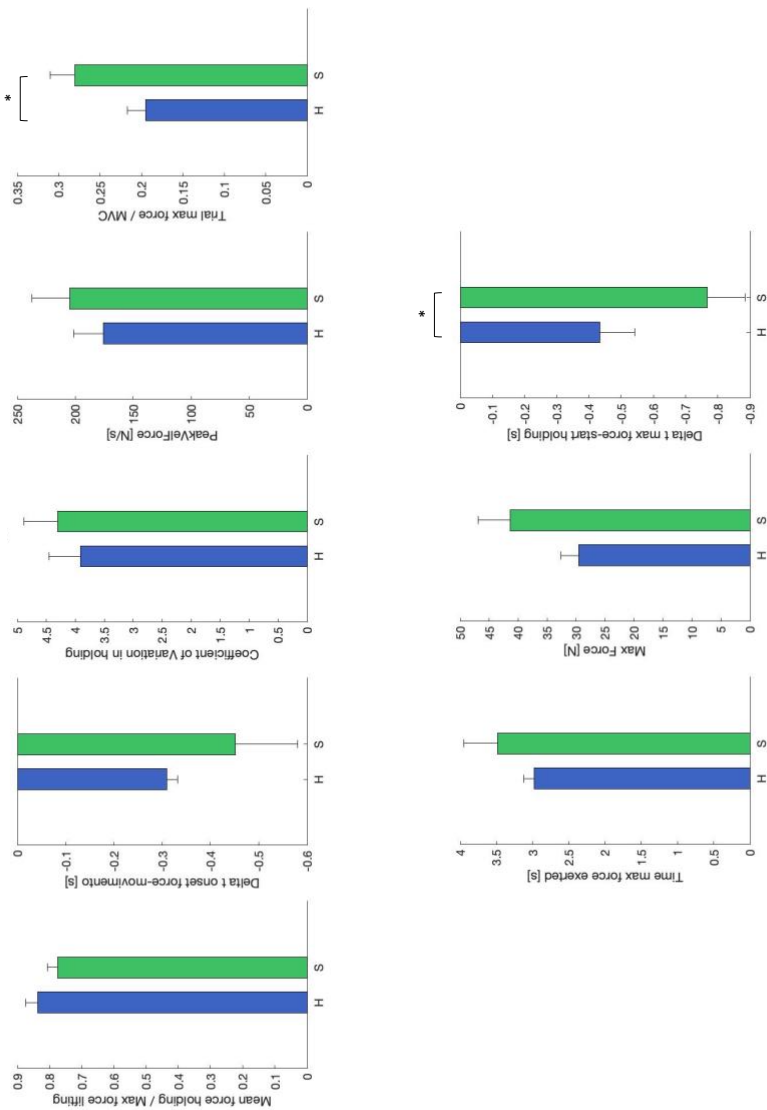
Figure 28 Results from lifting task. Top from left to right: ratio between mean force during holding and peak force during lifting, time between grip force onset and movement onset, coefficient of variation, peak ratio between force exerted and lifting velocity, normalized maximal total force; bottom from left to right: time when force reached its peak, maximal total force, time between the peak force and start of the holding phase. Green: patients with somatosensory deficits; Blue: healthy controls. Error bars show standard errors. * statistically significant between-groups comparisons (p<0.05).
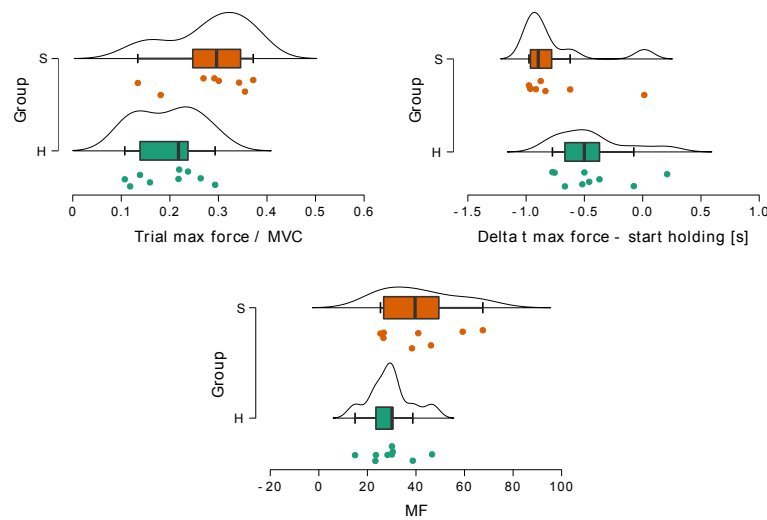
Figure 29 Raincloud plots of the normalized maximal force exerted during the lifting (top left), time interval between maximal force exertion and ending of lifting (top right) and absolute maximal force exerted (MF) (bottom) Green: healthy controls, Orange: stroke patients.

Discussion

This study aimed to assess the impairments in bimanual anticipatory grip force and bimanual force control in patients with cerebral stroke and somatosensory impairment. Within this aim we recruited a convenient sample of eleven healthy subjects and nine patients with stroke sequalae and mild functional UL impairment. We used a newly designed device that allow us measuring the force applied on it and its position in space to assess subjects' performance in three tasks: a fixed force matching task, a time varying forc matching task and a lifting task. Our analysis showed that in the patients we recruited the ability of modulating the bimanual force in force matching tasks was relatively preserved. However, the analysis of the lifting task suggested that patients presented some deficits in force modulation related to movement planning.

Although the overall patients' performance in the force matching tasks was not significantly different from the healthy subject's, we were able to measure some mild deficits both on terms of accuracy and grip force variability. Specifically, the patients were less accurate in matching a fixed target force, especially for greater target force level relatively their MVC. Also, there was a tendency to significance

114

in the between-group comparison in terms of the CV across different force levels (ANOVA group effect: F=3.83, p=0.66) suggesting that patients exerted a less steady bimanual force. However, there are some factors worth to mention that could explain the relatively good overall patients' performance in these tasks. Firstly, we recruited patients with mild to moderate UL functional impairment and all the patients had FMA-UL score of at least 50/66. Secondly, although all the patients reported subjective impaired tactile sensation, we purposely included also patients with very mild somatosensory impairment as documented by the EmNSA scores. Thirdly, the design of the task enabled patients to rely on the tactile feedback of both hands, potentially allowing the patients to compensate for tactile deficits in the affected hand. Lastly, in the matching tasks patients were provided with visual feedback of the target force and the force exerted. Therefore, on one hand it was not surprising that subjects with mild post-stroke impairment could perform in line with age-matched healthy controls in force matching tasks. On the other hand, our data suggest that bimanual grasping and visual feedback of the force exerted may help patients to compensate for force modulation impairments related to sensory deficits. Specifically, the stroke patient's reliability on visual feedback may partially explain the between-group difference in terms of grip force variability in the fixed-force matching task. However, it is relevant to mention that we were not able to entirely rule out the hypothesis that the relatively small sample size of this study may partially affect the results since the post-hoc power analysis revealed achieved power overall greater that 0.75 for "conditions"*"group" interaction but lower than 0.6 for between group comparisons.

These considerations apply also to the time-varying force matching task where no significant between-group difference was detected. We found that both groups were less accurate in reproducing the target force in phase 1 and 4, i.e. when the target force was ramping up and down respectively. In terms of bias error, the phase 4 was the most challenging and subjects systematically overshot the target force. This behavior is consistent with a delayed decreasing of the exerted force in the task's phase 4 and was found in both healthy controls and stroke survivors. Our data corroborated previous findings showing poorer performance both in terms of

accuracy and variability in matching a time-varying force compared to a fixed force (Kubota et al., 2012). Moreover, previous literature suggested that aging is associated with an impaired ability to rapidly vary the force exerted possibly making these tasks challenging for both patients with stroke and age-matched healthy controls included in our study (Kubota et al., 2012; Voelcker-Rehage & Alberts, 2005b).

Interestingly, although there was an inverse relationship between the subjects' accuracy and the target force level, the analysis on the CV showed an opposite trend: the higher the target force level, the lower the CV. However, this is not to be meant as a decrease of the absolute variability in the trials with the greater target force. In contrast, this suggested that the variability increase is not proportional to the force exerted.

The lifting task allowed us to detect the anticipatory grip force behavior in patients with somatosensory deficits. We did not find between-group significant difference in terms of time between the grip force onset and the movement start. The synchronization between the grip force and the holding force has been considered a peculiar feature of anticipatory behavior in object manipulation and has been widely investigated in healthy subjects and patients with sensory deficits due to either peripheric or CNS lesions (R. S. Johansson & Flanagan, 2009). In line with our results, previous studies showed that the time relationship between grip and load force is relatively preserved in stroke patients with sensory deficits (Hermsdörfer et al., 2003). It is conceivable that these patients may be able to use alternative cues, like visual input or previous learning to use residual internal predictive models (Hermsdörfer et al., 2003). In our experiment patients might also have taken advantage of the sensory information from the unaffected hand, that could have fed the forward model of the lifting action (Wolpert & Ghahramani, 2000). However, we found that patients exerted a greater normalized grip force during the lifting phase compared to healthy controls, suggesting an increased effort for lifting the BiSBox device. Notably this difference is likely not to be related to patients' strength deficits since we measured no significant difference in terms of MVC and we found a tendency to significant between-group difference in favor of

the SP group in the absolute maximal force exerted (t=1.925, p=0.07; Figure 29 bottom). In contrast, it is conceivable that our results corroborated previous research that found exaggerated grip force in patients with tactile sensory deficits due to stroke (Nowak et al., 2013). Moreover, we found that subjects in the SP group showed significantly longer delay between the time they reached the peak grip force and the end of the lifting. This may indirectly suggest that patients with stroke reached the peak force earlier, exerting a greater force, in order to make sure to avoid the device's slipping, and then took longer time to decrease the grip force and to approach the ending of the lifting (i.e the holding phase). In other words, patients were not able to estimate the grip force needed to lift the device and showed an altered timing of grip force modulation during the lifting phase. It is important to underline that the force matching tasks did not show any impairment in force modulation that could account for the between-group differences we measured in the lifting task. On one hand this may suggested that the lifting task unveiled specific motor planning impairment. On the other hand, this showed that during the force matching tasks patients might have relied on visual feedback to compensate for tactile sensory deficits. Finally, we were not able to find a learning effect across trials in the lifting task. We tried to account for this factor allowing the subjects to perform some trials before recording and eliminating the first three trials of the session. However, the greater force exerted by the patients may also be a consequence of an altered internal model of the device, which they hadn't had experienced before. The tactile sensation deficit, may have played a role in this behavior, altering the patients' sensorial experience of the object and making them slower than healthy controls in building its internal model (Nowak et al., 2004).

Noteworthy, in the present experiment we did not measure object's affordance. This concept was introduced in the late 70's and suggests that the mere vision of an object elicits a CNS pre-activation related to the different ways of possible interaction with it, even in the absence of the intent of acting. This ability is shaped by the object's physical properties the subjects had previously experienced or deduced by its observation. Although this concept is indeed related to motor planning and, therefore, to anticipatory motor control, and it is of interest for people

affected by stroke, we designed this experiment with the aim of ruling out as much as possible its influence. Object's affordance is in fact also involved in action selection and complex cognitive functions of paramount importance in motor behavior but of higher cognitive level then the predictive mechanism investigated in this study. Therefore, we design a setting where the experimenter made as clear as possible to the subject the device's grasping modality. Moreover, in the starting position the participants were asked to place their hands in the immediate proximities of the device's lateral force plates (avoiding touching them), with the aim of minimizing the UL's movements before the contact. Nevertheless, it would be informative for future studies to focus on a broader concept of anticipatory motor control, including in their investigations object's affordance and action selection impairment in patients with CNS stroke.

In conclusion, in the present study we used newly designed BiSBox device that allowed us to measure the grip force exerted along with kinematic parameters during a lifting task. Our analysis provided some evidence of impaired motor planning in patients with CNS stroke sequelae and somatosensory deficits. However, this study is affected by some limitations. Most importantly, the limited sample size did not provide sufficient statistical power in some comparisons, especially concerning the lifting task. Future works shall aim to reproduce these results with a greater sample, and to investigate learning effect across multiple repetition of lifting task in patients with stroke sequelae and sensory deficits.

Kinematic analysis of the index-to-nose task

The ability to perform fast and accurate reaching movements is essential for interacting with the environment using the upper limbs. Accurate control of fast UL movements requires that the motor system has access to information about the outcome of its commands. Although the somatosensory and visual feedback are the principal source of this information, relying only on such information leads to poor movement control. In fact, A sensorimotor feedback loop in human somatosensory system is indeed affected by a delay of the order of 80-150 ms which is remarkably long in the context of fast reaching (Scott, 2016). Therefore, a system that relies only on such a feedback control would result unstable and perform unnecessarily large out-of-phase corrections. A forward model could solve this issue providing the CNS with a prediction of the future sensory input that can feed an internal feedback loop before the actual sensory feedback is available (Mcnamee & Wolpert, 2019). The combination of forward model prediction and delayed sensory feedback ensures fast and stable movement performance.

There is compelling evidence that the cerebellum plays a key role in the implementation of a forward model (Kawato et al., 1987a; Tanaka et al., 2020; Wolpert & Ghahramani, 2000). Interestingly, recent literature suggested that the parietal cortex, and specifically the Posterior Parietal Cortex (PPC), is involved in the representation of the future state of the body and, through broad connections with the primary somatosensory cortex, contributes to the sense of proprioception (Cui, 2016; Desmurget et al., 1999; Parkinson et al., 2010; Reichenbach et al., 2014). Although upper limb reaching behavior in patients with somatosensory deficits caused by CNS lesions has been extensively studied, limited attention has been paid to the influence of these kind of deficits on predictive motor control.

The aim of this section was to analyze a 3-D reaching movement of stroke patients with cerebellar and somatosensory impairments and to compare their movements' kinematics with normative data on healthy age-matched subjects. With this aim we used an innovative technology for kinematic analysis based on a markerless system able to automatically reconstruct the human body's figure during movements.

Firstly, we tested the accuracy of this system on assessing upper limb's kinematics in comparison with the golden standard represented by an 8-camera optoelectronic motion capture system (Vicon, Oxford Metrics Ltd., Oxford, UK). Secondly, we used the markerless system to assess patients with stroke sequelae and healthy controls.

We hypothesized that patients would show abnormal kinematic pattern early after the movement onset and that error compensation during the movement would be consistent with a delayed control carried out by a feedback controller. The results would provide new insights in the mechanism underpinning the forward model in the context of upper limb movements.

On the Pose Estimation Software for Measuring Movement Features in the Finger-to-Nose Test[1]

Introduction

Upper Limb's (UL) movements are of paramount importance for effectively interact with the environment and to perform our daily activities. Among all the sensorimotor consequences of a cerebral stroke, UL impairments are one of the most disabling, leading to lack of independence and reduced quality of life (Hatem et al., 2016; Stinear et al., 2020). Stroke can affect all the domains involved in the UL movements, including somatosensation and strength along with motor control processes (Hatem et al., 2016). In clinical setting, sensorimotor and functional impairments of the UL are quantified using a variety of assessment scales in which the clinician visually scores the patient's ability of performing a defined action or movement (de los Reyes-Guzmán et al., 2014).

To overcome the lack of objectivity and the examiner- dependency of this clinical assessment, in the last decades new technological development has provided innovative and accurate tools for movement analysis. The most used tools for instrumental UL movement assessment are inertial measurement units (IMUs), optoelectronic systems for kinematic analysis and robotic devices (de los Reyes-Guzmán et al., 2014). Each of these tools are more appropriate and accurate in measuring specific movement's features. On the other hand, the use of such devices can alter the subject's performance introducing some additional sensorimotor inputs (like the sense of touch of the device or the device resistance to the motion) that can affect the movement performance (Schwarz et al., 2019).

Similar limitations have led to an increasing interest in adopting human pose estimation (HPE) software in the context of human motion analysis (Mehdizadeh et al., 2021). Beside the classical application fields, such as, sport performance

---

[1] © 2022 IEEE. Reprinted, with permission, from E. Martini, N. Valè, M. Boldo, A. Righetti, N. Smania and N. Bombieri, "On the Pose Estimation Software for Measuring Movement Features in the Finger-to-Nose Test," 2022 IEEE International Conference on Digital Health (ICDH), 2022, pp. 77-86, doi: 10.1109/ICDH55609.2022.00021.

analysis, human computer interaction, and action recognition, several research works started to adopt and evaluate such a computer vision technology for the analysis of pathological gait detection (Guo et al., 2021). In all these contexts, platforms based on human pose estimation software have proven to achieve good trade-off between accuracy, costs, portability, and easy of use. To the best of our knowledge, there is no work in literature that evaluates quantitatively the accuracy of pose estimation software in measuring UL movements, and in particular, in the UL kinematic assessment to extrapolate movement parameters. In this work we present an extended quantitative evaluation of HPE software for measuring movement parameters in the Finger-to-Nose Test - FNT (see Figure 30). We selected one of the most widespread and accurate pose estimation software (i.e., Openpose (Cao et al., 2021) and adopted a convolutional neural network trained for detecting detailed human body keypoints, including fingertips and nose. Then, we identified a meaning- ful set of kinematics features for the FNT and we defined the procedures to extrapolate each feature measurements from the sequence of keypoints provided by HPE software. We present the evaluation of the software accuracy by using an 8-camera infra-red motion capture system (i.e., Oxford Vicon) as ground truth on a set of 15 healthy and 5 post-stroke patients.

Finally, we addressed the problem of *automating* the param- eter extrapolation. Measuring the movement parameters for the FNT through both optoelectronics as well as video-based systems rely on the time segmentation of the video streams, in which start and stop of movements have to be identified. To avoid this error-prone manual step and subjectivity issues in the whole extrapolation pipeline, we propose an algorithm that implements the Automatic Time Segmentation (ATSA). We measured the accuracy of such an algorithm versus the time segmentation manually extrapolated by an operator from the video streams, on set of 26 healthy and 26 post-stroke subjects.
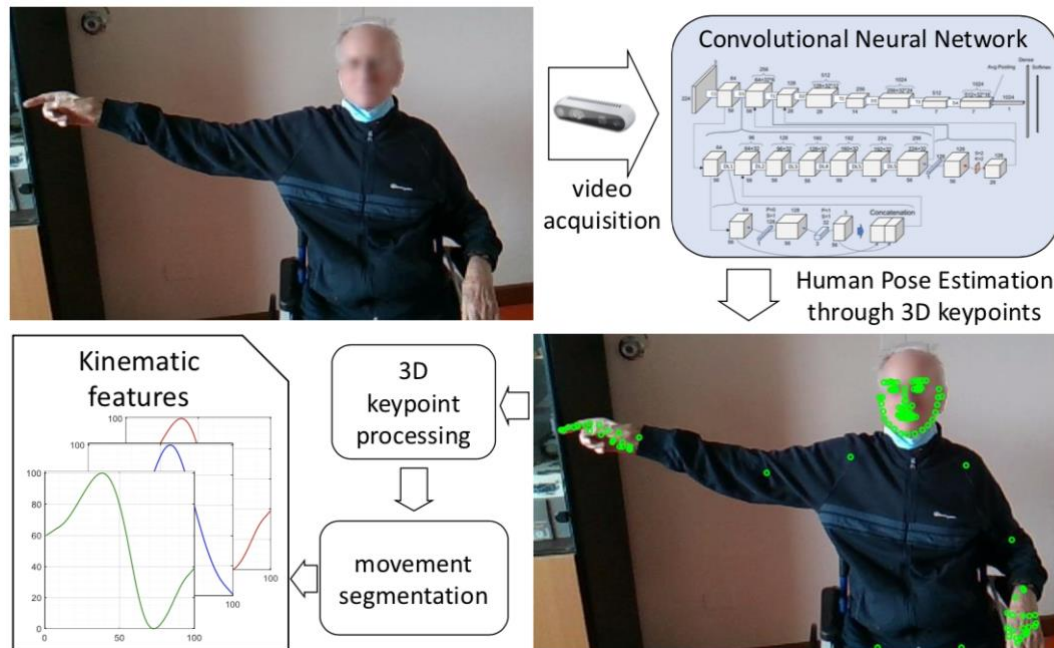
Figure 30 Extrapolation of movement features in the FNT through pose estimation software.

Background and related work

While strength, somatosensory and functional impairments have been widely studied and the literature have proposed a range of assessment measurements addressed to these domains, motor control impairments are more challenging to be measured (Santisteban et al., 2016). These impairments can arise as a consequence of primary sensorimotor deficits or from specific motor control processes' dysfunctions such as feedback or feedforward impairments (Frey et al., 2011). In these cases, the patient's strength and somatosensory functions could be normal, but when the patient is asked to perform an UL movement, this would be inaccurate, presenting a variety of abnormalities ranging from lack of smoothness, abnormal velocity and acceleration patterns or lack of coordination between different joints, eventually leading to inability to perform functional activities (Bastian et al., 1996). The assessment of motor control impairments in clinical practice is challenging as it requires the measurement of the upper limb's kinematics during the execution of a functional movement. In this context, reaching and pointing tasks are the most commonly investigated movements in clinical settings. Patients are asked to perform fast UL's movements to touch a target, usually with the index fingertip.

The target can be placed in front of them or can be a part of patient's body like the tip of his/her nose (index-to-nose task). The index-to-nose task (FNT) is commonly performed during the neurological exam to assess patient's UL motor control impairments (Schmitz-Hubsch et al., 2006). In the assessing of these pointing movements, clinicians focus their observation on movement tremor, deviations from the ideal trajectory, spatial errors in target reaching (dysmetria), excess of speed or slowness and multi-joints coordination. However, this kind of clinical evaluation via movement observation is subjective to personal interpretation, and affected by lack of sensitivity, poor reproducibility and resolution, and floor and ceiling effects (Krabben et al., 2011) and previous literature recommended the application of instrumental movement assessment in stroke rehabilitation (Kwakkel et al., 2017). Furthermore, a recent research suggested that the kinematic analysis of the FNT provides clinicians with information not available from standard movement observation (G. M. Johansson et al., 2017).

Although the literature is heterogeneous in defining the metrics of interest, previous reviews suggested a set of parameters to be used when assessing the UL movements (de los Reyes-Guzmán et al., 2014; Garro et al., 2021; Nordin et al., 2014; Zollo et al., 2011). Concerning the kinematics of the hand (the end-point in a reaching task) the review of De Los Reyes-Guzmàn et al. identified a set of metrics, each examining a specific aspect of UL's movement computed from hand's trajectory, speed and acceleration profile(de los Reyes-Guzmán et al., 2014). The mostly investigated include the time of execution, the maximum hand velocity throughout the movement, the path ratio (the ratio between the straight line linking the start position and the target and the length of the actual trajectory), the number of velocity peaks throughout the movement, the time to peak velocity, the target error and the jerk (de los Reyes-Guzmán et al., 2014).

The most used tools for instrumental UL movement assessment are inertial measurement units (IMUs), optoelectronic systems for kinematic analysis and robotic devices (de los Reyes-Guzmán et al., 2014). Each of these tools are more appropriate and accurate in measuring specific movement's features. The inertial sensors measure angular velocity and linear acceleration in orthogonal axis referred

to a reference system based on the sensor itself. However, recent versions of IMUs include magnetometers that allow identifying the orientation of the sensor respect to the Earth's magnetic field. IMUs have the advantage of being relatively inexpensive, and are particularly useful for measuring the subjects' level of activity in their daily life (Leuenberger et al., 2017). Specifically, previous studies used data from IMUs to compare the overall level of activity of the affected and unaffected arms (Lee et al., 2018). However, the fact that stroke subjects' UL movement are often slow and irregular, hampers their use in the assessment of specific and multi-joints movement like reaching tasks and require sophisticated feature extraction techniques (Krishna et al., 2019; Maceira-Elvira et al., 2019). The most commonly extracted features using IMUs include movement intensity, signal amplitude, signal energy and data from the frequency domain (Maceira-Elvira et al., 2019). Kinematic three-dimensional analysis involves retroreflective markers fixed to the patient's body that reflect the light emitted by the cameras (Roche et al., 2019). The cameras detect the marker's position in the 3-D space and related software are able to reconstruct the marker's trajectories and derive its velocity and acceleration patterns (Adans-Dester et al., 2020). Given that the markers are extremely light and small (around 1 cm^3), these systems have limited interference with patients' movement. However, the setting preparation is time consuming and the cameras are expensive. Moreover, the assessment is subjected by the examiner's precision of placing the markers on the landmarks. Optoelctronic systems are useful for assessing kinematics parameters of UL reaching while they are less accurate in estimating the movement's dynamics. In the context of a reaching task, the reconstruction of the markers' trajectories allows extracting a series of features including, velocity patterns, time and position of peak velocity, the number of velocity peak and others (de los Reyes-Guzmán et al., 2014).

Finally, robotic devices represent another cornerstone of the instrumental UL movement analysis in stroke subjects. Although they have been primarily used as a rehabilitative tool to assist the physiotherapist during the treatment, robotic devices can provide a variety of data including torques, forces and position that can be used to assess the patient's movements (Garro et al., 2021; Scott & Dukelow, 2011). In the last decades they have been widely used in this field allowing neuroscientists to

perform seminal studies on human UL movement control and stroke rehabilitation (Resulaj et al., 2009; Rodgers et al., 2019). Robotic devices allow the assessment of several UL's movement features referring to different domains. Interestingly, along with parameters related to primary sensorimotor impairments like strength or proprioceptive deficits, these devices provide data that clinicians can use to infer UL's motor control deficits including movement smoothness, peak velocity, spatial errors and trajectory's abnormalities (Nordin et al., 2014; Resulaj et al., 2009).

Measuring human pose variables using computer vision has been increasingly applied in the recent years to assess mobility and risks of fall as well as to identify gait features in parkinsonism and other neurological diseases (Rupprechter et al., 2021; Sabo et al., 2020). Quantifying gait pathology with commodity cameras increases access to quantitative motion analysis in clinics and at home and enables researchers to conduct large-scale studies of neurological and musculoskeletal disorders (Kidziński et al., 2020).

Several solutions have been also proposed to combine hu- man pose estimation with CNN architectures for classification between normal and pathological gait in humans, with ability to provide information about the detected alterations from the extracted skeletal (Rohan et al., 2020). To achieve high accuracy, the majority of these solutions rely on OpenPose (Cao et al., 2021), an open-source framework that uses a non-parametric representation (i.e., part affinity fields - PAFs) to associate body parts with individuals in the image.

Some solutions adopt the Kinect sensor to estimate the 3D skeleton. In (Antico et al., 2021), the authors compared the accuracy of the new Azure Kinect DK and shown that such a sensor is highly accurate in tracking body movements.

More advanced solutions have been recently proposed to implement 3D HPE with RGB cameras. An example is the mobile system presented by Guo et al. (Guo et al., 2019)to track humans and analyze their gait in canonical coordinates based on a single RGB-D camera. To alleviate the effects of viewpoint diversity, Wei et al. proposed a view-invariant 3D HPE module (Wei et al., 2020). Zimmermann et al.

demonstrated that HPE by leveraging both RGB and depth images performs better than using depth data alone (Zimmermann et al., 2018).

In (Mehdizadeh et al., 2021), the authors compared the accuracy of three different HPE software (AlphaPose, OpenPose, Detectron) for gait analysis by considering a 3D motion capture system as golden model. They underlined that there are important opportunities to evaluate models capable of 3D pose estimation in video data, improve the training of pose-tracking algorithms for older adult and clinical populations, and develop video-based 3D pose trackers specifically optimized for quantitative gait measurement. A similar comparison between 2D HPE with Openpose and the Vicon motion capture system has been presented in (Ota et al., 2021). The authors evaluated the software accuracy to measure pelvic segment angles, hip, knee, and ankle joint angles during treadmill walking and running. An orthogonal analysis of the 2D HPE accuracy has been conducted in (Åberg et al., 2021). The results underline that such a CNN-based method for extraction of gait parameters from video appears suitable for valid and reliable quantification of gait.

To the best of our knowledge, the quantitative evaluation of the pose estimation software at the state of the art in measuring UL movements is missing. This work focuses on measuring the achieved accuracy and understanding whether the discrepancy between this technology and a motion capture system can lead to different clinical interpretations.
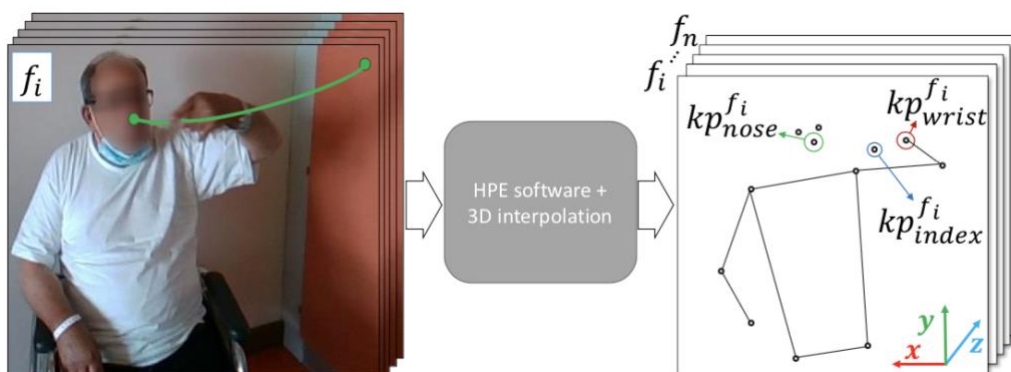
Figure 31 Overview of the per-frame elaboration of the human pose estimation software.

Methods

Kinematic testing protocol

An 8-camera motion capture system (Vicon, Oxford Metrics Ltd., Oxford, UK) was used to track the upper body during movements. The data, recorded at 100 Hz, were assumed as golden model. Six markers were placed by a physiotherapist on each subject's UL. The selected landmarks were: Styloid processes, Humeral Lateral and Medial epicondyles, Humeral Lesser tubercle, Acromion. Subjects were sitting on a chair, 45 cm high with a backrest, in the center of the room and were assessed while performing the FNT.

During each trial, study participants were instructed to reach at a self-selected speed their nose. In the starting position the subjects sat still with their shoulder abducted at 90°, fully extended elbow and hand closed into a fist except for the index. They kept this position until the examiner's "Start" signal. At this point they were asked to touch their nose with the index fingertip flexing their elbow. Each video take consisted of 7 consecutive index-to-nose movements for each UL with eyes open. Between each trial, subjects were provided with "stop" and "go" signals by a physiotherapist. The task was recorded by both the RGB-D camera and the opto-electronic system simultaneously. The resulting signals from the two devices have been synchronized by cross-correlation in post processing.

Participants

This study included healthy participants and post-stroke patients. Participants were recruited from the Neuromotor and Cognitive Rehabilitation Research Centre (CRRNC) of the University of Verona, Italy. All participants were informed regarding the experimental nature of the study and informed consent was obtained from all subjects. Healthy controls with no concomitant UL pain or mobility impairment and no history of neurological diseases were recruited. The local ethics committee approved the study. Post-stroke outpatients were recruited according to the following selection criteria. Inclusion criteria were: age ≥ 18, diagnosis of stroke confirmed by a specialist in neurology and by radiologic findings (CT or MRI),

time from stroke ≤ 1 year, Trunk Control Test score = 100/100, strength of shoulder abductors and elbow flexors ≥ 3/5 MRC (Medical Research Council Scale for Muscle Strength), signature of the informed consent. Exclusion criteria were the presence of severe cognitive, visual or communication impairments and other concomitant neurological or orthopedic diseases interfering with patients' capacity of providing the informed consent or performing the required task.

Data Analysis

The human pose estimation software retrieves each frame of the video sequence from an input camera as shown in Figure 31. For each frame fi, the software performs an inference step through a convolutional neural network (CNN) to extrapolate the set KPS of keypoints:

$$KPS = \{kp^{fi}_j : i = 1..|V\ F|, j = 1..|CNN\ kps|\} \qquad (20)$$

where |CNN kps| is the maximum number of keypoints detected thorugh the adopted CNN per frame, and |V F | is the number of video frames processed.

We selected Openpose (Cao et al., 2021), as it is one of the most accurate and widespread HPE solutions at the state of the art (Mehdizadeh et al., 2021). We selected the BODY 25 model trained with the COCO (T.-Y. Lin et al., 2014) and MPII datasets (Andriluka et al., 2014) to extrapolate a set K P S of 25 keypoints, including nose and wrist. We configured Openpose to include the hand detector feature (Simon et al., 2017), which allows us to extend the original set of keypoints with additional 20 keypoints to include the fingertip. We adopted an Intel RealSense D415 RGB-D as input camera. Each frame consists of an RGB image (848×480×3 8-bit matrix) and a depth image (848×480 16-bit matrix). To extract the 3D coordinates in space of each keypoint, the platform implements the interpolation of the 2D coordinates extrapolated by Openpose with the depth matrix information as for the back-projection algorithm (Hartley, 2004).

Each final keypoint $kp^{fi}_j = (x, y, z)$ represents a joint of the human skeleton, where x, y, and z are the 3D coordinates of the keypoint. In particular, we evaluated the movement features through the keypoints associated to the nose (kpfi nose), finger

tip (kpfi finger), and wrist (kpfi wrist), as shown in Figure 31 We define fonset and foffset the couple of video frames that identify the start (see Figure. 31) and stop (when the subject touches the nose with the index fingertip) of the FNT movement, respectively. We define tonset and toffset the time instants (time stamps) associated to frames fonset and foffset, respectively.

Previous studies on stroke subjects that included upper limb kinematic assessment focused on a variety of movement parameters referring to either time or spatial domains (de los Reyes-Guzmán et al., 2014; Shi et al., 2011). A recent literature review suggests the most relevant features in the assessment of stroke subjects. Following these indications, we focus on the following ten features.

1) Movement duration: In the time domain, the movement duration indicates the time interval from the start of the movement to the target reaching. The movement duration is clearly linked to the average velocity of the subject's hand and can be interpreted as a measure of movement efficiency. Previous studies suggested that stroke subjects perform slower movements compared to healthy age-matched controls (Adans-Dester et al., 2020). We define movement duration T as follows:

$$T = \text{toffset} - \text{tonset} \qquad (21)$$

2) Length of the hand trajectories: In the spatial domain, the total displacement measures the length (in cm) of the hand trajectory in the three-dimensional space (Wu et al., 2007a). This measure can be interpreted as an indication of directness of the movement. The longer the hand path, the less direct and efficient is the movement. Referring to stroke subjects, straighter movements with shorted hand trajectories has been linked to improved movement planning and multi-joints coordination abilities (Archambault et al., 1999). Considering the distance between two 3D keypoints:

$$\text{dist}(a, b) = \sqrt{(x_a - x_b)^2 + (y_a - y_b)^2 + (z_a - z_b)^2} \qquad (22)$$

we define the trajectory length l of the hand as the sum of the absolute distances (Δp) between subsequent positions of the wrist keypoint:

$$\Delta p = \{\text{dist}(kp_{wrist}^{fi}, kp_{wrist}^{fi-1}): i = 2..n\} \tag{23}$$

$$l = \sum_{i=2}^{n} \Delta p_i \tag{24}$$

3) Normalized cartesian velocity shape: Cartesian velocity is the magnitude of the velocity vector of the index finger. The shape of the velocity pattern is commonly used by clinicians to evaluate from a behavioural perspective the quality of the subject's movement. It is well known that the kinematic profile of a pointing task is rather consistent across healthy subjects. The velocity pattern of the index finger shows a roughly symmetric bell-shape with the velocity peak approximately at half of the movement (Day et al., 1998). In the clinical practice, when a 3D movement analysis is performed, the velocity pattern evaluation is performed by visually inspecting the hand velocity as a function of the movement progression, expressed as a percentage of the entire movement. To compare movements from subjects with different anthropometric features, it is necessary to normalize the data regarding absolute speed and time execution of the movement. Eqn 25 defines the velocity displacement vector v in terms of position distances Δp (eqn(23) by considering kpfi wrist as observed keypoint) over the time elapsed between subsequent positions Δt:

$$v = \left\{\frac{\Delta p_i}{\Delta t_i}: i = 2..n\right\} \tag{25}$$

$$\Delta t = \{t_i - t_{i-1}: i = 2..n\} \tag{26}$$

We define the normalized cartesian velocity v_{norm} and the normalized time vector t_{norm} as follows:

$$v_{norm} = \left\{\frac{v_i - v_{min}}{v_{max} - v_{min}}: i = 2..n\right\} \tag{27}$$

$$t_{\text{norm}} = \left\{ \frac{t_i - t_1}{t_n - t_1} : i = 2..n \right\} \qquad (28)$$

Where

$$v_{\text{max}} = \max_{i \in \{2..n\}} v_i \qquad (29)$$

$$v_{\text{min}} = \min_{i \in \{2..n\}} v_i \qquad (30)$$

4) Average velocity: It represents the mean three- dimensional velocity of the hand relative to the subject's body. The mean velocity can be considered as a general measure of efficiency of the upper limb movement. In order for a movement to be effectively used in the domestic and daily environment, this has to be sufficiently precise and fast. On the other hand, the overall mean velocity of the movement is a relatively rough parameter and does not capture any specific abnormalities in the velocity pattern of the movement. Previous studies showed that stroke subjects perform the FNT slower than healthy controls (Day et al., 1998; Honda et al., 2020). However, especially in stroke subjects, a faster pointing movement does not necessarily mean a more precise and effective reaching. We define the average velocity as $v_{(avg)} = \frac{l}{T}$, l and T from Eqns. 24 and 21, respectively.

5) Peak velocity: The absolute value of the peak velocity is the maximum of the absolute three-dimensional speed throughout the entire movement. It is a measure of how fast the subject can perform a reaching movement irrespective to its precision. The higher the correlation between the peak velocity and the mean velocity, the more consistent and repetitive the movements are. In contrast, great values of velocity peak in association with relatively slow average velocity suggest high speed variability and possibly longer and sub-optimal trajectories. The literature suggests that moderately impaired stroke subjects have lower amplitude in peak velocity (Johansson et al., 2017). Eqn 29 defines this feature.

6) Percentage of movement time with max velocity: The percentage of movement when the maximum of velocity occurs is the proportion of movement time spent between the start of the movement and the velocity peak (Johansson et al., 2017).

This feature is related to the ability of movement planning and feed-forward motor control (Wu et al., 2007b). It is well known that in healthy subjects the velocity peak is reached roughly at half of the movement, while previous reports showed that stroke subjects tend to show left-shifted velocity profile, due to the earlier occurrence of the maximum of velocity (Johansson et al., 2017). This common behavior can be interpreted as a strategy to improve the control in the latter part of the movement, when the hand is slowing down. This could help the subjects to improve the precision of the pointing, which is the ultimate goal of a pointing task such as the FNT. The time percentage of movement of maximum velocity $t_{max\%}$ is the jth element of the normalized time vector t_{norm} (Eqn 28), where j is the index of the maximum element in velocity vector v (Eqn 25):

$$t_{\mathrm{max\backslash\%}} = t_{norm\,j} \cdot 100 \tag{31}$$

$$j = argmax_{i \in \{2..n\}} v_i \tag{32}$$

7) Percentage of spatial position at max velocity: The peak of the velocity can be described in terms of position relative to the hand path length. Along with temporal occurrence, in healthy subjects the velocity peak is reached around the half of the movement path. In stroke subjects however the spatial and temporal relative occurrence of the maximum of speed may not coincide. For example, while it has been previously reported that patients with stroke tend to anticipate the timing of velocity peak (Johansson et al., 2017), this may not be the case for the spatial position of the peak. Overall, this feature provides information about the symmetry of the movement in the acceleration and deceleration phases. Eqn 33 represents this feature by dividing the sum of the first j elements of Δp with the trajectory length l (Eqn 24), where j is the index of the absolute maximum in velocity vector v (Eqn 25):

$$\Delta p_{\mathrm{max\backslash\%}} = \frac{\sum_{i=2}^{j} \Delta p_i}{l} \cdot 100 \tag{33}$$

$$j = argmax_{i \in \{2..n\}} v_i \tag{34}$$

8) Number of velocity relative peaks: Along with the over- all speed and accuracy of the movement, previous studies on upper limb kinematic included in their analysis the movement smoothness. Although this feature can be estimated in different ways, the most common one involves the sum of the local maximum of the three-dimensional velocity throughout the movement (G. M. Johansson et al., 2017; K.-C. Lin et al., 2007; Wu et al., 2007a). A perfectly smooth reaching should include only one local peak of velocity (in this case an absolute peak of velocity) while the presence of more peaks suggest that a number of corrections have been performed during the movement. The vector of velocity peaks v$_{peaks}$ is composed by the local maxima of the velocity vector vi, obtained in (6), as follows:

$$v_{\text{peaks}} = \{v_i | i \in \{2..n-1\} \wedge v_i > v_{i-1} \wedge v_i > v_{i+1}\} \tag{35}$$

9) Early movement velocity after 150 ms: The early phase of a reaching movement is of particular interest from a motor control perspective. Given that the proprioceptive feedback is affected by an intrinsic delay of 150/200 ms, in this time window after movement onset, the feedback is not yet available, and movement is led only by feed-forward motor control. From a clinical perspective, the hand speed within this time window is of paramount importance in a reaching task kinematic analysis. It has been previously showed that velocity abnormalities in this early movement phase are likely to be related of inverse model impairment in patients with cerebellar lesions (Bhanpuri et al., 2014). This parameter is impossible to assess in a daily clinical setting when patients are assessed by a physician without the use of accurate systems for upper limb movement analysis. We define this feature as follows:

$$v_{(150ms)} = \{v_i | i \in \{2..n\} \wedge t_i = 0.150\} \tag{36}$$

10) Normalized cartesian acceleration shape: The acceleration phase is said to be related to the pre-planned aspects of movement where asymmetries between the acceleration and deceleration phases suggests impairments in feed-forward motor control (Grosskopf & Kuhtz-Buschbeck, 2006). The acceleration phase is defined

as the movement sections between the movement start and the absolute velocity peak. In contrast, the deceleration phase is defined as the remaining part of the reaching, until the touch of the nose. We define the acceleration displacement vector a in Eqn 37 by dividing the velocity v (Eqn 25) with the time elapsed between subsequent positions Δt. The normalized cartesian acceleration norm is obtained as for equation 40:

$$a = \left\{ \frac{v_i}{t_i - t_{i-1}} : i = 3..n \right\} \tag{37}$$

$$a_{(max)} = \max_{i \in \{3..n\}} a_i \tag{38}$$

$$a_{(min)} = \min_{i \in \{3..n\}} a_i \tag{39}$$

$$a_{\text{norm}} = \frac{a_i - a_{\min}}{a_{\max} - a_{\min}} : i = 3..n \tag{40}$$

At the state of the art, the couple f_{onset} and f_{offset} (and the corresponding t_{onset} and t_{offset}) are identified manually for each FNT movement by an operator. Coderre et al. (Coderre et al., 2010) suggested a semi-automatic method for such a task through a sliding backward algorithm. It consists of a first coarse segmentation step, by which the operator manually identifies the movements from the video sequence. Then, from each phase, they extrapolate t_{onset} and t_{offset} by comparing the wrist velocity against a velocity threshold (5% of the maximum wrist velocity). The threshold allows the algorithm to distinguish the stationary from the movement state. Even though this approach achieves a fair accuracy w.r.t. the totally manual segmentation, it requires a manual and subjective intervention. In addition, due to the natural fluctuation of the wrist velocity between subsequent movements, it becomes sensitively inaccurate without the manual intervention.
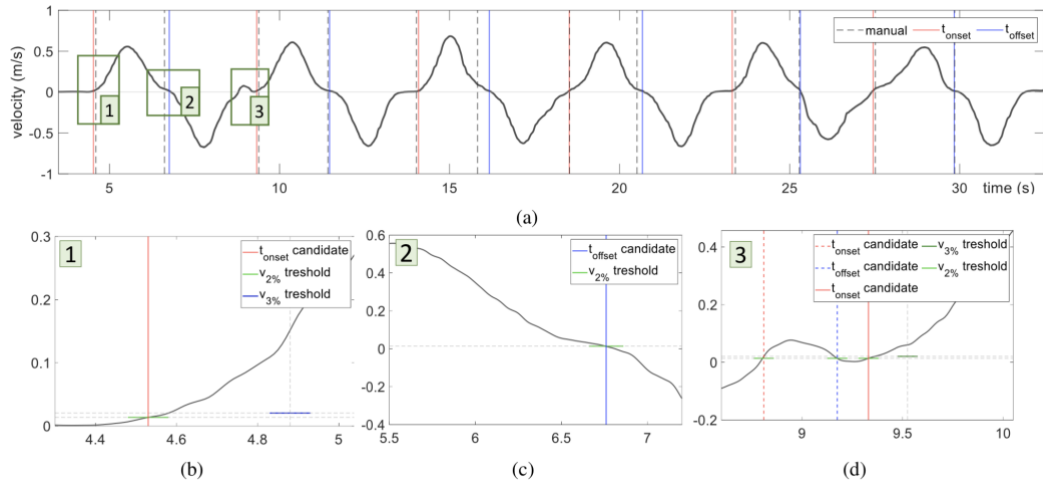
Figure 32 Example of automatic vs. manual segmentation: (a) Wrist velocity of a sequence of seven movements. Numbered boxes zoom in the first three couples of onset and offset instants identified by the proposed algorithm from the velocity vector and those identified manually from the video images. (b) First condition holding that identifies an onset. (c) Duration condition holding that discards a false positive segment

We propose an Automatic Time Segmentation Algorithm - ATSA (Figure 33) that implements the fully automatic movement segmentation in $O(|V\,F\,|)$ by analysing the velocity displacement vector (Eqn 25) of the wrist. In our experimental setup, for a fair comparison w.r.t. the manual segmentation, we considered the 2D velocity of the wrist (axes x and y in Figure 31) as it is the velocity observable by the human operator. Then, we propose two velocity thresholds, which identify the start of the voluntary movement and the confirmation of the temporally continuous movement. We heuristically identified these two values in 2% and 3% of the maximum wrist velocity ($v2\%$ and $v3\%$ in the following). The algorithm definition is independent from these values.

Starting from frame f0, the algorithm extrapolates every couples of instants t_{onset} and t_{offset} that represent the movements in the video. For each frame, it searches for a candidate onset instant to that satisfies the following conditions:

- Every t_{onset} identified in the previous frames has to be coupled with a corresponding t_{offset}, so that the T_{onset} and T_{offset} have the same number of elements. This allows us to detect only complete FNT movements.

136

- Wrist velocity at instant i (v_i in the algorithm) is higher than the velocity threshold $v_{2\%}$, while t_{i-1} is lower than $v_{2\%}$. This allows identifying t_i as the start of the voluntary movement.

- After an interval of $k_{3\%}$ frames, the wrist velocity has to become greater than the second threshold $v_{3\%}$. This allows to confirm the temporally continuous movement and to avoid false positive movements due to fluctuations. Figure 32 shows, for example, the onset candidate (red line) identified in the first movement of the sequence of Figure 32 a.

Algorithm 1 Onset-Offset segmentation algorithm.

1: INITIALIZE $T_{\text{onset}} = \emptyset$, $T_{\text{offset}} = \emptyset$, $j = 0$
2: **for** each frame f_i ($i = 0, .., |VF| - k_{3\%}$) **do**
3:      {Step 1: Identification of candidate t_{onset}}
4:      **if** $(|T_{\text{onset}}| = |T_{\text{offset}}|) \wedge (v_i > v_{2\%}) \wedge$
         $\wedge (v_{i-1} \le v_{2\%}) \wedge (v_{i+k_{3\%}} > v_{3\%})$ **then**
5:          $T_{\text{onset}} \leftarrow T_{\text{onset}} \cup \{t_i\}$
6:          $j \leftarrow i$

7:          {Step 2: Identification of candidate t_{offset}}
8:      **else if** $(|T_{\text{onset}}| > |T_{\text{offset}}|) \wedge (v.x_i \le v_{2\%}) \wedge$
         $\wedge (v_{i-1} > v_{2\%})$ **then**
9:          $T_{\text{offset}} \leftarrow T_{\text{offset}} \cup \{t_i\}$
10:          **if** $t_i - t_j \le k_{\text{duration}}$ **then**
11:             $T_{\text{onset}} \leftarrow T_{\text{onset}} - \{t_j\}$
12:             $T_{\text{offset}} \leftarrow T_{\text{offset}} - \{t_i\}$
13:          **end if**
14:      **end if**
15: **end for**

Figure 33 Onset-Offset automatic segmentation algorithm.

The algorithm (Figure 33) identifies the subsequent offset by searching for the instant in which the wrist velocity goes lower than the first threshold (e.g., Figure 32c).

To prevent false positive due to larger shakes, the algorithm also implements a movement duration check (line 10, Figure 33). If the difference between the

candidate offset and onset is below a pre-defined duration threshold ($k_{duration}$), both candidates are discarded (e.g., Figure 32d). Following the definitions of voluntary movement and temporally continuous movement proposed in literature (Daunoraviciene et al., 2018; Wagner et al., 2008), and by considering the architectural characteristics of our camera (i.e., sampling rate), we set $k_{3\%} = 35$ frames and $k_{duration} = 0.4$ s for our experimental analysis.

Results

To measure the accuracy of the HPE software, 15 control subjects (7 males and 8 females) and 5 patients were involved. To measure the accuracy of the automatic segmentation algorithm, 26 control subjects (13 males and 13 females) and 20 patients with stroke (10 males and 10 females) participated in the study. The mean age of the control subjects was 28.2 ± 5.1 years and that of the patients was 63.4 ± 13.4 years. Clinical and demographic data are reported in Table 4

Table 4 Post-stroke group clinical and demographic features.

Patient	Sex	Age	Affected limb	Time since stroke onset (days)	Type of ictus
0	Male	53	Right	39	Ischemic
1	Male	55	Right	207	Ischemic
2	Female	63	Left	181	Hemorrhagic
3	Male	60	Right	36	Hemorrhagic
4	Male	59	Left	59	Ischemic

Accuracy of the extracted features

The values of the features presented were compared using the opto-electronic system as ground truth. For this analysis, data from 15 healthy controls and 5 stroke patients were included: 30 video takes were recorded for healthy subjects and 10 for post-stroke patients, each consisting of 7 index-to-nose trials. Marker-less and marker-based data were manually split in onset and offset by a clinician watching the videos. Due to errors during the acquisition, 2 video takes have been excluded from the analysis (healthy subject n.3 left arm, and healthy subjects n. 7 right arm) leading to a total of 38 video takes and 266 movements analyzed. Table 5 reports the measure of each feature extrapolated from the markerless system (Openpose) and the corresponding accuracy, which is defined as the difference w.r.t. the

measure extrapolated with the MoCap. In general, no significant difference in the measurements between the control group and the post-stroke group (i.e., mean absolute error - MAE) has been observed for every feature.

Accuracy of time segmentation

The accuracy of the automatic segmentation algorithm has been evaluated w.r.t. the manual segmentation performed by experienced clinicians who analyzed the videos. For this analysis 26 healthy controls and 20 stroke patients were included. Each subject completed 2 video takes (one for each arm) leading to a total of 364 index-to nose movements for healthy controls and 280 for stroke patients. Figure 34 shows the results. Overall, we measured a MAE of the automatic approach equal to 0.057s (0.051s for the control group, and 0.066s for the post-stroke group).

Finally, we evaluated the impact of the automatic segmentation step on the accuracy of the HPE software in measuring the movement features. As expected, we found that ATSA affects the overall software accuracy. On the other hand, the differences between the measures extrapolated with the HPE software with manual segmentation with those extrapolated with the automatic segmentation are negligible (see Table 6 vs. Table 5 for automatic vs. manual, respectively). In particular, considering the MoCap as ground truth, ATSA increases the error of the HPE software less than 1.7% in measuring the trajectory length and position percentage of maximum velocity. The additional error is less than 3% when measuring the maximum velocity, average velocity, and time percentage of maximum velocity. The error increases up to 5% for the number of velocity peaks and velocity after 150 ms.

Overall, the normalized shape of velocity and acceleration are closely approximated (see Table 7), with correlation coefficient $\rho > 0.93$ and pval < 0.001.

Table 5 Kinematic outcomes of the Finger-to-Nose test in all participants. The features are obtained with the markerless system, and the error is the difference between the markerless system values and the golden model. Features from both systems are obtained with manual time segmentation, performed by an expert clinician

| Subject	Arm	Trajectory Length (m)		Maximum Velocity (m/s)		Average Velocity (m/s)		Time Percentage of Max Velocity (%)		Position Percentage of Max Velocity (%)		Number of Velocity Peaks (#movements)		Velocity after 150 ms (m/s)	
		Measure	Error	Measure	Error	Measure	Error	Measure	Error	Measure	Error	Measure	Error	Measure	Error
Control Group															
0	R	0.668	0.012	0.943	0.069	0.450	0.022	31.000	-1.000	36.000	-2.000	1.000	0.000	0.369	0.002
0	L	0.693	0.029	1.098	0.045	0.575	0.017	39.000	0.000	44.000	-4.000	1.000	0.000	0.448	-0.045
1	R	0.629	-0.009	1.520	0.189	0.715	-0.024	48.000	1.000	55.000	2.000	1.000	0.000	0.769	0.111
1	L	0.582	0.005	1.293	-0.109	0.783	0.033	40.000	9.000	50.000	5.000	1.000	0.000	0.927	-0.316
2	R	0.656	0.014	0.924	0.031	0.557	-0.007	50.000	9.000	52.000	10.000	1.000	0.000	0.356	-0.013
2	L	0.664	0.066	0.850	0.064	0.558	0.052	47.000	8.000	49.000	6.000	1.000	0.000	0.401	-0.068
3	R	0.656	0.020	1.140	0.120	0.681	0.066	40.000	-5.000	40.000	-7.000	1.000	0.000	0.512	0.048
4	R	0.690	-0.003	0.992	-0.020	0.652	0.003	51.000	-1.000	52.000	-3.000	1.000	0.000	0.472	-0.007
4	L	0.711	0.055	1.183	0.101	0.719	0.056	43.000	13.000	46.000	6.000	1.000	0.000	0.630	-0.306
5	R	0.646	-0.020	1.040	-0.052	0.616	-0.019	47.000	5.000	50.000	5.000	1.000	0.000	0.486	-0.032
5	L	0.632	0.054	1.118	0.011	0.670	0.045	39.000	-9.000	39.000	-14.000	1.000	0.000	0.613	0.074
6	R	0.704	0.034	0.841	0.041	0.524	0.025	45.000	8.000	48.000	10.000	1.000	0.000	0.358	-0.017
6	L	0.661	0.074	1.075	0.167	0.620	0.065	48.000	9.000	49.000	-1.000	1.000	0.000	0.512	-0.130
7	L	0.666	0.051	1.334	0.087	0.800	0.097	45.000	2.000	46.000	-2.000	1.000	0.000	0.592	-0.023
8	R	0.640	-0.010	1.000	0.048	0.599	-0.010	48.000	4.000	50.000	4.000	1.000	0.000	0.469	-0.029
8	L	0.725	0.065	1.258	0.140	0.733	0.066	50.000	8.000	53.000	7.000	1.000	0.000	0.571	-0.048
9	R	0.732	0.033	1.062	0.074	0.633	0.020	46.000	2.000	44.000	0.000	1.000	0.000	0.362	-0.091
9	L	0.639	0.021	0.995	0.038	0.588	0.020	45.000	-2.000	46.000	-2.000	1.000	0.000	0.392	0.041
10	R	0.609	0.025	1.051	-0.048	0.593	0.017	46.000	-7.000	42.000	-8.000	1.000	0.000	0.285	0.101
10	L	0.692	0.053	1.122	0.117	0.663	0.056	50.000	1.000	49.000	1.000	1.000	0.000	0.444	0.017
11	R	0.782	0.000	1.192	-0.132	0.761	-0.007	42.000	0.000	39.000	-3.000	1.000	0.000	0.503	-0.011
11	L	0.800	0.037	1.277	0.076	0.705	0.032	47.000	-2.000	49.000	-6.000	1.000	0.000	0.648	-0.077
12	R	0.579	0.019	0.968	0.058	0.555	0.014	49.000	5.000	50.000	5.000	1.000	0.000	0.327	0.025
12	L	0.619	0.057	0.990	0.102	0.544	0.049	47.000	0.000	51.000	0.000	1.000	0.000	0.359	0.040
13	R	0.713	0.077	0.648	0.141	0.324	0.022	48.000	4.000	49.000	4.000	1.000	0.000	0.127	-0.000
13	L	0.744	0.108	0.665	0.190	0.364	0.049	48.000	1.000	52.000	3.000	2.000	1.000	0.126	0.025
14	R	0.700	0.003	0.875	-0.028	0.441	0.001	63.000	1.000	56.000	-1.000	1.000	0.000	0.065	0.011
14	L	0.642	0.003	1.030	0.005	0.596	0.018	54.000	1.000	51.000	0.000	1.000	0.000	0.220	-0.008
MAE			0.034		0.081		0.033		4.214		4.286		0.036		0.061
Post-Stroke Group															
0	R*	0.583	0.023	1.060	0.030	0.447	0.050	65.000	4.000	65.000	12.000	2.000	1.000	0.087	0.001
0	L	0.646	0.034	1.088	-0.016	0.545	0.033	57.000	2.000	54.000	0.000	1.000	0.000	0.204	-0.003
1	R*	0.551	-0.017	0.778	-0.073	0.415	0.008	43.000	4.000	44.000	5.000	1.000	0.000	0.155	0.018
1	L	0.678	-0.001	1.059	0.033	0.626	-0.010	48.000	4.000	50.000	5.000	1.000	0.000	0.417	-0.012
2	R	0.724	0.007	1.039	-0.008	0.569	0.006	52.000	2.000	55.000	2.000	1.000	0.000	0.355	-0.001
2	L*	0.804	0.072	0.872	0.057	0.354	0.023	29.000	4.000	39.000	7.000	1.000	0.000	0.120	0.041
3	R*	0.683	0.015	0.668	-0.092	0.350	-0.002	48.000	2.000	44.000	0.000	1.000	0.000	0.034	0.053
3	L	0.639	-0.036	0.695	-0.175	0.385	-0.022	58.000	3.000	53.000	-4.000	1.000	0.000	0.022	0.109
4	R	0.653	0.015	1.224	0.083	0.631	0.043	50.000	10.000	57.000	14.000	1.000	0.000	0.406	-0.024
4	L*	0.635	0.050	1.140	0.135	0.532	0.059	36.000	4.000	44.000	6.000	1.000	0.000	0.460	0.010
MAE			0.027		0.149		0.025		3.900		5.500		0.100		0.027
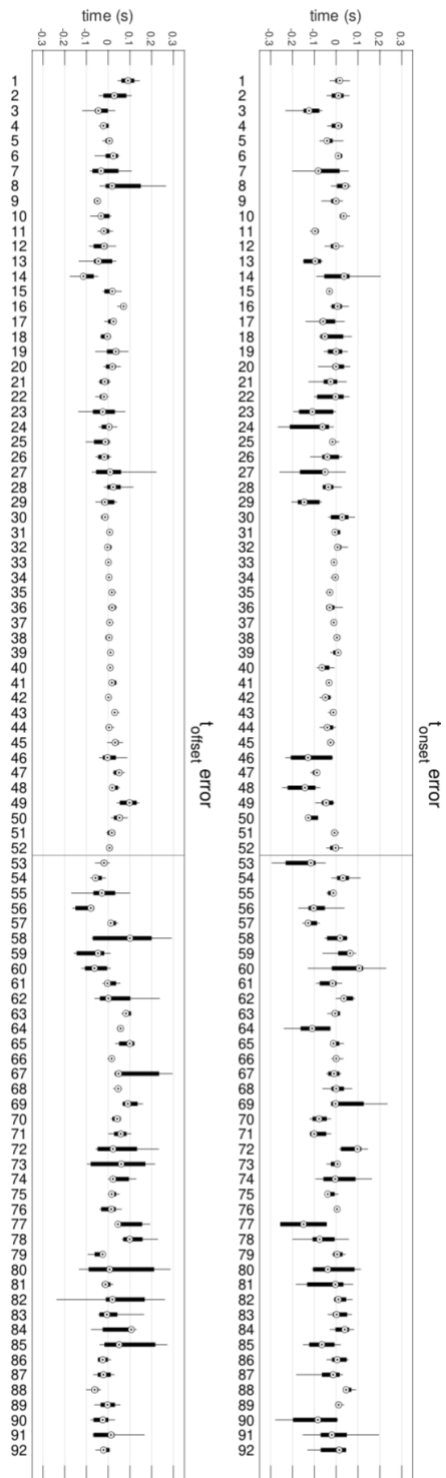
Figure 34 Distribution of the differences between onset/offset start time detected by the
ATSA and onset/offset start time detected by manual segmentation, assumed as ground
truth.

Table 6 Kinematic outcomes of the FNT in all participants. The measures are obtained with the markerless system, and the error is the difference between the markerless system values and the golden model. Features from the markerless system are obtained with ATSA, while ground-truth features come from the manual time segmentation, performed by an expert clinician.

Subject	Arm	Movement Duration (s)		Trajectory Length (m)		Maximum Velocity (m/s)		Average Velocity (m/s)		Time Percentage of Max Velocity (%)		Position Percentage of Max Velocity (%)		Number of Velocity Peaks (#movements)		Velocity after 150 ms (m/s)	
		Measure	Error	Measure	Error	Measure	Error	Measure	Error	Measure	Error	Measure	Error	Measure	Error	Measure	Error
Control Group																	
0	R	1.374	-0.071	0.665	0.009	0.937	0.064	0.488	0.059	33.000	1.000	35.000	-3.000	1.000	0.000	0.335	-0.032
0	L	1.208	0.003	0.692	0.028	1.107	0.054	0.582	0.025	42.000	3.000	48.000	0.000	1.000	0.000	0.366	-0.126
1	R	0.789	-0.080	0.598	-0.040	1.290	-0.041	0.742	0.004	39.000	-8.000	53.000	0.000	1.000	0.000	1.064	-0.406
1	L	0.773	-0.004	0.593	0.016	1.353	-0.049	0.769	0.019	42.000	11.000	51.000	6.000	1.000	0.000	0.892	-0.350
2	R	1.159	-0.023	0.653	0.011	0.927	0.034	0.566	0.002	49.000	8.000	52.000	10.000	1.000	0.000	0.411	0.043
2	L	1.217	0.022	0.664	0.066	0.845	0.059	0.546	0.041	49.000	10.000	50.000	7.000	1.000	0.000	0.373	-0.097
3	R	1.034	-0.030	0.662	0.025	1.153	0.133	0.604	-0.010	37.000	-8.000	40.000	-7.000	1.000	0.000	0.461	-0.004
3	L	1.100	0.056	0.691	-0.002	1.006	-0.006	0.616	-0.033	47.000	-5.000	50.000	-5.000	1.000	0.000	0.513	0.034
4	R	1.056	0.086	0.721	0.065	1.191	0.109	0.697	0.034	44.000	14.000	47.000	7.000	1.000	0.000	0.531	-0.405
4	L	0.984	-0.064	0.638	-0.028	1.045	-0.048	0.639	0.003	42.000	0.000	49.000	3.000	1.000	0.000	0.660	0.143
5	R	0.990	0.034	0.637	0.058	1.155	0.047	0.653	0.028	36.000	-12.000	36.000	-17.000	1.000	0.000	0.603	0.064
5	L	1.293	-0.068	0.698	0.028	0.875	0.075	0.549	0.049	39.000	2.000	45.000	7.000	1.000	0.000	0.463	0.089
6	R	1.207	0.139	0.673	0.087	1.057	0.148	0.559	0.004	45.000	6.000	48.000	-2.000	1.000	0.000	0.329	-0.312
6	L	0.793	-0.085	0.640	0.026	1.362	0.115	0.821	0.118	50.000	7.000	49.000	1.000	1.000	0.000	0.618	0.002
7	R	1.013	-0.071	0.628	-0.022	1.002	0.051	0.620	0.011	46.000	2.000	50.000	4.000	1.000	0.000	0.547	0.049
8	R	0.987	0.012	0.724	0.064	1.255	0.137	0.757	0.089	46.000	4.000	49.000	3.000	1.000	0.000	0.625	0.005
8	L	1.141	-0.017	0.731	0.032	1.071	0.083	0.641	0.027	47.000	3.000	44.000	0.000	1.000	0.000	0.411	-0.043
9	R	1.086	-0.004	0.638	0.021	1.014	0.057	0.589	0.021	46.000	-1.000	46.000	-2.000	1.000	0.000	0.360	0.009
9	L	1.017	-0.003	0.603	0.019	1.094	-0.006	0.593	0.017	42.000	-11.000	39.000	-11.000	1.000	0.000	0.310	0.126
10	R	1.023	-0.047	0.694	0.055	1.169	0.165	0.673	0.066	47.000	-2.000	47.000	-1.000	1.000	0.000	0.467	0.040
10	L	1.008	0.025	0.749	-0.034	1.239	-0.086	0.796	0.028	38.000	-4.000	41.000	-1.000	1.000	0.000	0.771	0.257
11	R	1.029	-0.097	0.786	0.023	1.338	0.137	0.754	0.081	43.000	-6.000	50.000	-5.000	1.000	0.000	0.777	0.051
11	L	1.060	0.015	0.580	0.021	0.975	0.064	0.551	0.011	47.000	3.000	50.000	5.000	1.000	0.000	0.326	0.023
12	R	1.147	-0.007	0.618	0.056	1.055	0.167	0.546	0.052	45.000	-2.000	51.000	0.000	1.000	0.000	0.453	0.134
12	L	1.982	-0.133	0.709	0.073	0.704	0.197	0.358	0.056	42.000	-2.000	43.000	-2.000	1.000	0.000	0.116	-0.011
13	R	1.987	-0.073	0.740	0.105	0.648	0.173	0.375	0.059	47.000	0.000	51.000	2.000	2.000	0.000	0.127	0.026
13	L	1.391	-0.159	0.700	0.003	0.879	-0.023	0.500	0.060	50.000	-12.000	43.000	-14.000	1.000	0.000	0.166	0.113
14	L	1.125	-0.026	0.649	0.011	1.043	0.018	0.568	-0.010	55.000	2.000	53.000	2.000	1.000	0.000	0.205	-0.023
MAE			**0.052**		**0.037**		**0.084**		**0.036**		**5.321**		**4.536**		**0.036**		**0.108**
Post-Stroke Group																	
0	R*	1.189	-0.224	0.574	0.015	1.052	0.022	0.494	0.097	58.000	-3.000	61.000	8.000	1.000	0.000	0.144	0.057
0	L	1.279	0.193	0.653	0.041	1.099	-0.006	0.510	-0.003	56.000	1.000	54.000	0.000	1.000	0.000	0.166	-0.038
1	R*	1.363	-0.065	0.559	-0.009	0.857	0.007	0.414	0.008	39.000	0.000	41.000	2.000	1.000	0.000	0.180	0.024
1	L	1.127	0.007	0.691	0.013	1.081	0.054	0.637	0.000	41.000	-3.000	51.000	6.000	1.000	0.000	0.645	0.228
2	R	1.116	-0.157	0.702	-0.015	1.044	-0.003	0.639	0.075	47.000	-3.000	52.000	-1.000	1.000	0.000	0.586	0.231
2	L*	2.074	-0.139	0.773	0.041	0.874	-0.059	0.376	0.044	32.000	7.000	39.000	7.000	1.000	0.000	0.144	0.024
3	R*	2.165	0.204	0.693	0.025	0.709	-0.050	0.321	-0.032	49.000	3.000	49.000	5.000	1.000	0.000	0.064	0.030
3	L	1.853	0.171	0.664	-0.011	0.719	-0.151	0.361	-0.045	56.000	1.000	51.000	-6.000	1.000	0.000	0.044	0.021
4	R	1.059	-0.030	0.649	0.011	1.202	0.061	0.600	0.011	47.000	7.000	55.000	12.000	1.000	0.000	0.449	0.044
4	L*	1.216	-0.009	0.636	0.051	1.115	0.110	0.526	0.053	40.000	8.000	45.000	7.000	1.000	0.000	0.301	-0.159
MAE			**0.120**		**0.023**		**0.052**		**0.037**		**3.600**		**5.400**		**0.000**		**0.086**

Table 7 Mean Absolute Error (MAE), Root-Mean-Square Deviation (RMSD), and Correlation Coefficient (pval < 0.001) between the velocity/acceleration shape from the marker-less system and the marker-based system. Shapes from the marker-less system are obtained using both manual segmentation and automatic segmentation

Subject	Arm	Velocity and Acceleration Shape					
		MAE (m/s)		RMSD (m/s)		Correlation Coefficient (ϱ)	
Segmentation		manual	auto	manual	auto	manual	auto
Control Group							
0	R	0.045	0.066	0.057	0.079	0.992	0.972
0	L	0.026	0.067	0.031	0.076	0.997	0.978
1	R	0.059	0.137	0.076	0.164	0.982	0.873
1	L	0.125	0.152	0.142	0.173	0.913	0.868
2	R	0.058	0.046	0.071	0.056	0.984	0.991
2	L	0.090	0.120	0.103	0.132	0.942	0.903
3	R	0.074	0.046	0.102	0.062	0.952	0.984
4	R	0.012	0.042	0.015	0.047	0.931	0.733
4	L	0.179	0.195	0.224	0.237	0.999	0.991
5	R	0.052	0.054	0.064	0.075	0.786	0.754
5	L	0.059	0.082	0.071	0.105	0.983	0.977
6	R	0.043	0.047	0.052	0.062	0.977	0.947
6	L	0.203	0.146	0.235	0.200	0.991	0.988
7	L	0.068	0.144	0.095	0.169	0.760	0.857
8	R	0.065	0.052	0.077	0.068	0.776	0.761
8	L	0.102	0.056	0.111	0.067	0.970	0.884
9	R	0.074	0.089	0.084	0.103	0.982	0.980
9	L	0.067	0.066	0.094	0.096	0.939	0.984
10	R	0.079	0.097	0.092	0.124	0.973	0.955
10	L	0.053	0.065	0.067	0.086	0.962	0.962
11	R	0.042	0.071	0.057	0.090	0.966	0.929
11	L	0.049	0.073	0.058	0.091	0.991	0.986
12	R	0.050	0.042	0.064	0.059	0.987	0.962
12	L	0.041	0.069	0.050	0.082	0.989	0.966
13	R	0.050	0.064	0.060	0.087	0.988	0.994
13	L	0.127	0.101	0.168	0.146	0.996	0.987
14	R	0.035	0.088	0.051	0.114	0.987	0.987
14	L	0.041	0.054	0.054	0.064	0.949	0.949
AVG		**0.070**	**0.083**	**0.087**	**0.104**	**0.984**	**0.932**
Post-Stroke Group							
0	R*	0.088	0.149	0.135	0.219	0.990	0.963
0	L	0.042	0.023	0.056	0.027	0.990	0.989
1	R*	0.058	0.033	0.073	0.041	0.925	0.856
1	L	0.023	0.119	0.027	0.138	0.988	0.997
2	R	0.052	0.079	0.068	0.095	0.987	0.993
2	L*	0.036	0.094	0.045	0.115	0.997	0.917
3	R*	0.064	0.056	0.087	0.070	0.981	0.971
3	L	0.091	0.073	0.132	0.088	0.990	0.935
4	R	0.054	0.044	0.070	0.058	0.980	0.988
4	L*	0.055	0.102	0.074	0.125	0.957	0.979
AVG		**0.056**	**0.077**	**0.077**	**0.098**	**0.979**	**0.959**

Discussion

The present study aimed to assess the accuracy of a marker- less system for motion analysis of the FNT in healthy controls and patients affected by cerebral stroke. We focused on a set of clinically meaningful movement features and we compared the values obtained using the hpe software device with a the values obtained with a marker-based system, commonly considered the golden model. Our comparison showed that the markerless device is significantly accurate in estimating all the features investigated, except for the early movement's velocity. Therefore, it can represent a useful tool for the UL movement analysis in people affected by stroke. Kinematic motion analysis is widely used in clinical practice, especially for the assessment of gait. In contrast, the UL movement analysis presents several peculiar challenges that have hampered its diffusion. Firstly, while the locomotion is clearly the most relevant activity performed with the lower limbs, the UL can perform a variety of functionally relevant tasks like pointing, reaching and grasping in different directions. Consequently, there is a lack of agreement on standard protocols for the kinematic assessment of the UL. Secondly, the mechanic complexity of the UL allows the same task to be performed with a remarkable inter-subjects variability hampering the comparison between subjects. Lastly, in contrast to the locomotion, where a well-defined movement, the step, is repeated several times making relatively easy the segmentation of a single gait cycle, it is typically hard to define accurately the movement onset in most of the UL common tasks.

In the present paper we proposed an assessment protocol of UL movement aiming to overcome these issues. We chose the FNT since it is a well known task commonly assessed in the usual neurological examination. This task is easy to standardize since the starting point and the target are intrinsically defined maximizing its repeatability in different settings. Moreover, we proposed a method for automatically identify the movement's start and end allowing automatic segmentation. Notably, the ATSA offers some advantages avoiding examiner-dependency and fastening the analysis process. The problem of movement segmentation has been often overlooked in the literature, and several studies didn't mention how they tackle this issue (Adans-Dester et al., 2020; Honda et al., 2020; Wu et al., 2007b). Overall, the most commonly used method to identify movement

onset uses a velocity threshold (3-5% of peak velocity or 2-5 cm/s) and identifies the instant when the hand speed overcomes this threshold (Chen et al., 2021; Coderre et al., 2010; Grosskopf & Kuhtz-Buschbeck, 2006; G. M. Johansson et al., 2017), or using pressure-sensitive switches (K.-C. Lin et al., 2007). However, it has been suggested that this method should not be considered reliable when assessing stroke subjects' UL movements (Coderre et al., 2010). Coderre and colleagues proposed a complex method for identifying the movement onset based on the integration of hand speed and position relative to the starting point (Coderre et al., 2010). In their study participants performed the task using an exoskeleton robot making easier to define the starting position across trials but inevitably affecting the patients' movement (Schwarz et al., 2019). Therefore it can be argued that our method improve the procedures described in the existing literature and, on the other hand, did not include any additional devices that could alter the subjects' natural movement. In the present analysis, the application of our ATSA showed that when compared to manual segmentation performed by two clinicians via a frame-by-frame analysis, the automatic labelling had a mean error of 0.57s. This error led to a mean absolute error in the movement duration of 0.052s and 0.098s for healthy controls and patients with stroke respectively. Notably, considering the sample rate of the hpe software's camera, this time error corresponds to a 3 to 6 frames, a remarkable accurateness since, even by a single- frame manual analysis it is sometimes hard to identify the exact movement's start and end and there can be disagreement between raters. Moreover, for movement's duration, the literature suggested a relative Minimal Detectable Change (rMDC) of 38-98%, far greater than the error associated with our automatic segmentation being between 18% and 0.6% of the entire movement's duration (Wagner et al., 2008). An exception was the early movement's velocity computed after 150ms from the movement's onset. The error between the values obtained with hpe software and with the MoCap system seemed to be too large to be considered reliable. However, this error is likely to depend almost entirely on the automatic segmentation method and not on the hpe software analysis per se. Moreover, this feature is rarely used in common clinical assessment and it has mainly been used for research purposes (Bhanpuri et al.,

2014). Our analysis suggests that to compute this feature, manual movement's segmentation should be recommended.

A recent systematic review on UL kinematic analysis identified most used and clinically meaningful kinematic metrics referring to different movement domains (Schwarz et al., 2019). Based on these recommendations our analysis included parameters on movement accuracy, planning, smoothness and efficiency. We then com- pared the metrics' values obtained with the hpe software and MoCap systems. Overall, the accurateness of the hpe software system did not change between the analysis of healthy controls and patients with stroke. Movement duration, trajectory length, average and maximum velocity, time and position percentage of peak velocity reported a relative mean absolute error of 3- 5%. The question about whether this error could affect clinical interpretation of the measurement is crucial. Only few studies attempted to estimate psychometric properties of UL kinematic analysis during different tasks (Alt Murphy et al., 2013; Wagner et al., 2008). Noteworthy, Wagner and colleagues estimated the rMDC of a series of kinematic metrics in the FNT in subjects with cerebral stroke using a MoCap system (Wagner et al., 2008). Their finding suggested that the (rMDC) for the features we analyzed are significantly greater than the mean absolute errors that we found between hpe software and MoCap. Specifically, authors suggested the rMDC being 24- 61% for the peak velocity value and 45-81% for the time to peak velocity. Moreover, another study that analyzed the FNT in patients with stroke suggested that a peak velocity difference of 0.6 m/s, and 8% of time to peak velocity can differentiate between mild and moderate stroke subjects (G. M. Johansson et al., 2017). On the other hand, when assessing the effect of a rehabilitation treatment on kinematic parameters in a reaching task, previous researches found that an increase of 9% of the time percentage of peak velocity and of 6% of the spatial percentage of peak velocity were statistically significant (Adans-Dester et al., 2020; K.-C. Lin et al., 2007). The early velocity after 150ms from the movement onset has been rarely investigated in the literature, although it provides useful information on the anticipatory motor control and movement planning and it has previously been associated with ballistic movement's accuracy in cerebellar stroke patients (Bhanpuri et al., 2014). We measured values of early velocity compatible to their

previous results. However for this feature we found a mean absolute error of extremely variable across subjects ranging from 1% to 90%. It is conceivable that this amount of error for some subjects refers to inaccuracy of automatic identification of movements' onset specifically for subjects with stroke. These results suggest that for computing this specific feature, when assessing subjects with cerebral stroke, manual segmentation should be recommended. Along with numeric parameters, velocity and acceleration pattern inspection provides useful information to clinicians. In terms of hand's velocity pattern, the comparison between the measures obtained with the hpe software system and the MoCap system showed very strong correlations both for healthy controls and patients with stroke with mean rho values being 0.941 and 0.947 respectively.

To conclude, the comparison with the literature suggests that the hpe software system can provide reliable and accurate kinematic data that clinicians can use for improving the clinical UL assessment in patients with stroke.

Finally, from a clinical setting perspective, markerless movement analysis provides some relevant advantages com- pare to standard MoCap systems. Firstly, the assessment is less time consuming since there is no more the need of place the markers on the subjects' landmarks. Secondly, the hpe software system is portable and allows performing the analysis in wards, gyms and ambulatory care settings. Lastly, these devices are remarkably cheaper than MoCap systems available in the market.

Motor control impairment in upper limbs' reaching task in people with cerebellar and somatosensory deficits

Introduction

The ability of performing fast and accurate movements using Upper Limbs (ULs) is one of the most remarkable aspects of human motor behavior. However, the apparent ease with which we reach, grasp, and manipulate different objects in our daily life conceals the complex mechanisms involved in movement planning, execution and control. The study of these mechanisms has attracted a rich body of literature in the last decades and different models have been proposed (Feldman, 2015; Todorov & Jordan, 2002; Wolpert & Ghahramani, 2000). Overall, there is compelling evidence that the Central Nervous System (CNS) uses internal models of the motor system and environmental dynamic properties to optimize sensorimotor behavior (Mcnamee & Wolpert, 2019). These models act as a representation of the external word allowing an organism to simulate and predict the consequences of its actions without performing it (Mcnamee & Wolpert, 2019). Specifically, a forward model integrates a copy of the motor command (often referred as "efference copy") with sensory information about limbs' position and predicts the future body's state and sensory feedback (M. I. Jordan, 1996b).

Although its existence has been questioned in some recent works (Press et al., 2020), the literature suggested that a forward model is essential to perform fast and accurate ULs movements offering a solution for the problem of intrinsic latency that affects the somatosensory system (Wolpert & Flanagan, 2001). A sensorimotor feedback loop in human somatosensory system is indeed affected by a delay of the order of 80-150ms which is remarkably long in the context of fast reaching (Scott, 2016). Therefore, a system that relies only on such a feedback control would result unstable and perform unnecessarily large out-of-phase corrections. A forward model could solve this issue providing the CNS with a prediction of the future sensory input that can feed an internal feedback loop before the actual sensory feedback is available (Mcnamee & Wolpert, 2019). Such internal model is thought to be responsible for a range of ULs' sensorimotor behavior ranging from grip force modulation while grasping and moving an object (Flanagan & Wing, 1997; R. S. Johansson & Flanagan, 2009), to perception attenuation of self-produced tactile

stimuli (Bays et al., 2006; Bays & Wolpert, 2007a) and it is likely to be involved in the sense of agency (Pareés et al., 2014; Shergill et al., 2005).

The cerebellum has been suggested to play a key role in the implementation of a forward model (Kawato et al., 1987a; Tanaka et al., 2020; Wolpert & Ghahramani, 2000). Its cortex receives projections from the motor areas of the cerebral cortex, which can convey information about the motor command via pontine nuclei, and from the spinal cord through the spinocerebellar tracts that provides proprioceptive information. The cerebellum is therefore located in an ideal position to integrate in its cortex the efference copy with the somatosensory information and provide the cerebral motor, premotor and parietal cortices with the output of a forward model through the deep cerebellar nuclei via the thalamus (Bostan et al., 2013; D'Angelo, 2018). Moreover, recent neurophysiological studies showed that the current activity of the deep cerebellar nuclei can predict the future input to the cerebellar cortex via the mossy fibers corroborating the idea that the predictive computations involved in the forward model are represented in this cerebro-cerebellar loop (Tanaka et al., 2019).

The crucial role of the cerebellum is suggested also by studies on patients with cerebellar lesions. These patients manifest typical UL sensorimotor symptoms that are collected under the umbrella of the cerebellar ataxia syndrome, which includes clumsiness, lacking smoothness and multi-joint coordination, spatial errors while pointing to a target (i.e. dysmetria) and irregular movements repetitions (Day et al., 1998; Lisberger & Thach, 2013; Manto et al., 2012).

Some of the typical UL motor dysfunctions in patients with cerebellar lesions have been described as the consequence of an impaired forward or inverse model. On one hand spatial errors of overshooting or undershooting the target during reaching (i.e. dysmetria) was showed to be effectively modeled as an impairment of an inverse model and a miscalculation of UL's inertia (Bhanpuri et al., 2014). On the other hand, the lack of smoothness, the excessive oscillations approaching the target and errors in movement planning have been interpreted as the consequence of patients' inability of anticipating the consequences of voluntary movements, consistent with an impairment of a forward model (Frey et al., 2011). Relying only

on delayed somatosensory feedback for motor control, these subjects perform instable UL reaching movements with exaggerated oscillations while approaching the target (Bhanpuri et al., 2014; Cabaraux et al., 2020; Frey et al., 2011; Manto et al., 2012; Wolpert & Ghahramani, 2000). According to this idea, in these patients the cerebellum receives the efference copy based on a theoretically correct limbs' position estimation provided by the somatosensory system. However, cerebellar lesions may impair the computation of the predicted body's state, i.e., the output of the forward model. Being the information provided for internal feedback correction unreliable, the system is forced to rely mainly on delayed feedback control, using information on ULs' position provided by the dorsal columns to the somatosensory areas of the parietal cortex. This would lead to the typical excessive oscillations observed in cerebellar patients in the last phase of a reaching movement. Moreover, the inability of predicting the consequences of the voluntary movement and result in impaired movement's planning.

Recent literature suggested that, along with the cerebellum, the forward model's neural underpinning consist of a complex cerebro-cerebellar network including the sensorimotor cortex, and the Posterior Parietal Cortex (PPC). The PCC is indeed involved in the representation of the future state of the body and, through broad connections with the primary somatosensory cortex, contributes to the sense of proprioception (Cui, 2016; Desmurget et al., 1999; Parkinson et al., 2010; Reichenbach et al., 2014). Moreover, imaging studies provided evidence that the activity of the secondary somatosensory area in the parietal cortex (SII) represents the output of the forward model, suggesting its involvement in the representation of the sensory consequences of voluntary actions (Shergill et al., 2013). Interestingly, similar to cerebellar patients, patients with CNS lesions involving the spinothalamocortical pathway, the thalamus, the primary somatosensory cortex and other parietal areas involved in the proprioception sense, show dysmetria, lack of smoothness and irregular movements, a syndrome often called sensory ataxia (Ghika et al., 1994; Melo & Bogousslavsky, 1992; Osumi et al., 2018, Caplan, 2012). This behavior is exacerbated when patients are prevented from using vision to compensate for proprioceptive deficits (Klingner & Witte, 2018). Although it has

been previously suggested that patients with sensory ataxia due to stroke showed signs of both feedback and feedforward motor control deficits, limited attention has been paid in describing the role of somatosensory information in the forward model. (Osumi et al., 2018).

Here we proposed a theoretical framework for interpreting sensory and cerebellar ataxia as different forward model's dysfunctions. Given the architecture of the forward model, it is conceivable that a somatosensory deficit would impair the ability of predicting the consequences of a voluntary movement. From a computational perspective, the impairment of the ULs' position sense due to CNS stroke, would affect the initial body's state estimate from which the movement is planned through the sensorimotor transformations (Soechting & Flanders, 1989b, 1989a). Although the vision system can partially compensate for these deficits, planning the movement from unreliable information would result in inappropriate motor command and, eventually, an altered efference copy. In principle, the forward model in these patients is preserved (given that the cerebellum is intact), however the unreliable efference copy would affect the output of the forward model itself. Moreover, the lesion of CNS structures involved in the position sense would compromise patient's ability of correcting the movements using the feedback motor control in the absence of vision. This interpretation is in line with previous literature suggesting analogies between sensorimotor deficits of cerebellar patients and patients with impaired proprioception. In fact, these patients have been reported to have difficulties in anticipating interaction torques originating from voluntary movements as a consequence of the inability of sending predictive signals that can anticipate motor errors (Frey et al., 2011). Also, brain stimulation studies using transcranic magnetic stimulation to suppress activity of the posterior parietal cortex, impaired the healthy subject's ability to correct movements trajectories from unexpected perturbation if unable to see the hand (Reichenbach et al., 2014).

The idea that the cerebellum and the posterior parietal cortex are crucial for predictive aspects of UL movement control during reaching tasks been corroborated

by several lesional studies that investigated sensorimotor UL behavior of patients with CNS lesions.

However, to the best of our knowledge, this is the first attempt to describe UL motor deficits in cerebellar and sensory ataxia in pointing task using a single theoretical framework for sensorimotor control. The present observational study assessed the kinematic profile of an UL pointing task in patients with CNS lesions and healthy controls. We aimed to compare movement's kinematics in patients with cerebellar lesions and patients with somatosensory impairment testing our theoretical framework. Our hypothesis is that, although both groups would be characterized by ataxic behavior, different movement features' alterations would be detected. Specifically, we expect the cerebellar patients to present altered motor planning with relatively preserved feedback motor control, performing effective trajectories corrections. In contrast, we expect patients with somatosensory impairment to be significantly reliant on vision and to present impaired forward and feedback motor control showing larger pointing spatial errors and anticipated velocity peaks trying to slow down to visually guide the last movement's phase.

METHODS

Participants

Patients with cerebral stroke and young healthy volunteers (HS) were recruited. Participants were recruited from the Neuromotor and Cognitive Rehabilitation Research Centre (CRRNC) of the University of Verona, Italy. For healthy controls, the exclusion criteria were the presence of musculoskeletal injuries or any other neurological condition, history of surgery or pain affecting upper limbs, normal or corrected to normal visual and auditory abilities. For stroke subjects, the inclusion criteria were: age ≥ 18 year old, diagnosis of stroke confirmed by a specialist in neurology and by radiologic findings (CT or MR), lesion in somatosensory areas including thalamic somatosensory nuclei, parietal cortex, posterior limb of the internal capsule, cerebellum, cerebellar pedunculi, strength of shoulder abductors and elbow flexors ≥ 3/5 MRC (Medical Research Council Scale for Muscle

Strength), limited to full UL capacity (Fugle-Mayer assessment scale score (FMA) ≥ 31) (Hoonhorst et al., 2015).

Exclusion criteria were the presence of severe cognitive, visual or communication impairments and other concomitant neurological or orthopaedic diseases interfering with patients' capacity of providing the informed consent or performing the required task.

The assessment procedure in this study were approved (approval number 2320CESC) by the local Ethics Committee (Comitato Etico per la Sperimentazione Clinica delle Province di Verona e Rovigo) and was carried out according to the Declaration of Helsinki. All participants provided written informed consent to participate in the study.

Clinical assessment

Strength, function, and proprioception of upper limb were assessed using a battery of clinical scales. The Motricity Index (MI) is a well-known scale for the assessment of limb strength testing pinch grip, elbow flexion and shoulder abduction (score range 0-99, greater score indicates better performance) (Collin & Wade, 1990). The Fugl-Meyer assessment scale for upper limb (FMA-UL) is a measure of UL function that includes 33 items assessing reflex, activity, muscle strength and movement control (score range 0-66, greater score indicates better performance) (Fugl-Meyer et al., 1975). The Erasmus MC modifications to the Nottingham Sensory Assessment (EmNSA) was used to assess proprioceptive deficits of patients with stroke. It includes tasks investigating light touch, pressure, pinprick, sharp-blunt discrimination, and proprioception (score range 0-40, greater score indicates better performance)(Stolk-Hornsveld et al., 2006). To assess the limb's ataxia in patients with cerebellar lesions the International Cooperative Ataxia Rating Scale (ICARS) was used. It is composed in 4 subscales investigating posture and gait disorders, kinetic function, speech disorder and oculomotor disorders. In this study only the section 2 (kinetinc function) was administered. This section includes 7 tasks resulting in a score ranging from 0 to 52 where the higher the score the more severe the impairment (Schmitz-Hübsch et al., 2006).

Instrumental assessment

The index-to-nose task was assessed: subjects sat comfortably on an armchair, abducted the shoulder at 90° and extended the elbow. From this starting position, they were asked to touch the tip of their nose with the index fingertip at a self-selected speed. Patients were told that they were supposed to prioritize the reaching accuracy over the movement's velocity. This task was chosen as it is one of the most common UL movement assessed during a clinical neurologic evaluation both for patients with cerebellar disorders and patients with proprioception impairments. Moreover, it is included in the ICARS scale, which is a well-known validated clinical scale for the assessment of UL's ataxia (Schmitz-Hübsch et al., 2006). All the subjects performed the task seven times with both upper limbs in two conditions: eyes open (EO) and eyes closed (EC). Between each trial, subjects were provided with "stop" and "go" signals by a physiotherapist. The task was recorded by an RGB-D camera Intel RealSense D415 RGB-D placed 2m in front of the subjects and keypoints were extracted using Openpose software (Cao et al., 2021).

Data Analysis

We extracted eight movement's features related to movement's accuracy, efficiency and anticipatory motor control and motor planning. The analyzed parameters are listed in Table 8. For a formal definition of the features readers may refer to (Martini et al., 2022).

154

Table 8 Outline of the analyzed movevent's features

Feature	Notation	Description
Movement duration	**time**	The movement duration indicates the time interval from the start of the movement to the target reaching. In the present analysis the movement's onset and offset were manually identified via a frame-by-frame video inspection. It is considered a measure of movement's efficiency.
Average velocity	**Vel**	It represents the mean three-dimensional velocity of the hand relative to the subject's body. It is considered a measure of movement's efficiency.
Peak velocity	**PeakVel**	The absolute value of the peak velocity is the maximum of the absolute three-dimensional speed throughout the entire movement. It is considered a measure of movement's efficiency.
Percentage of movement time where peak velocity was reached	$t_{max\%}$	The percentage of movement duration when the maximum of velocity occurs is the proportion of movement time spent between the start of the movement and the velocity peak. It is considered a measure of motor planning.
Percentage of movement trajectory where peak velocity was reached	$p_{max\%}$	The percentage of movement trajectory when the maximum of velocity occurs. It is considered a measure of motor planning.
Early movement velocity	**EV**	The absolute three-dimensional velocity 150ms after the movement's onset. It is considered a measure of motor planning and movement's efficiency.
Dysmetria along the x axis	**DysmX**	The distance between index fingertip and the nose tip on the horizontal axis when the finger's velocity drops to 0 m/s for the first time. Positive values indicate target's overshooting and negative values indicate target's undershooting. It is considered a measure of motor accuracy.
Dysmetria	**Dysm**	The absolute distance between index fingertip and the nose tip on the frontal plane when the finger's velocity drops to 0 m/s for the first time. It is considered a measure of motor accuracy.

Patients were divided into two groups according to the lesion site: one group including patients with lesion involving thalamic somatosensory nuclei, parietal cortex, posterior limb of the internal capsule (SP) and the other group including patients with lesion involving the cerebellum or cerebellar pedunculi (CP). For each subject the features' values were averaged across movements and descriptive statistics was carried out. Data distribution was checked using the Shapiro-Wilk test. A repeated measure 2x3 ANOVA was used with "Eyes Open" (EO) and "Eyes

Closed" (EC) as within-group factor and "group" as a between group factor. Post hoc analyses were carried out using Holm-Bonferroni test. Data from the impaired limb were used for stroke patients while data from the non-dominant arm were used for healthy controls. For these analyses, the absolute value of the x axis dysmetria was used. Associations between movement's parameters were tested using a spearman's or Pearson's correlation according to data distribution. All the analysis were carried out using JASP software (Version 0.15).

Results

A convenient sample of 12 healthy subjects (HS), 12 patients with somatosensory deficits (SP) and 9 patients with cerebellar lesions (CP). Demographic and clinical data of the included subjects are listed in Table 9 and Table 10 respectively.

Table 9 Demographic characteristics of the included subjects. Data are reported as mean ± standard deviation.

Group	Age (years) Mean ± sd	Laterality (R/L)	Sex (M/F)
HS (n=12)	29.0 ± 2.9	11/1	7/5
SP (n=12)	62.4 ± 13.6	12/0	7/5
CP (n=9)	66.9 ± 25.2	9/0	8/1

Table 10 Clinical characteristics of the included patients. Between groups comparison was performed using t-test for unpaired samples or chi-square test for categorial variable

	SP (n=12)		CP (n=9)		Between group comparison
	mean	sd	mean	sd	p-value
Time since stroke onset (months)	2.6	1.8	3.6	4.2	n.s.
Affected arm (R/L)	7/5		6/2		
FMA-UL	52.2	12.7	58.9	5.4	n.s.
MI	80.2	23.0	86.6	10.7	n.s.
ICARS			24.3	10.3	
EmNSA	30.2	9.8			

The repeated measure ANOVA showed significant group effect for the movement's duration (time) (F=4.083 p=0.027 η_p^2=0.22), average velocity (Vel) (F=13.591 p<.001 η_p^2=0.48), peak velocity (PeakVel) (F=10.696 p<.001 η_p^2=0.41) and early movement velocity (EV) (F=12.759 p<.001 η_p^2=0.47) (Figure 35, Table 11). Post hoc analysis revealed that SP group was overall slower than HS group (time: t=2.76 p=0.029 Cohen's d=0.49; Vel: t=-4.277 p<.001 Cohen's d=-0.76; PeakVel: t=-3.640 p=.002 Cohen's d=0.64; EV: t=-4.130 p<.001 Cohen's d=-0.73). Similarly, CP were slower than HS as for average velocity (t=-4.58 p<.001 Cohen's d=-0.81), peak velocity (t=-4.18 p=.001 Cohen's d=-0.74 and early velocity (t=-4.45 p<.001 Cohen's d=-0.79) The ANOVA analysis of absolute value of dysmetria along the horizontal axis (x axis) found a significant effect of group. The post hoc comparisons showed that patients in the CP had smaller deviation from the target in the x axis than HS group (t=-3.119 p=0.012 Cohen's d=-0.55) (Figure 35). Moreover, a within group effect on movement duration was found (F=4.52 p=0.04 η_p^2=0.14) and the post hoc analysis showed that overall the subjects took more time to point at their nose in EC condition compared to the EO condition (time: t=2.13 p=0.04 Cohen's d=0.38) (Figure 35). Post-hoc within-groups analysis found tendency to significant difference in the SP group (t=-3.029 p_{holm}=0.06).

Interestingly we found that functional UL impairment assessed with the FMA-UL was not associated with any of the movement parameters for SP and CP. Analogously the somatosensory deficit measured with the EmNSA did not correlate with any of the analyzed features. In contrast, ICARS score was inversely correlated to the early velocity and the peak velocity in the EC condition: the greater the severity of the cerebellar ataxia, the slower the movement, both in terms of initial velocity and peak velocity. Moreover, only in the CP group we found that the dysmetria along the horizontal axis was directly associated with the absolute value of the peak velocity and the position of the velocity peak through the index finger's trajectory ($p_{max\%}$). Specifically, those patients that reached the velocity peak after the half of the movement trajectory length tended to overshoot the target, while patients who reached the velocity peak earlier undershoot the target (Figure 36).

157

Table 11 Repeated measure ANOVA results. *: group effect of the repeated measure
ANOVA. Data are reported as mean ± standard deviation.

| Feature	Condition	HS	SP	CP	Between group comparison*
time	EO	1.140 ± 0.277	1.934 ± 0.996	1.932 ± 0.449	F=4.083 p=0.027 η_p^2=0.22
	EC	1.160 ± 0.234	2.729 ± 2.299	2.165 ± 0.698	
Vel	EO	0.590 ± 0.133	0.388 ± 0.146	0.361± 0.089	F=13.581 p<.001 η_p^2=0.48
	EC	0.571 ± 0.130	0.345 ± 0.147	0.310 ± 0.066	
PeakVel	EO	0.878 ± 0.199	0.637 ± 0.189	0.591 ± 0.134	F=10.696 p<.001 η_p^2=0.41
	EC	0.854 ± 0.194	0.596 ± 0.181	0.538 ± 0.101	
$t_{max\%}$	EO	45.250 ± 4.070	41.250 ± 10.323	39.222 ± 7.678	n.s.
	EC	44.000 ± 4.472	40.583 ± 14.902	36.750 ± 8.013	
$p_{max\%}$	EO	46.417 ± 7.229	44.250 ± 8.966	42.333 ± 8.617	n.s.
	EC	47.583 ± 47.583	49.200 ± 15.069	43.625 ± 9.899	
EV	EO	0.624 ± 0.155	0.408 ± 0.165	0.373 ± 0.088	F=12.759 p<.001 η_p^2=0.47
	EC	0.610 ± 0.149	0.359 ± 0.162	0.322 ± 0.072	
DysmX (absolute value)	EO	0.051 ± 0.017	0.039 ± 0.031	0.017 ± 0.018	F=4.866 p=.015 η_p^2=0.25
	EC	0.047 ± 0.029	0.034 ± 0.033	0.020 ± 0.012	
Dysm	EO	0.053 ± 0.019	0.052 ± 0.034	0.028 ± 0.018	n.s.
	EC	0.052 ± 0.026	0.047 ± 0.036	0.031 ± 0.016	
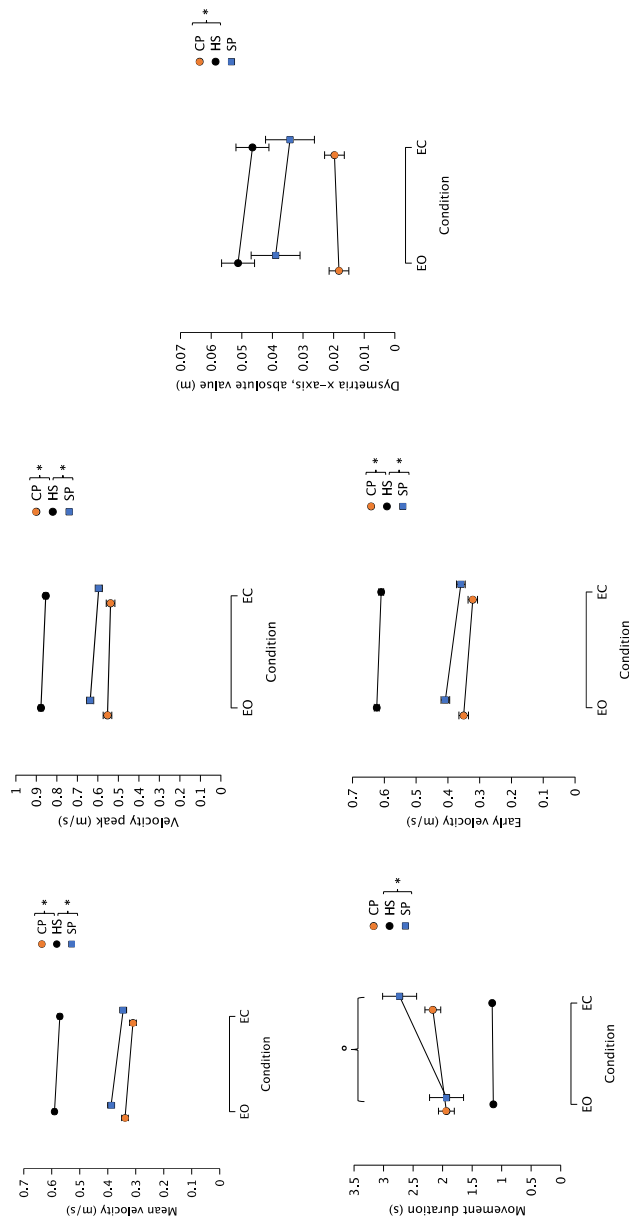
Figure 35 Post hoc plots of the repeated measure ANOVA. Top left: mean velocity; top center: velocity peak; bottom left: movement duration; bottom center: early velocity; right: dysmetria along the horizontal axis. *: post hoc between group comparison p<0.05; °: post hoc within group comparison p<0.05. CP: Cerebellar Patients; HS: Healthy Subjects; SP: patients with sensory impairment; EO: Eyes Open; EC: Eyes Closed. Error bars represents standard error of the mean.
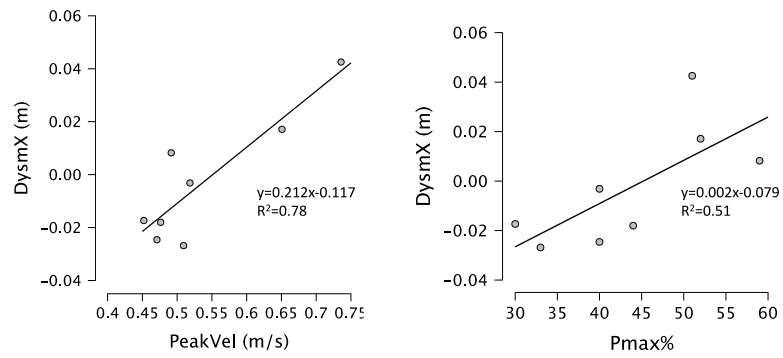
Figure 36 Scatter plots for the x-axis dysmetria as a function of peak velocity (left) and position of the velocity peak (right) in the CP group.

Discussion

The present study aimed to compare UL movement's kinematics in an index-to-nose task in patients with cerebellar lesions and patients with somatosensory impairment with young healthy controls. We performed this analysis to test our theoretical framework aiming to describe patient's sensory and cerebellar ataxic behavior as a consequence of a forward model impairment. With this aim we extrapolated a series of movement features related to anticipatory motor control and motor planning ($t_{max\%}$, $p_{max\%}$, EV) movement's accuracy (DysmX, Dysm) and movement's efficiency (time, Vel, PeakVel). Overall, the included stroke patients performed the movement less efficiently than HS, being slower in terms of early velocity, peak velocity and average velocity. This was not surprising given that some patients had functional and strength impairment measured with FMA-UL and MI and was already reported in studies investigating UL kinematics in stroke subjects (G. M. Johansson et al., 2017; Thrane et al., 2020). However, neither UL strength or function or proprioception (assessed with EmNSA) was associated with movement's velocity, suggesting that movement slowness was not related to primary sensorimotor impairment. This was partially in contrast with previous studies that found that UL strength was strongly associated with reaching speed (Wagner et al., 2006, 2007). However, this strong association was found particularly in the acute phase after stroke (Wagner et al., 2006) and only a small amount of variance of reaching performance was found to be explained by sensorimotor impairments in the subacute phase of recovery (Wagner et al., 2007). On the other hand, in CP group ICARS score was inversely correlated to movement early and mean velocity. That is the more severe the ataxia, the slower the movement was performed. It is conceivable that patients with more severe cerebellar ataxia performed slower movements to try to compensate their ataxic behavior and control oscillations, especially when visual feedback was provided.

In line with previous literature, SP group was the most affected by the lack of visual feedback. The results from movement duration analysis showed that these patients slowed down the movement in the EC condition more than the other groups, corroborating previous findings (Miall et al., 2019). This was not surprising as previous literature extensively described the importance of visual feedback for

patients with somatosensory deficits (Klingner & Witte, 2018). In this study, to assess movement accuracy we quantified dysmetria as the absolute value of the distance between the index fingertip and the tip of the nose when the hand's velocity reaches 0m/s for the first time after movement onset. Moreover, we analyzed the x axis (horizontal axis) component of the finger-nose distance, since previous literature suggested that this component of dysmetria is of relevance for patients with cerebellar ataxia (Bhanpuri et al., 2014). Unexpectedly, the CP group showed significant lower values of the x axis dysmetria compared to HC. Some factors might explain this result. Firstly, it is noteworthy that in HS group, in contrast to the CP group, this component of dysmetria is relevantly larger than the y axis component (perpendicular to the movement direction) and account almost for all the index-nose distance at the end of the movement. This suggested that the x axis dysmetria in healthy subjects should be considered as natural inter-subject variability in the way of touching their nose. Although instructed to touch their nose with the index fingertip, some subjects naturally performed the movement touching the nose with their index knuckle or the middle phalanx. Accordingly, almost all healthy overshot the target as confirmed by the signed values of the DysmX. Secondly, the values of the measured x-axis dysmetria are limited to few centimeters, and, although statistically significant, these between-group difference could be considered as not behaviorally relevant. Finally, although this is an appropriate parameter to assess movement accuracy, it could not capture ataxic oscillations approaching the target unless patients stopped completely their hand. The included patients had not such severe ataxia and this could explain the remarkable accuracy we measured with this parameter.

Our analysis did not find between group differences in terms of movement planning parameters ($t_{max\%}$, $p_{max\%}$). It is well known that in healthy subjects the velocity peak is reached roughly at half of the movement, while previous reports showed that stroke subjects tend to present left-shifted velocity profile, due to the earlier occurrence of the maximum of velocity (G. M. Johansson et al., 2017). Although in the present study no between-group difference was found, these parameters were differently associated with other movement's features within the three groups.

Specifically, in HS and SP groups the $p_{max\%}$ was not correlated to other movement's parameters suggesting that the velocity peak position may depend only on the trajectory length. In these groups irrespective to the movement's velocity, the velocity peak was reached between 40% and 50% of trajectory length as previous seminal studies found (G. M. Johansson et al., 2017). In contrast, the $t_{max\%}$ was significantly and directly associated with the movement peak velocity. In other words, patients who performed the movement with slower velocity reached the velocity peak earlier compared to the faster patients. This is in line with previous findings suggesting that patients with stroke tend to anticipate the timing of velocity peak (G. M. Johansson et al., 2017). Extending the second phase of the movement, stroke patients tried to maximize the movement accuracy, facilitating the control of the hand while approaching the target. It is conceivable that this behavior could be an attempt to compensate for sensory feedback impairment in the SP group.

The position of the velocity peak in a reaching movement is commonly associated to movement planning. Our results showed that only in the CP group the $p_{max\%}$ was directly associated with the DysmX. Subjects that reached the velocity peak in the second half of the movement trajectory overshot the target while subjects that reached the velocity peak in the first half, undershot their nose. This could suggest that for cerebellar patients the target overshooting or undershooting in an index-to-nose task may be related to an impairment in movement planning rather than to an altered feedback control, as hypothesized and supported by previous literature (Cabaraux et al., 2020). In this respect a previous study analyzed a fast reaching movement using a manipulandum in patients with cerebellar ataxia and found that the amount of the target over- or undershooting was inversely associated to the early movement velocity (Bhanpuri et al., 2013). This finding supported the idea that cerebellar lesions may disrupt UL's inverse model and that dysmetria related to cerebellar ataxia may be a consequence to an altered internal model of the UL. Our results did not corroborate this hypothesis. Although we did find evidence for impaired motor planning in the CP group, in our task the early velocity was not associated with target's over-undershooting. It is conceivable that the relative complexity of index-to-nose task compared to the task investigated by Bhanpuri and colleagues jeopardized this association. In fact, in contrast to their setting, the

index-to-nose task is a three-dimensional pointing movement with significantly wider amplitude. Eventually, it is important to underline that the relatively small sample size may have hampered the analysis power and prevent to find significant between-group differences, especially when comparing features related to movement planning.

To summarize, the kinematic analysis of the finger-to-nose task allowed us to investigate UL movement dysfunction in patients with somatosensory deficits and cerebellar lesions due to stroke. As hypothesized, we found some evidence of impaired motor planning in patients with cerebellar lesion since the spatial error in pointing the nose was associated with the position of the velocity peak and absolute value of peak velocity. These associations could be interpreted as patients' difficulties in adjusting hand's velocity to the planned trajectory. We speculate that this behavior found only in the CP group could be related to an impairment of the forward model as previous literature suggested (Frey et al., 2011; Nowak et al., 2007; Tanaka et al., 2020). Also, we found that patients in the SP group were the most affected by the absence of vision in the as they significantly reduced the movement velocity in the EC condition. This is in line with a strong research body that underlined the crucial role of visual feedback in movement control for patients with somatosensory deficits. Moreover, the association between slower velocity peak and anticipated $t_{max\%}$ could be a sign of impaired sensory feedback and this association was found only in the SP group and not in the CP group. In conclusion, our analysis did not provide conclusive evidence of forward model impairment in patients with somatosensory deficits (Osumi et al., 2018). In contrast, in line previous literature we suggested impairment in using sensory feedback to control UL reaching movement in patients with impaired somatosensation and impaired motor planning and forward model in patients with cerebellar lesions.

General discussion and conclusions

The goal of this project was to investigate different aspects of the anticipatory motor control in healthy subjects and in stroke patients with cerebellar and somatosensory impairment.

In the first section of this dissertation, we aimed to provide further evidence on the role of the forward model in sensorimotor function of the upper limb. We focused on the sensory attenuation phenomenon, and we performed new analysis on previously recorded data on force matching tasks (Bays & Wolpert, 2007a; Shergill et al., 2005; Wolpe et al., 2016). In the Shergill's and Wolpe's studies subjects were delivered with a target force exerted by a motor torque through a lever on their left index fingertip. Then they were asked to match that force with their right index finger by either directly press on their left index through the lever on top of the left index (self condition) or indirectly controlling a slider that was actioning the motor torque attached to the lever (slider condition) (see Figure 3). In the Bays' study, authors used a setting with two levers to perform the force matching task: one lever acted on the left index finger as previously described experiment and one measured the matching force exerted with the right index finger. This setting allowed the authors to manipulate the lateral separation between the two levers and the gain between the force measured by the passive lever and the force produced by the active lever. In the self conditions of the Shergill's and Wolpe's studies and when the two levers were vertically aligned in the Bays' study, authors found that subjects underestimated the force they were exerting, overshooting the target force. In contrast they were more accurate in the slider condition or in case of lateral separation between the two levers (and the hands). Their findings supported the idea that when a forward model can predict the sensory consequence of a voluntary action, this prediction is then used to attenuate the consequent tactile sensations. When this computation was not possible given the artificial setting (i.e. in the slider condition), such attenuation was not measured. Although this strong line of research, recently some studies argued against the forward model hypothesis (Press et al., 2020; Roussel et al., 2013; Thomas et al., 2020; Yon et al., 2020). Taking

together, these recent studies proposed that the previous findings on sensory tactile attenuation in force matching tasks (Bays et al., 2005, 2006; Bays & Wolpert, 2007a; Shergill et al., 2003, 2005, 2013, 2014; Wolpe et al., 2016, 2018) were the results of a general unpredictive gating mechanism that occurs whenever a limb is actively moved (Press et al., 2020).

To disentangle between these two hypotheses, we performed a new analysis focused on the trial-to-trial variability in force matching in conditions with different level of attenuation. The underlying idea of our project was that the amount of attenuation depends on the accurateness of the prediction: the more accurate it is, the more attenuated is the perception. Notably, the accuracy of the prediction is herein to be intended in terms of spatial and temporal coherence rather than intensity. We found that the within-subject relative level of attenuation between two conditions was associated to the within-subject trial to trial variability. These results corroborated the forward model hypothesis: the involvement of a forward model in modulating the intensity of the tactile perception in these conditions, might be responsible for an extra source of sensory noise, eventually translated in the measured increased matching force's trial-to-trial variability. Moreover, we modeled the subjects' responses in the analyzed force matching tasks, and we found that a model in which the attenuation factor is the ratio between the matching forces in the self and slider conditions condition best captured the subjects' behavior. We propose that our results are relevant from different perspectives. On one hand, our analysis underlined the strong connection between motor and sensory aspects of actions: when performing a voluntary action, from the motor command the prediction of the sensory consequences of the movement influences and modulates the intensity of the perception of the consequent sensory stimuli. These aspects should be taken into account by research on motor control, especially concerning the upper limbs. On the other hand, our analysis suggested, in line with previous evidence (Shergill et al., 2005, 2014), that impairment in the forward model may result in misperception of self-generated tactile stimuli compared to healthy adults. Further research should focus on this topic investigating selective predictive motor control impairment and its sensory consequences in different cohorts. Several questions on the SA phenomenon remains unanswered and the physiological

meaning of such phenomenon is still unclear. Previous studies suggested that the attenuation of the predictive part of sensory feedback has the scope of enhancing the salience of unexpected external stimuli (Bays & Wolpert, 2007a). Other studies highlighted the importance of such mechanism in discriminating between self-generated and externally generated stimuli contributing to the sense of agency. Our findings don't provide further evidence on the physiological purpose of the SA phenomenon. Further research should aim to investigate this issue with new experimental procedure, possibly investigating other sensory domains in addition to tactile stimuli.

In the second section of this dissertation, we aimed to investigate anticipatory grip force modulation deficits during a bimanual object lifting task in patients with stroke and somatosensory deficits. The lift of an object is a complex action that involves both the control of the upper limb and the hand-object interaction. This behavior has been widely investigated by assessing the anticipatory grip force modulation during the lifting of an object of known properties (Flanagan et al., 2001; R. S. Johansson & Edin, 1993; Y. Li et al., 2011; Nowak et al., 2005). When moving the UL while grasping an object, predictive state estimation was usually associated with an increase of grip force before the UL movement onset. This anticipatory reaction is crucial in order to prevent the object slippage during the movement (Flanagan & Wing, 1997; Frenkel-Toledo et al., 2019). In contrast to the robust literature body concerning unimanual object lifting, bimanual force modulation in lifting task has not been widely investigated. In order to identify specific impairments in the anticipatory grip force exertion, we firstly investigated patients' ability of bimanually modulating the grip force. In the first chapter we validated our experimental procedure on a sample of young and elderly healthy volunteers. Subjects were assessed in a fixed-force matching task and a time-varying force matching task. The target force was shown on a computer screen and visual feedback of the exerted force was provided (Figure 20). Our setting allowed us to detect older subjects' significant lower accuracy and force stability compared to younger subjects. This was expected given that aging is associated with a variation in the metabolic processes of the brain (Hyder & Rothman, 2012; A.-L. Lin & Rothman, 2014) and with a degenerative process of the neuromuscular

system affecting nerves conduction velocity (Jagga et al., 2011; Norris et al., 1953; Palve & Palve, 2018). In the second chapter we modified the BiSBox device to include a depth camera enabling the device's position tracking. We recruited a convenient sample of healthy subjects and patients with somatosensory impairment due to CNS stroke. Previous findings suggested that sensory information is important for maintaining a precise forward model of dynamic grip force control (Hermsdörfer et al., 2008). However, limited research investigated objects' lifting tasks in patients with sensory deficits due to CNS lesions. Some studies found that stroke subjects presented delayed grip force onset (Blennerhassett et al., 2008; Hermsdörfer et al., 2003; Nowak et al., 2013) and, likely to compensate for these deficits, produced exaggerate grip force (Nowak et al., 2013). In contrast, other reports found that tactile sensitivity deficits seemed not to affect the timing onset of grip forces in respect to the load forces (Hermsdörfer et al., 2003).

In our study, subjects performed a fixed-force matching task, a time-varying force matching task, and a lifting task. Our analysis showed that in the patients we recruited the ability of modulating the bimanual force in force matching tasks was relatively preserved. However, the analysis of the lifting task suggested that patients presented some deficits in force modulation related to movement planning. Specifically, the lifting task allowed us to detect the anticipatory grip force behavior in patients with somatosensory deficits. In line with previous results, (Hermsdörfer et al., 2003), we found that the synchronization between the grip force and the holding force was preserved in the stroke patients. It is conceivable that these patients may be able to use alternative cues, like visual input, or previous learning, to use residual internal predictive models (Hermsdörfer et al., 2003). However, our results showed that patients exerted an exaggerated grip force to carry out the lifting, likely to compensate for sensory deficits and to ensure to avoid object slipping. It is conceivable that these patients may be able to use alternative cues, like visual input or previous learning to use residual internal predictive models (Hermsdörfer et al., 2003). This may indirectly suggest that sensory patients were not able to estimate the grip force needed to lift the device and showed an altered timing of grip force modulation during the lifting phase. The tactile sensation deficit, may have played a role in this behavior, altering the patients' sensorial

experience of the object and making them slower than healthy controls in building its internal model (Nowak et al., 2004).

In the last section of this dissertation, we aimed to use an accurate low-cost movement analysis system to assess predictive upper limb behavior of a fast and repetitive reaching task in patients with cerebellar lesions and patients with somatosensory deficits. Previous literature suggested that a forward model enabling to predict the sensory and kinematic consequences of a voluntary UL action is essential to perform fast and accurate reaching and pointing movements (Wolpert & Ghahramani, 2000). The cerebellum has been identified as an ideal locus for the neural underpinning of such predictive model (Kawato et al., 1987b; Tanaka et al., 2020; Wolpert & Ghahramani, 2000). However, limited research has focused on the role of proprioception in feedforward motor control and on the effects of somatosensory deficits on a forward model of the UL. We developed an accurate low-cost system for the kinematic assessment of the index-to-nose task and we compared a group of young healthy subjects, and stroke patients with cerebellar lesions or proprioceptive impairment. This system was composed of an Intel RealSense D415 RGB-D as input camera and we selected one of the most widespread and accurate pose estimation software Openpose (Cao et al., 2021) and adopted a convolutional neural network trained for detecting detailed human body keypoints, including fingertips and nose. In the first chapter we tested the accuracy of our system using an optoelectronic motion analysis system as a gold standard (Vicon, Oxford Metrics Ltd., Oxford, UK). We found that our system was overall accurate in measuring the most common kinematic parameters in pointing tasks including movement velocity, spatial accuracy of pointing, and position of the velocity peak throughout the movement trajectory. In the second chapter we used this experimental setting to measure a set of reaching parameters referring to movement accuracy, efficiency and motor planning in a cohort of healthy controls and patients affected by CNS stroke involving the cerebellum or the somatosensory cortex and thalamus.

We proposed a theoretical framework for interpreting sensory and cerebellar ataxia as different forward model's dysfunctions. As expected, we found that the included

stroke patients performed the movement less efficiently than healthy controls, being slower in terms of early velocity, peak velocity and average velocity. Interestingly patients' movement speed was not associated with functional UL impairments, suggesting that specific motor control deficits might play a role forcing the patients to slow down hand velocity to compensate. As hypothesized, our results suggested that patients with somatosensory deficit were the most affected by the absence of visual feedback significantly reducing movement speed when performing the task with closed eyes. Moreover, we found that patients with cerebellar lesions showed signs of impaired movement planning. Specifically, for cerebellar patients the target overshooting or undershooting in an index-to-nose task may be related to an impairment in movement planning rather than to an altered feedback control, as suggested by previous literature (Cabaraux et al., 2020). We speculate that this behavior found only in the CP group could be related to an impairment of the forward model as previous literature suggested (Frey et al., 2011; Nowak et al., 2007; Tanaka et al., 2020). In contrast, we did not find direct evidence of impaired motor planning and forward motor control in patients with somatosensory deficits.

Overall, we investigated different aspects of predictive motor control related to forward models of the upper limb. On one hand our results corroborated previous findings on the role of forward models in tactile perception. On the other hand, this dissertation underlined the importance of assessing predictive motor control in patients affected by CNS lesions. Future research should focus on the role of anticipatory motor control in motor learning and on the design of rehabilitation treatment for forward model dysfunctions.

References

Aagten-Murphy, D., & Bays, P. M. (2019). Independent working memory resources for egocentric and allocentric spatial information. *PLOS Computational Biology*, *15*(2), e1006563. https://doi.org/10.1371/journal.pcbi.1006563

Åberg, A. C., Olsson, F., Åhman, H. B., Tarassova, O., Arndt, A., Giedraitis, V., Berglund, L., & Halvorsen, K. (2021). Extraction of gait parameters from marker-free video recordings of Timed Up-and-Go tests: Validity, inter- and intra-rater reliability. *Gait & Posture*, *90*, 489–495. https://doi.org/10.1016/j.gaitpost.2021.08.004

Adans-Dester, C., Fasoli, S. E., Fabara, E., Menard, N., Fox, A. B., Severini, G., & Bonato, P. (2020). Can kinematic parameters of 3D reach-to-target movements be used as a proxy for clinical outcome measures in chronic stroke rehabilitation? An exploratory study. *Journal of NeuroEngineering and Rehabilitation*, *17*(1), 106. https://doi.org/10.1186/s12984-020-00730-1

Alt Murphy, M., Willén, C., & Sunnerhagen, K. S. (2013). Responsiveness of Upper Extremity Kinematic Measures and Clinical Improvement During the First Three Months After Stroke. *Neurorehabilitation and Neural Repair*, *27*(9), 844–853. https://doi.org/10.1177/1545968313491008

Andriluka, M., Pishchulin, L., Gehler, P., & Schiele, B. (2014). 2D Human Pose Estimation: New Benchmark and State of the Art Analysis. *2014 IEEE Conference on Computer Vision and Pattern Recognition*, 3686–3693. https://doi.org/10.1109/CVPR.2014.471

Antico, M., Balletti, N., Laudato, G., Lazich, A., Notarantonio, M., Oliveto, R., Ricciardi, S., Scalabrino, S., & Simeone, J. (2021). Postural control assessment via Microsoft Azure Kinect DK: An evaluation study. *Computer Methods and Programs in Biomedicine*, *209*, 106324. https://doi.org/10.1016/j.cmpb.2021.106324

Archambault, P., Pigeon, P., Feldman, A. G., & Levin, M. F. (1999). Recruitment and sequencing of different degrees of freedom during pointing movements involving the trunk in healthy and hemiparetic subjects. *Experimental Brain Research*, *126*(1), 55–67. https://doi.org/10.1007/s002210050716

Armstrong, C. A., & Oldham, J. A. (1999). A comparison of dominant and non-dominant hand strengths. *The Journal of Hand Surgery: British & European Volume*, *24*(4), 421–425.

Avanzino, L., Ravaschio, A., Lagravinese, G., Bonassi, G., Abbruzzese, G., & Pelosin, E. (2018). Adaptation of feedforward movement control is abnormal in patients with cervical dystonia and tremor. *Clinical Neurophysiology*, *129*(1), 319–326. https://doi.org/10.1016/j.clinph.2017.08.020

Ballardini, G., Ponassi, V., Galofaro, E., Carlini, G., Marini, F., Pellegrino, L., Morasso, P., & Casadio, M. (2019). Interaction between position sense and force control in bimanual tasks. *Journal of Neuroengineering and Rehabilitation*, *16*(1), 1–13.

Ballardini, G., Ponassi, V., Galofaro, E., Pellegrino, L., Solaro, C., Muller, M., & Casadio, M. (2019). Bimanual control of position and force in people with

multiple sclerosis: preliminary results. *2019 IEEE 16th International Conference on Rehabilitation Robotics (ICORR)*, 1147–1152.

Bastian, A. J., Martin, T. A., Keating, J. G., & Thach, W. T. (1996). Cerebellar ataxia: abnormal control of interaction torques across multiple joints. *Journal of Neurophysiology*, *76*(1), 492–509. https://doi.org/10.1152/jn.1996.76.1.492

Bays, P. M., Flanagan, J. R., & Wolpert, D. M. (2006). Attenuation of Self-Generated Tactile Sensations Is Predictive, not Postdictive. *PLoS Biology*, *4*(2), e28. https://doi.org/10.1371/journal.pbio.0040028

Bays, P. M., & Wolpert, D. M. (2007a). Predictive attenuation in the perception of touch. In Haggard Patrick, Rosetti Yves, & Kawato Mitsuo (Eds.), *Attention & Performance XXII, Sensorimotor Foundations of Higher Cognition* (pp. 339–358).

Bays, P. M., & Wolpert, D. M. (2007b). Computational principles of sensorimotor control that minimize uncertainty and variability. In *Journal of Physiology* (Vol. 578, Issue 2, pp. 387–396). https://doi.org/10.1113/jphysiol.2006.120121

Bays, P. M., Wolpert, D. M., & Flanagan, J. R. (2005). Perception of the consequences of self-action is temporally tuned and event driven. *Current Biology*, *15*(12), 1125–1128. https://doi.org/10.1016/j.cub.2005.05.023

Bhanpuri, N. H., Okamura, A. M., & Bastian, A. J. (2013). Predictive modeling by the cerebellum improves proprioception. *Journal of Neuroscience*, *33*(36), 14301–14306. https://doi.org/10.1523/JNEUROSCI.0784-13.2013

Bhanpuri, N. H., Okamura, A. M., & Bastian, A. J. (2014). Predicting and correcting ataxia using a model of cerebellar function. *Brain*, *137*(7), 1931–1944. https://doi.org/10.1093/brain/awu115

Binkofski, F., & Buccino, G. (2018). *The role of the parietal cortex in sensorimotor transformations and action coding* (pp. 467–479). https://doi.org/10.1016/B978-0-444-63622-5.00024-3

Birznieks, I., Burstedt, M. K. O., Edin, B. B., & Johansson, R. S. (1998). *Mechanisms for Force Adjustments to Unpredictable Frictional Changes at Individual Digits During Two-Fingered Manipulation.* www.physiology.org/journal/jn

Blakemore, S.-J., Frith, C. D., & Wolpert, D. M. (2001). The cerebellum is involved in predicting the sensory consequences of action. *Neuroreport*, *12*(9), 1879–1884. https://doi.org/10.1097/00001756-200107030-00023

Blennerhassett, J. M., Carey, L. M., & Matyas, T. A. (2008). Clinical Measures of Handgrip Limitation Relate to Impaired Pinch Grip Force Control after Stroke. *Journal of Hand Therapy*, *21*(3), 245–253. https://doi.org/10.1197/j.jht.2007.10.021

Boecker, H., Lee, A., Mühlau, M., Ceballos-Baumann, A., Ritzl, A., Spilker, M. E., Marquart, C., & Hermsdörfer, J. (2005). Force level independent representations of predictive grip force–load force coupling: A PET activation study. *NeuroImage*, *25*(1), 243–252. https://doi.org/10.1016/j.neuroimage.2004.10.027

Bostan, A. C., Dum, R. P., & Strick, P. L. (2013). Cerebellar networks with the cerebral cortex and basal ganglia. *Trends in Cognitive Sciences*, *17*(5), 241–254. https://doi.org/10.1016/j.tics.2013.03.003

Cabaraux, P., Gandini, J., Kakei, S., Manto, M., Mitoma, H., & Tanaka, H. (2020). Dysmetria and errors in predictions: The role of internal forward model. In *International Journal of Molecular Sciences* (Vol. 21, Issue 18, pp. 1–21). MDPI AG. https://doi.org/10.3390/ijms21186900

Cabeza, R. (2001). Functional neuroimaging of cognitive aging. *HANDBOOK OF FUNCTIONAL NEUROIMAGING OF COGNITION.*

Cao, Z., Hidalgo, G., Simon, T., Wei, S.-E., & Sheikh, Y. (2021). OpenPose: Realtime Multi-Person 2D Pose Estimation Using Part Affinity Fields. *IEEE Transactions on Pattern Analysis and Machine Intelligence*, *43*(1), 172–186. https://doi.org/10.1109/TPAMI.2019.2929257

Caspers, S., & Zilles, K. (2018). *Microarchitecture and connectivity of the parietal lobe* (pp. 53–72). https://doi.org/10.1016/B978-0-444-63622-5.00003-6

Chapman, C. E., Bushnell, M. C., Miron, D., Duncan, G. H., & Lund, J. P. (1987). Sensory perception during movement in man. *Experimental Brain Research*, *68*(3). https://doi.org/10.1007/BF00249795

Chen, Z.-J., He, C., Gu, M.-H., Xu, J., & Huang, X.-L. (2021). Kinematic Evaluation via Inertial Measurement Unit Associated with Upper Extremity Motor Function in Subacute Stroke: A Cross-Sectional Study. *Journal of Healthcare Engineering*, *2021*, 1–7. https://doi.org/10.1155/2021/4071645

Coderre, A. M., Amr Abou Zeid, Dukelow, S. P., Demmer, M. J., Moore, K. D., Demers, M. J., Bretzke, H., Herter, T. M., Glasgow, J. I., Norman, K. E., Bagg, S. D., & Scott, S. H. (2010). Assessment of upper-limb sensorimotor function of subacute stroke patients using visually guided reaching. *Neurorehabilitation and Neural Repair*, *24*(6), 528–541. https://doi.org/10.1177/1545968309356091

Cole, K. J., Steyers, C. M., & Graybill, E. K. (2003). The effects of graded compression of the median nerve in the carpal canal on grip force. *Experimental Brain Research*, *148*(2), 150–157. https://doi.org/10.1007/s00221-002-1283-6

Collin, C., & Wade, D. (1990). Assessing motor impairment after stroke: a pilot reliability study. *Journal of Neurology, Neurosurgery & Psychiatry*, *53*(7), 576–579. https://doi.org/10.1136/jnnp.53.7.576

Córdova Bulens, D., Crevecoeur, F., Thonnard, J.-L., & Lefèvre, P. (2018). Optimal use of limb mechanics distributes control during bimanual tasks. *Journal of Neurophysiology*, *119*(3), 921–932.

Cui, H. (2016). Forward prediction in the posterior parietal cortex and dynamic brain-machine interface. *Frontiers in Integrative Neuroscience*, *10*(OCT2016). https://doi.org/10.3389/fnint.2016.00035

D'ANGELO, E. (2011). NEURAL CIRCUITS OF THE CEREBELLUM: HYPOTHESIS FOR FUNCTION. *Journal of Integrative Neuroscience*, *10*(03), 317–352. https://doi.org/10.1142/S0219635211002762

D'Angelo, E. (2018). Physiology of the cerebellum. In *Handbook of Clinical Neurology* (Vol. 154, pp. 85–108). Elsevier B.V. https://doi.org/10.1016/B978-0-444-63956-1.00006-0

Daunoraviciene, K., Ziziene, J., Griskevicius, J., Pauk, J., Ovcinikova, A., Kizlaitiene, R., & Kaubrys, G. (2018). Quantitative assessment of upper

extremities motor function in multiple sclerosis. *Technology and Health Care*, *26*, 647–653. https://doi.org/10.3233/THC-182511

Davidson, S. (2016). A Spinal Circuit for Mechanically-Evoked Itch. *Trends in Neurosciences*, *39*(1), 1–2. https://doi.org/10.1016/j.tins.2015.12.001

Davis, N. J. (2007). Memory and coordination in bimanual isometric finger force production. *Experimental Brain Research*, *182*(1), 137–142.

Day, B. L., Thompson, P. D., Harding, A. E., & Marsden, C. D. (1998). Influence of vision on upper limb reaching movements in patients with cerebellar ataxia. In *Brain* (Vol. 121).

de los Reyes-Guzmán, A., Dimbwadyo-Terrer, I., Trincado-Alonso, F., Monasterio-Huelin, F., Torricelli, D., & Gil-Agudo, A. (2014). Quantitative assessment based on kinematic measures of functional impairments during upper extremity movements: A review. *Clinical Biomechanics*, *29*(7), 719–727. https://doi.org/10.1016/j.clinbiomech.2014.06.013

Desmurget, M., Epstein, C. M., Turner, R. S., Prablanc, C., Alexander, G. E., & Grafton, S. T. (1999). Role of the posterior parietal cortex in updating reaching movements to a visual target. *Nature Neuroscience*, *2*(6), 563–567. https://doi.org/10.1038/9219

Dogge, M., Custers, R., & Aarts, H. (2019). Moving Forward: On the Limits of Motor-Based Forward Models. In *Trends in Cognitive Sciences* (Vol. 23, Issue 9, pp. 743–753). Elsevier Ltd. https://doi.org/10.1016/j.tics.2019.06.008

Ehrsson, H. H., Fagergren, A., Johansson, R. S., & Forssberg, H. (2003). Evidence for the Involvement of the Posterior Parietal Cortex in Coordination of Fingertip Forces for Grasp Stability in Manipulation. *Journal of Neurophysiology*, *90*(5), 2978–2986. https://doi.org/10.1152/jn.00958.2002

Feinberg, I. (1978). Efference Copy and Corollary Discharge: Implications for Thinking and Its Disorders*. *Schizophrenia Bulletin*, *4*(4), 636–640. https://doi.org/10.1093/schbul/4.4.636

Feldman, A. G. (2015). *Referent control of action and perception*. Springer New York. https://doi.org/10.1007/978-1-4939-2736-4

Ferrand, L., & Jaric, S. (2006). Force coordination in static bimanual manipulation: Effect of handedness. *Motor Control*, *10*(4), 359–370.

Fjell, A. M., McEvoy, L., Holland, D., Dale, A. M., Walhovd, K. B., & Initiative, A. D. N. (2014). What is normal in normal aging? Effects of aging, amyloid and Alzheimer's disease on the cerebral cortex and the hippocampus. *Progress in Neurobiology*, *117*, 20–40.

Flanagan, J. R., King, S., Wolpert, D. M., & Johansson, R. S. (2001). Sensorimotor prediction and memory in object manipulation. *Canadian Journal of Experimental Psychology/Revue Canadienne de Psychologie Expérimentale*, *55*(2), 87–95. https://doi.org/10.1037/h0087355

Flanagan, J. R., & Wing, A. M. (1997). The Role of Internal Models in Motion Planning and Control: Evidence from Grip Force Adjustments during Movements of Hand-Held Loads. In *The Journal of Neuroscience* (Vol. 17, Issue 4).

Flanagan, J. R., & Wing, AlanM. (1995). The stability of precision grip forces during cyclic arm movements with a hand-held load. *Experimental Brain Research*, *105*(3), 455–464. https://doi.org/10.1007/BF00233045

Fozard, J. L., Vercruyssen, M., Reynolds, S. L., Hancock, P. A., & Quilter, R. E. (1994). Age differences and changes in reaction time: the Baltimore Longitudinal Study of Aging. *Journal of Gerontology*, *49*(4), P179–P189.

Frenkel-Toledo, S., Yamanaka, J., Friedman, J., Feldman, A. G., & Levin, M. F. (2019). Referent control of anticipatory grip force during reaching in stroke: an experimental and modeling study. *Experimental Brain Research*, *237*(7), 1655–1672. https://doi.org/10.1007/s00221-019-05498-y

Frey, S. H., Fogassi, L., Grafton, S., Picard, N., Rothwell, J. C., Schweighofer, N., Corbetta, M., & Fitzpatrick, S. M. (2011). Neurological Principles and Rehabilitation of Action Disorders. *Neurorehabilitation and Neural Repair*, *25*(5_suppl), 6S-20S. https://doi.org/10.1177/1545968311410940

Fugl-Meyer, A. R., Jääskö, L., Leyman, I., Olsson, S., & Steglind, S. (1975). The post-stroke hemiplegic patient. 1. a method for evaluation of physical performance. *Scandinavian Journal of Rehabilitation Medicine*, *7*(1), 13–31.

Fujiyama, H., Van Soom, J., Rens, G., Gooijers, J., Leunissen, I., Levin, O., & Swinnen, S. P. (2016). Age-related changes in frontal network structural and functional connectivity in relation to bimanual movement control. *Journal of Neuroscience*, *36*(6), 1808–1822.

Galganski, M. E., Fuglevand, A. J., & Enoka, R. M. (1993). Reduced control of motor output in a human hand muscle of elderly subjects during submaximal contractions. *Journal of Neurophysiology*, *69*(6), 2108–2115.

Galofaro, E., Ballardini, G., Boggini, S., Foti, F., Nisky, I., & Casadio, M. (2019). Assessment of bimanual proprioception during an orientation matching task with a physically coupled object. *2019 IEEE 16th International Conference on Rehabilitation Robotics (ICORR)*, 101–107. https://doi.org/10.1109/ICORR.2019.8779415

Garro, F., Chiappalone, M., Buccelli, S., de Michieli, L., & Semprini, M. (2021). Neuromechanical Biomarkers for Robotic Neurorehabilitation. *Frontiers in Neurorobotics*, *15*. https://doi.org/10.3389/fnbot.2021.742163

Geschwind, N., & Kaplan, E. (1998). A human cerebral deconnection syndrome: A preliminary report. *Neurology*, *50*(5), 1201.

Ghika, J., Bogousslavsky, J., Henderson, J., Maeder, P., & Regli, F. (1994). The jerky dystonic unsteady hand: A delayed motor syndrome in posterior thalamic infarctions. *Journal of Neurology*, *241*(9), 537–542. https://doi.org/10.1007/BF00873516

Goble, D. J., Coxon, J. P., van Impe, A., de Vos, J., Wenderoth, N., & Swinnen, S. P. (2010). The neural control of bimanual movements in the elderly: Brain regions exhibiting age-related increases in activity, frequency-induced neural modulation, and task-specific compensatory recruitment. *Human Brain Mapping*, *31*(8), 1281–1295. https://doi.org/10.1002/hbm.20943

Goldenberg, G. (2013). *Apraxia*. Oxford University Press. https://doi.org/10.1093/acprof:oso/9780199591510.001.0001

Gordon, A. M., Westling, G., Cole, K. J., & Johansson, R. S. (1993). Memory representations underlying motor commands used during manipulation of

common and novel objects. *Journal of Neurophysiology*, *69*(6), 1789–1796. https://doi.org/10.1152/jn.1993.69.6.1789

Gorniak, S. L., Plow, M., McDaniel, C., & Alberts, J. L. (2014). Impaired object handling during bimanual task performance in multiple sclerosis. *Multiple Sclerosis International*, *2014*.

Grosskopf, A., & Kuhtz-Buschbeck, J. P. (2006). Grasping with the left and right hand: a kinematic study. *Experimental Brain Research*, *168*(1–2), 230–240. https://doi.org/10.1007/s00221-005-0083-1

Guo, Y., Deligianni, F., Gu, X., & Yang, G.-Z. (2019). 3-D Canonical Pose Estimation and Abnormal Gait Recognition With a Single RGB-D Camera. *IEEE Robotics and Automation Letters*, *4*(4), 3617–3624. https://doi.org/10.1109/LRA.2019.2928775

Guo, Y., Gu, X., & Yang, G.-Z. (2021). MCDCD: Multi-Source Unsupervised Domain Adaptation for Abnormal Human Gait Detection. *IEEE Journal of Biomedical and Health Informatics*, *25*(10), 4017–4028. https://doi.org/10.1109/JBHI.2021.3080502

Hartley, R. (2004). *Multiple view geometry in computer vision*. Cambridge University Press.

Hatem, S. M., Saussez, G., della Faille, M., Prist, V., Zhang, X., Dispa, D., & Bleyenheuft, Y. (2016). Rehabilitation of Motor Function after Stroke: A Multiple Systematic Review Focused on Techniques to Stimulate Upper Extremity Recovery. *Frontiers in Human Neuroscience*, *10*. https://doi.org/10.3389/fnhum.2016.00442

Hausmann, M., GuÈntuÈrkuÈn, O., & Corballis, M. (2003). Age-related changes in hemispheric asymmetry depend on sex. *Laterality: Asymmetries of Body, Brain and Cognition*, *8*(3), 277–290.

Henningsen, H., Ende-Henningsen, B., & Gordon, A. M. (1995). Asymmetric control of bilateral isometric finger forces. *Experimental Brain Research*, *105*(2), 304–311.

Hermans, L., Levin, O., Maes, C., Van Ruitenbeek, P., Heise, K.-F., Edden, R. A. E., Puts, N. A. J., Peeters, R., King, B. R., & Meesen, R. L. J. (2018). GABA levels and measures of intracortical and interhemispheric excitability in healthy young and older adults: an MRS-TMS study. *Neurobiology of Aging*, *65*, 168–177.

Hermsdörfer, J., Elias, Z., Cole, J. D., Quaney, B. M., & Nowak, D. A. (2008). Preserved and Impaired Aspects of Feed-Forward Grip Force Control After Chronic Somatosensory Deafferentation. *Neurorehabilitation and Neural Repair*, *22*(4), 374–384. https://doi.org/10.1177/1545968307311103

Hermsdörfer, J., Hagl, E., Nowak, D. A., & Marquardt, C. (2003). Grip force control during object manipulation in cerebral stroke. *Clinical Neurophysiology*, *114*(5), 915–929. https://doi.org/10.1016/S1388-2457(03)00042-7

Heuninckx, S., Wenderoth, N., Debaere, F., Peeters, R., & Swinnen, S. P. (2005). Neural basis of aging: the penetration of cognition into action control. *Journal of Neuroscience*, *25*(29), 6787–6796.

Heuninckx, S., Wenderoth, N., & Swinnen, S. P. (2008). Systems neuroplasticity in the aging brain: recruiting additional neural resources for successful motor performance in elderly persons. *Journal of Neuroscience*, *28*(1), 91–99.

Honda, T., Mitoma, H., Yoshida, H., Bando, K., Terashi, H., Taguchi, T., Miyata, Y., Kumada, S., Hanakawa, T., Aizawa, H., Yano, S., Kondo, T., Mizusawa, H., Manto, M., & Kakei, S. (2020). Assessment and Rating of Motor Cerebellar Ataxias With the Kinect v2 Depth Sensor: Extending Our Appraisal. *Frontiers in Neurology*, *11*. https://doi.org/10.3389/fneur.2020.00179

Hoonhorst, M. H., Nijland, R. H., van den Berg, J. S., Emmelot, C. H., Kollen, B. J., & Kwakkel, G. (2015). How Do Fugl-Meyer Arm Motor Scores Relate to Dexterity According to the Action Research Arm Test at 6 Months Poststroke? *Archives of Physical Medicine and Rehabilitation*, *96*(10), 1845–1849. https://doi.org/10.1016/j.apmr.2015.06.009

Hsu, J. (1996). *Multiple comparisons: theory and methods*. CRC Press.

Hu, X., Loncharich, M., & Newell, K. M. (2011). Visual information interacts with neuromuscular factors in the coordination of bimanual isometric force. *Experimental Brain Research*, *209*(1), 129–138.

Hu, X., & Newell, K. M. (2011). Aging, visual information, and adaptation to task asymmetry in bimanual force coordination. *Journal of Applied Physiology*, *111*(6), 1671–1680.

Hunter, S. K., Pereira, H. M., & Keenan, K. G. (2016). The aging neuromuscular system and motor performance. *Journal of Applied Physiology*, *121*(4), 982–995.

Hyder, F., & Rothman, D. L. (2012). Quantitative fMRI and oxidative neuroenergetics. *Neuroimage*, *62*(2), 985–994.

Iandolo, R., Carè, M., Shah, V. A., Schiavi, S., Bommarito, G., Boffa, G., Giannoni, P., Inglese, M., Mrotek, L. A., & Scheidt, R. A. (2019). A two alternative forced choice method for assessing vibrotactile discrimination thresholds in the lower limb. *Somatosensory & Motor Research*, *36*(2), 162–170.

Incel, N. A., Ceceli, E., Durukan, P. B., Erdem, H. R., & Yorgancioglu, Z. R. (2002). Grip strength: effect of hand dominance. *Singapore Medical Journal*, *43*(5), 234–237.

Jagga, M., Lehri, A., & Verma, S. K. (2011). Effect of aging and anthropometric measurements on nerve conduction properties-A review. *Journal of Exercise Science and Physiotherapy*, *7*(1), 1.

Jaric, S., Collins, J. J., Marwaha, R., & Russell, E. (2006). Interlimb and within limb force coordination in static bimanual manipulation task. *Experimental Brain Research*, *168*(1–2), 88–97.

Jaric, S., Knight, C. A., Collins, J. J., & Marwaha, R. (2005). Evaluation of a method for bimanual testing coordination of hand grip and load forces under isometric conditions. *Journal of Electromyography and Kinesiology*, *15*(6), 556–563.

Jin, X., Uygur, M., Getchell, N., Hall, S. J., & Jaric, S. (2011). The effects of instruction and hand dominance on grip-to-load force coordination in manipulation tasks. *Neuroscience Letters*, *504*(3), 330–335.

Jin, Y., Kim, M., Oh, S., & Yoon, B. (2019). Motor control strategies during bimanual isometric force control among healthy individuals. *Adaptive Behavior*, *27*(2), 127–136.

Jin, Y., Seong, J., Cho, Y., & Yoon, B. (2019). Effects of aging on motor control strategies during bimanual isometric force control. *Adaptive Behavior*, *27*(4), 267–275.

Johansson, G. M., Grip, H., Levin, M. F., & Häger, C. K. (2017). The added value of kinematic evaluation of the timed finger-to-nose test in persons post-stroke. *Journal of NeuroEngineering and Rehabilitation*, *14*(1). https://doi.org/10.1186/s12984-017-0220-7

Johansson, R. S., & Cole, K. J. (1994). Grasp stability during manipulative actions. *Canadian Journal of Physiology and Pharmacology*, *72*(5), 511–524. https://doi.org/10.1139/y94-075

Johansson, R. S., & Edin, B. B. (1993). PREDICTIVE FEED-FORWARD SENSORY CONTROL DURING GRASPING AND MANIPULATION IN MAN. In *Biomedical Research* (Vol. 14).

Johansson, R. S., & Flanagan, J. R. (2009). Coding and use of tactile signals from the fingertips in object manipulation tasks. *Nature Reviews Neuroscience*, *10*(5), 345–359. https://doi.org/10.1038/nrn2621

Johansson, R. S., & Westling, G. (1984). Roles of glabrous skin receptors and sensorimotor memory in automatic control of precision grip when lifting rougher or more slippery objects. *Experimental Brain Research*, *56*(3). https://doi.org/10.1007/BF00237997

Johnson, P. B., Ferraina, S., Bianchi, L., & Caminiti, R. (1996). Cortical Networks for Visual Reaching: Physiological and Anatomical Organization of Frontal and Parietal Lobe Arm Regions. *Cerebral Cortex*, *6*(2), 102–119. https://doi.org/10.1093/cercor/6.2.102

Jordan, M. I. (1996a). Computational aspects of motor control and motor learning. In *Handbook of Perception and Action* (pp. 71–120). https://doi.org/10.1016/S1874-5822(06)80005-8

Jordan, M. I. (1996b). *Computational aspects of motor control and motor learning* (pp. 71–120). https://doi.org/10.1016/S1874-5822(06)80005-8

Jordan, M., & Rumelhart, D. (1992). Forward models: Supervised learning with a distal teacher. *Cognitive Science*, *16*(3), 307–354. https://doi.org/10.1016/0364-0213(92)90036-T

Kalaska, J. F., Caminiti, R., & Georgopoulos, A. P. (1983). Cortical mechanisms related to the direction of two-dimensional arm movements: relations in parietal area 5 and comparison with motor cortex. *Experimental Brain Research*, *51*(2). https://doi.org/10.1007/BF00237200

Kalisch, T., Wilimzig, C., Kleibel, N., Tegenthoff, M., & Dinse, H. R. (2006). Age-related attenuation of dominant hand superiority. *PLoS One*, *1*(1), e90.

Kang, N., & Cauraugh, J. H. (2014). Bimanual force variability and chronic stroke: asymmetrical hand control. *PloS One*, *9*(7).

Kang, N., & Cauraugh, J. H. (2018). Coherence and interlimb force control: effects of visual gain. *Neuroscience Letters*, *668*, 86–91.

Kapur, S., Zatsiorsky, V. M., & Latash, M. L. (2010). Age-related changes in the control of finger force vectors. *Journal of Applied Physiology*, *109*(6), 1827–1841.

Kawato, M., Furukawa, K., & Suzuki, R. (1987a). A hierarchical neural-network model for control and learning of voluntary movement. *Biological Cybernetics*, *57*(3), 169–185. https://doi.org/10.1007/BF00364149

Kawato, M., Furukawa, K., & Suzuki, R. (1987b). A hierarchical neural-network model for control and learning of voluntary movement. *Biological Cybernetics*, *57*(3), 169–185. https://doi.org/10.1007/BF00364149

Kawato, M., Kuroda, T., Imamizu, H., Nakano, E., Miyauchi, S., & Yoshioka, T. (2003). Internal forward models in the cerebellum: fMRI study on grip force and load force coupling. *Progress in Brain Research*, 171–188. https://doi.org/10.1016/S0079-6123(03)42013-X

Kelly, G., & Shanley, J. (2016). Rehabilitation of ataxic gait following cerebellar lesions: Applying theory to practice. *Physiotherapy Theory and Practice*, *32*(6), 430–437. https://doi.org/10.1080/09593985.2016.1202364

Kennedy, D. M., Boyle, J. B., Wang, C., & Shea, C. H. (2016). Bimanual force control: cooperation and interference? *Psychological Research*, *80*(1), 34–54.

Kidziński, Ł., Yang, B., Hicks, J. L., Rajagopal, A., Delp, S. L., & Schwartz, M. H. (2020). Deep neural networks enable quantitative movement analysis using single-camera videos. *Nature Communications*, *11*(1), 4054. https://doi.org/10.1038/s41467-020-17807-z

Kilteni, K., & Ehrsson, H. (2020). Predictive attenuation of touch and tactile gating are distinct perceptual phenomena. *BioRxiv*.

Kilteni, K., Engeler, P., Boberg, I., Maurex, L., & Ehrsson, H. H. (2021). No evidence for somatosensory attenuation during action observation of self-touch. *European Journal of Neuroscience*, *54*(7), 6422–6444. https://doi.org/10.1111/ejn.15436

Kilteni, K., Engeler, P., & Ehrsson, H. H. (2020). Efference Copy Is Necessary for the Attenuation of Self-Generated Touch. *IScience*, *23*(2). https://doi.org/10.1016/j.isci.2020.100843

Klingner, C. M., & Witte, O. W. (2018). Somatosensory deficits. In *Handbook of Clinical Neurology* (Vol. 151, pp. 185–206). Elsevier B.V. https://doi.org/10.1016/B978-0-444-63622-5.00009-7

Körding, K. P., Ku, S., & Wolpert, D. M. (2004). Bayesian integration in force estimation. *Journal of Neurophysiology*, *92*(5), 3161–3165. https://doi.org/10.1152/jn.00275.2004

Körding, K. P., & Wolpert, D. M. (2004). *Bayesian integration in sensorimotor learning*. www.nature.com/nature

Krabben, T., Molier, B. I., Houwink, A., Rietman, J. S., Buurke, J. H., & Prange, G. B. (2011). Circle drawing as evaluative movement task in stroke rehabilitation: an explorative study. *Journal of NeuroEngineering and Rehabilitation*, *8*(1), 15. https://doi.org/10.1186/1743-0003-8-15

Krishna, R., Pathirana, P. N., Horne, M., Power, L., & Szmulewicz, D. J. (2019). Quantitative Assessment of Cerebella Ataxia, through Automated Limb-Coordination tests. *2019 41st Annual International Conference of the IEEE Engineering in Medicine and Biology Society (EMBC)*, 6850–6853. https://doi.org/10.1109/EMBC.2019.8856694

Krishnan, V., & Jaric, S. (2010). Effects of task complexity on coordination of inter-limb and within-limb forces in static bimanual manipulation. *Motor Control*, *14*(4), 528–544.

Kubota, H., Demura, S., & Kawabata, H. (2012). Laterality and age-level differences between young women and elderly women in controlled force exertion (CFE). *Archives of Gerontology and Geriatrics*, *54*(2), e68–e72.

Kwakkel, G., Lannin, N. A., Borschmann, K., English, C., Ali, M., Churilov, L., Saposnik, G., Winstein, C., van Wegen, E. E. H., Wolf, S. L., Krakauer, J. W., & Bernhardt, J. (2017). Standardized Measurement of Sensorimotor Recovery in Stroke Trials: Consensus-Based Core Recommendations from the Stroke Recovery and Rehabilitation Roundtable. *Neurorehabilitation and Neural Repair*, *31*(9), 784–792. https://doi.org/10.1177/1545968317732662

Lafargue, G., Paillard, J., Lamarre, Y., & Sirigu, A. (2003). Production and perception of grip force without proprioception: is there a sense of effort in deafferented subjects? *European Journal of Neuroscience*, *17*(12), 2741–2749.

Lee, S. I., Adans-Dester, C. P., Grimaldi, M., Dowling, A. v., Horak, P. C., Black-Schaffer, R. M., Bonato, P., & Gwin, J. T. (2018). Enabling Stroke Rehabilitation in Home and Community Settings: A Wearable Sensor-Based Approach for Upper-Limb Motor Training. *IEEE Journal of Translational Engineering in Health and Medicine*, *6*, 1–11. https://doi.org/10.1109/JTEHM.2018.2829208

Leuenberger, K., Gonzenbach, R., Wachter, S., Luft, A., & Gassert, R. (2017). A method to qualitatively assess arm use in stroke survivors in the home environment. *Medical & Biological Engineering & Computing*, *55*(1), 141–150. https://doi.org/10.1007/s11517-016-1496-7

Li, K., & Wei, N. (2014). Fingertip force variability on the left and right hand during low-level sustained precision pinch. *2014 7th International Conference on Biomedical Engineering and Informatics*, 302–306.

Li, Y., Randerath, J., Goldenberg, G., & Hermsdörfer, J. (2011). Size–weight illusion and anticipatory grip force scaling following unilateral cortical brain lesion. *Neuropsychologia*, *49*(5), 914–923. https://doi.org/10.1016/j.neuropsychologia.2011.02.018

Lin, A.-L., & Rothman, D. L. (2014). What have novel imaging techniques revealed about metabolism in the aging brain? *Future Neurology*, *9*(3), 341–354.

Lin, C.-H., Chou, L.-W., Wei, S.-H., Lieu, F.-K., Chiang, S.-L., & Sung, W.-H. (2014). Influence of aging on bimanual coordination control. *Experimental Gerontology*, *53*, 40–47.

Lin, C.-H., Sung, W.-H., Chiang, S.-L., Lee, S.-C., Lu, L.-H., Wang, P.-C., & Wang, X.-M. (2019). Influence of aging and visual feedback on the stability of hand grip control in elderly adults. *Experimental Gerontology*, *119*, 74–81.

Lin, K.-C., Wu, C.-Y., Wei, T.-H., Gung, C., Lee, C.-Y., & Liu, J.-S. (2007). Effects of modified constraint-induced movement therapy on reach-to-grasp movements and functional performance after chronic stroke: a randomized controlled study. *Clinical Rehabilitation*, *21*(12), 1075–1086. https://doi.org/10.1177/0269215507079843

Lin, T.-Y., Maire, M., Belongie, S., Hays, J., Perona, P., Ramanan, D., Dollár, P., & Zitnick, C. L. (2014). *Microsoft COCO: Common Objects in Context* (pp. 740–755). https://doi.org/10.1007/978-3-319-10602-1_48

Lisberger, S., & Thach, T. (2013). The Cerebellum. In E. Kandel, J. Schwartz, T. Jessell, S. Siegelbaum, & A. J. Hudspeth (Eds.), *Principles of Neural Science* (Fifth Edition, pp. 960–981). McGraw-Hill.

Lodha, N., Coombes, S. A., & Cauraugh, J. H. (2012). Bimanual isometric force control: Asymmetry and coordination evidence post stroke. *Clinical Neurophysiology*. https://doi.org/10.1016/j.clinph.2011.08.014

Lodha, N., Naik, S. K., Coombes, S. A., & Cauraugh, J. H. (2010). Force control and degree of motor impairments in chronic stroke. *Clinical Neurophysiology*, *121*(11), 1952–1961.

Long, J., Tazoe, T., Soteropoulos, D. S., & Perez, M. A. (2016). Interhemispheric connectivity during bimanual isometric force generation. *Journal of Neurophysiology*, *115*(3), 1196–1207.

Maceira-Elvira, P., Popa, T., Schmid, A.-C., & Hummel, F. C. (2019). Wearable technology in stroke rehabilitation: towards improved diagnosis and treatment of upper-limb motor impairment. *Journal of NeuroEngineering and Rehabilitation*, *16*(1), 142. https://doi.org/10.1186/s12984-019-0612-y

Macerollo, A., Chen, J. C., Parees, I., Sadnicka, A., Kassavetis, P., Bhatia, K. P., Kilner, J. M., Rothwell, J. C., & Edwards, M. J. (2016). Abnormal movement-related suppression of sensory evoked potentials in upper limb dystonia. *European Journal of Neurology*, *23*(3), 562–568. https://doi.org/10.1111/ene.12890

Macerollo, A., Chen, J. C., Parés, I., Kassavetis, P., Kilner, J. M., & Edwards, M. J. (2015). Sensory attenuation assessed by sensory evoked potentials in functional movement disorders. *PLoS ONE*, *10*(6). https://doi.org/10.1371/journal.pone.0129507

Maes, C., Gooijers, J., de Xivry, J.-J. O., Swinnen, S. P., & Boisgontier, M. P. (2017). Two hands, one brain, and aging. *Neuroscience & Biobehavioral Reviews*, *75*, 234–256.

Manto, M., Bower, J. M., Conforto, A. B., Delgado-García, J. M., da Guarda, S. N. F., Gerwig, M., Habas, C., Hagura, N., Ivry, R. B., Mariën, P., Molinari, M., Naito, E., Nowak, D. A., Oulad Ben Taib, N., Pelisson, D., Tesche, C. D., Tilikete, C., & Timmann, D. (2012). Consensus Paper: Roles of the Cerebellum in Motor Control—The Diversity of Ideas on Cerebellar Involvement in Movement. *The Cerebellum*, *11*(2), 457–487. https://doi.org/10.1007/s12311-011-0331-9

Marini, F., Squeri, V., Morasso, P., & Masia, L. (2016). Wrist proprioception: amplitude or position coding? *Frontiers in Neurorobotics*, *10*, 13.

Martin, T. A., Keating, J. G., Goodkin, H. P., Bastian, A. J., & Thach, W. T. (1996). Throwing while looking through prisms: I. Focal olivocerebellar lesions impair adaptation. *Brain*, *119*(4), 1183–1198. https://doi.org/10.1093/brain/119.4.1183

Martini, E., Vale, N., Boldo, M., Righetti, A., Smania, N., & Bombieri, N. (2022). On the Pose Estimation Software for Measuring Movement Features in the Finger-to-Nose Test. *2022 IEEE International Conference on Digital Health (ICDH)*, 77–86. https://doi.org/10.1109/ICDH55609.2022.00021

Maschke, M., Gomez, C. M., Ebner, T. J., & Konczak, J. (2004). Hereditary Cerebellar Ataxia Progressively Impairs Force Adaptation During Goal-Directed Arm Movements. *Journal of Neurophysiology*, *91*(1), 230–238. https://doi.org/10.1152/jn.00557.2003

Mattar, A. A. G., & Gribble, P. L. (2005). Motor Learning by Observing. *Neuron*, *46*(1), 153–160. https://doi.org/10.1016/j.neuron.2005.02.009

Mcnamee, D., & Wolpert, D. M. (2019). Internal Models in Biological Control. *Annu Rev Control Robot Auton Syst.*, *2*, 339–364. https://doi.org/10.1146/annurev-control-060117-105206

McNeil, C. J., Doherty, T. J., Stashuk, D. W., & Rice, C. L. (2005). Motor unit number estimates in the tibialis anterior muscle of young, old, and very old men. *Muscle & Nerve: Official Journal of the American Association of Electrodiagnostic Medicine*, *31*(4), 461–467.

Mehdizadeh, S., Nabavi, H., Sabo, A., Arora, T., Iaboni, A., & Taati, B. (2021). Concurrent validity of human pose tracking in video for measuring gait parameters in older adults: a preliminary analysis with multiple trackers, viewing angles, and walking directions. *Journal of NeuroEngineering and Rehabilitation*, *18*(1), 139. https://doi.org/10.1186/s12984-021-00933-0

Melo, T. P., & Bogousslavsky, J. (1992). Hemiataxia-hypesthesia: a thalamic stroke syndrome. *Journal of Neurology, Neurosurgery & Psychiatry*, *55*(7), 581–584. https://doi.org/10.1136/jnnp.55.7.581

Miall, R. C., Rosenthal, O., Ørstavik, K., Cole, J. D., & Sarlegna, F. R. (2019). Loss of haptic feedback impairs control of hand posture: a study in chronically deafferented individuals when grasping and lifting objects. *Experimental Brain Research*, *237*(9), 2167–2184. https://doi.org/10.1007/s00221-019-05583-2

Mitchell, M., Martin, B. J., & Adamo, D. E. (2017). Upper limb asymmetry in the sense of effort is dependent on force level. *Frontiers in Psychology*, *8*, 643.

Monteiro, T. S., Zivari Adab, H., Chalavi, S., Gooijers, J., King, B. (Bradley) R., Cuypers, K., Mantini, D., & Swinnen, S. P. (2020). Reduced Modulation of Task-Related Connectivity Mediates Age-Related Declines in Bimanual Performance. *Cerebral Cortex*, *30*(8), 4346–4360.

Monzée, J., Lamarre, Y., & Smith, A. M. (2003). The Effects of Digital Anesthesia on Force Control Using a Precision Grip. *Journal of Neurophysiology*, *89*(2), 672–683. https://doi.org/10.1152/jn.00434.2001

Morrison, S., & Newell, K. M. (1998). Interlimb coordination as a function of isometric force output. *Journal of Motor Behavior*, *30*(4), 323–342.

Mountcastle, V. (1997). The columnar organization of the neocortex. *Brain*, *120*(4), 701–722. https://doi.org/10.1093/brain/120.4.701

Mulliken, G. H., Musallam, S., & Andersen, R. A. (2008). Forward estimation of movement state in posterior parietal cortex. *Proceedings of the National Academy of Sciences*, *105*(24), 8170–8177. https://doi.org/10.1073/pnas.0802602105

Murase, N., Kaji, R., Shimazu, H., Katayama-Hirota, M., Ikeda, A., Kohara, N., Kimura, J., Shibasaki, H., & Rothwell, J. C. (2000). Abnormal premovement gating of somatosensory input in writer's cramp. In *Brain* (Vol. 123).

Mutha, P. K., Haaland, K. Y., & Sainburg, R. L. (2013). Rethinking motor lateralization: specialized but complementary mechanisms for motor control of each arm. *PloS One*, *8*(3), e58582.

Nair, D. G., Purcott, K. L., Fuchs, A., Steinberg, F., & Kelso, J. A. S. (2003). Cortical and cerebellar activity of the human brain during imagined and executed unimanual and bimanual action sequences: a functional MRI study. *Cognitive Brain Research*, *15*(3), 250–260.

Nordin, N., Xie, S., & Wünsche, B. (2014). Assessment of movement quality in robot- assisted upper limb rehabilitation after stroke: a review. *Journal of NeuroEngineering and Rehabilitation*, *11*(1), 137. https://doi.org/10.1186/1743-0003-11-137

Norris, A. H., Shock, N. W., & Wagman, I. H. (1953). Age changes in the maximum conduction velocity of motor fibers of human ulnar nerves. *Journal of Applied Physiology*, *5*(10), 589–593.

Nowak, D. A., Glasauer, S., & Hermsdörfer, J. (2013). Force control in object manipulation—A model for the study of sensorimotor control strategies. *Neuroscience & Biobehavioral Reviews*, *37*(8), 1578–1586. https://doi.org/10.1016/j.neubiorev.2013.06.003

Nowak, D. A., Glasauer, S., Meyer, L., Mai, N., & Hermsdörfer, J. (2002). The role of cutaneous feedback for anticipatory grip force adjustments during object movements and externally imposed variation of the direction of gravity. *Somatosensory & Motor Research*, *19*(1), 49–60. https://doi.org/10.1080/08990220120113048

Nowak, D. A., Glauser, S., & Hermsdorfer, J. (2004). How predictive is grip force control in the complete absence of somatosensory feedback? *Brain*, *127*(1), 182–192. https://doi.org/10.1093/brain/awh016

Nowak, D. A., Hermsdörfer, J., Glasauer, S., Philipp, J., Meyer, L., & Mai, N. (2001). The effects of digital anaesthesia on predictive grip force adjustments during vertical movements of a grasped object. *European Journal of Neuroscience*, *14*(4), 756–762. https://doi.org/10.1046/j.0953-816x.2001.01697.x

Nowak, D. A., Hermsdörfer, J., Marquardt, C., & Topka, H. (2003). Moving objects with clumsy fingers: how predictive is grip force control in patients with impaired manual sensibility? *Clinical Neurophysiology*, *114*(3), 472–487. https://doi.org/10.1016/S1388-2457(02)00386-3

Nowak, D. A., Topka, H., Timmann, D., Boecker, H., & Hermsdörfer, J. (2007). The role of the cerebellum for predictive control of grasping. *Cerebellum*, *6*(1), 7–17. https://doi.org/10.1080/14734220600776379

Nowak, D. A., Voss, M., Huang, Y.-Z., Wolpert, D. M., & Rothwell, J. C. (2005). High-frequency repetitive transcranial magnetic stimulation over the hand area of the primary motor cortex disturbs predictive grip force scaling. *European Journal of Neuroscience*, *22*(9), 2392–2396. https://doi.org/10.1111/j.1460-9568.2005.04425.x

Oldfield, R. C. (1971). The assessment and analysis of handedness: The Edinburgh inventory. *Neuropsychologia*. https://doi.org/10.1016/0028-3932(71)90067-4

O'Sullivan, I., Burdet, E., & Diedrichsen, J. (2009). Dissociating variability and effort as determinants of coordination. *PLoS Comput Biol*, *5*(4), e1000345.

Osumi, M., Sumitani, M., Otake, Y., & Morioka, S. (2018). A "matched" sensory reference can guide goal-directed movements of the affected hand in central post-stroke sensory ataxia. *Experimental Brain Research*, *236*(5), 1263–1272. https://doi.org/10.1007/s00221-018-5214-6

Ota, M., Obata, T., Akine, Y., Ito, H., Ikehira, H., Asada, T., & Suhara, T. (2006). Age-related degeneration of corpus callosum measured with diffusion tensor imaging. *Neuroimage*, *31*(4), 1445–1452.

Ota, M., Tateuchi, H., Hashiguchi, T., & Ichihashi, N. (2021). Verification of validity of gait analysis systems during treadmill walking and running using human pose tracking algorithm. *Gait & Posture*, *85*, 290–297. https://doi.org/10.1016/j.gaitpost.2021.02.006

Palve, S. S., & Palve, S. B. (2018). Impact of aging on nerve conduction velocities and late responses in healthy individuals. *Journal of Neurosciences in Rural Practice*, *9*(1), 112.

Pareés, I., Brown, H., Nuruki, A., Adams, R. A., Davare, M., Bhatia, K. P., Friston, K., & Edwards, M. J. (2014). Loss of sensory attenuation in patients with functional (psychogenic) movement disorders. *Brain*, *137*(11), 2916–2921. https://doi.org/10.1093/brain/awu237

Parkinson, A., Condon, L., & Jackson, S. R. (2010). Parietal cortex coding of limb posture: In search of the body-schema. *Neuropsychologia*, *48*(11), 3228–3234. https://doi.org/10.1016/j.neuropsychologia.2010.06.039

Parry, R., Sarlegna, F. R., Jarrassé, N., & Roby-Brami, A. (2021). Anticipation and compensation for somatosensory deficits in object handling: Evidence from a patient with large fiber sensory neuropathy. *Journal of Neurophysiology*, *126*(2), 575–590. https://doi.org/10.1152/jn.00517.2020

Patel, P., Zablocki, V., & Lodha, N. (2019). Bimanual force control differs between increment and decrement. *Neuroscience Letters*, *701*, 218–225.

Preilowski, B. F. B. (1972). Possible contribution of the anterior forebrain commissures to bilateral motor coordination. *Neuropsychologia*, *10*(3), 267–277.

Press, C., Kok, P., & Yon, D. (2020). The Perceptual Prediction Paradox. In *Trends in Cognitive Sciences* (Vol. 24, Issue 1, pp. 13–24). Elsevier Ltd. https://doi.org/10.1016/j.tics.2019.11.003

Rantanen, T., Guralnik, J. M., Foley, D., Masaki, K., Leveille, S., Curb, J. D., & White, L. (1999). Midlife hand grip strength as a predictor of old age disability. *Jama*, *281*(6), 558–560.

Reichenbach, A., Thielscher, A., Peer, A., Bülthoff, H. H., & Bresciani, J.-P. (2014). A key region in the human parietal cortex for processing proprioceptive hand feedback during reaching movements. *NeuroImage*, *84*, 615–625. https://doi.org/10.1016/j.neuroimage.2013.09.024

Resulaj, A., Kiani, R., Wolpert, D. M., & Shadlen, M. N. (2009). Changes of mind in decision-making. *Nature*, *461*(7261), 263–266. https://doi.org/10.1038/nature08275

Rizzolatti, G., Fabbri-Destro, M., Nuara, A., Gatti, R., & Avanzini, P. (2021). The role of mirror mechanism in the recovery, maintenance, and acquisition of motor abilities. *Neuroscience & Biobehavioral Reviews*, *127*, 404–423. https://doi.org/10.1016/j.neubiorev.2021.04.024

Rizzolatti, G., & Matelli, M. (2003). Two different streams form the dorsal visual system: anatomy and functions. *Experimental Brain Research*, *153*(2), 146–157. https://doi.org/10.1007/s00221-003-1588-0

Roche, N., Bonnyaud, C., Reynaud, V., Bensmail, D., Pradon, D., & Esquenazi, A. (2019). Motion analysis for the evaluation of muscle overactivity: A point of view. *Annals of Physical and Rehabilitation Medicine*, *62*(6), 442–452. https://doi.org/10.1016/j.rehab.2019.06.004

Rodgers, H., Bosomworth, H., Krebs, H. I., van Wijck, F., Howel, D., Wilson, N., Aird, L., Alvarado, N., Andole, S., Cohen, D. L., Dawson, J., Fernandez-Garcia, C., Finch, T., Ford, G. A., Francis, R., Hogg, S., Hughes, N., Price, C. I., Ternent, L., … Shaw, L. (2019). Robot assisted training for the upper limb after stroke (RATULS): a multicentre randomised controlled trial. *The Lancet*, *394*(10192), 51–62. https://doi.org/10.1016/S0140-6736(19)31055-4

Rohan, A., Rabah, M., Hosny, T., & Kim, S.-H. (2020). Human Pose Estimation-Based Real-Time Gait Analysis Using Convolutional Neural Network. *IEEE Access*, *8*, 191542–191550. https://doi.org/10.1109/ACCESS.2020.3030086

Roussel, C., Hughes, G., & Waszak, F. (2013). A preactivation account of sensory attenuation. *Neuropsychologia*, *51*(5), 922–929. https://doi.org/10.1016/j.neuropsychologia.2013.02.005

Rubio-Garrido, P., Pérez-de-Manzo, F., Porrero, C., Galazo, M. J., & Clascá, F. (2009). Thalamic Input to Distal Apical Dendrites in Neocortical Layer 1 Is Massive and Highly Convergent. *Cerebral Cortex*, *19*(10), 2380–2395. https://doi.org/10.1093/cercor/bhn259

Rudisch, J., Müller, K., Kutz, D. F., Brich, L., Sleimen-Malkoun, R., & Voelcker-Rehage, C. (2020). How age, cognitive function and gender affect bimanual force control. *Frontiers in Physiology*, *11*, 245.

Rupprechter, S., Morinan, G., Peng, Y., Foltynie, T., Sibley, K., Weil, R. S., Leyland, L.-A., Baig, F., Morgante, F., Gilron, R., Wilt, R., Starr, P., Hauser, R. A., & O'Keeffe, J. (2021). A Clinically Interpretable Computer-Vision Based Method for Quantifying Gait in Parkinson's Disease. *Sensors*, *21*(16), 5437. https://doi.org/10.3390/s21165437

Sabo, A., Mehdizadeh, S., Ng, K.-D., Iaboni, A., & Taati, B. (2020). Assessment of Parkinsonian gait in older adults with dementia via human pose tracking in video data. *Journal of NeuroEngineering and Rehabilitation*, *17*(1), 97. https://doi.org/10.1186/s12984-020-00728-9

Sainburg, R. L. (2002). Evidence for a dynamic-dominance hypothesis of handedness. *Experimental Brain Research*, *142*(2), 241–258.

Sala-Llonch, R., Bartrés-Faz, D., & Junqué, C. (2015). Reorganization of brain networks in aging: a review of functional connectivity studies. *Frontiers in Psychology*, *6*, 663.

Sale, M. V, & Semmler, J. G. (2005). Age-related differences in corticospinal control during functional isometric contractions in left and right hands. *Journal of Applied Physiology*, *99*(4), 1483–1493.

Salimpour, Y., & Shadmehr, R. (2014a). Motor costs and the coordination of the two arms. *Journal of Neuroscience*, *34*(5), 1806–1818.

Salimpour, Y., & Shadmehr, R. (2014b). Motor costs and the coordination of the two arms. *Journal of Neuroscience*, *34*(5), 1806–1818.

Santisteban, L., Térémetz, M., Bleton, J.-P., Baron, J.-C., Maier, M. A., & Lindberg, P. G. (2016). Upper Limb Outcome Measures Used in Stroke Rehabilitation Studies: A Systematic Literature Review. *PLOS ONE*, *11*(5), e0154792. https://doi.org/10.1371/journal.pone.0154792

Schmidt, R. A., Lee, T. D., Winstein, C., Wulf, G., & Zelaznik, H. N. (1988). *Motor control and learning: A behavioral emphasis*. Human kinetics.

Schmitz-Hubsch, T., du Montcel, S. T., Baliko, L., Berciano, J., Boesch, S., Depondt, C., Giunti, P., Globas, C., Infante, J., Kang, J.-S., Kremer, B.,

Mariotti, C., Melegh, B., Pandolfo, M., Rakowicz, M., Ribai, P., Rola, R., Schols, L., Szymanski, S., … Klockgether, T. (2006). Scale for the assessment and rating of ataxia: Development of a new clinical scale. *Neurology*, *66*(11), 1717–1720. https://doi.org/10.1212/01.wnl.0000219042.60538.92

Schmitz-Hübsch, T., Tezenas du Montcel, S., Baliko, L., Boesch, S., Bonato, S., Fancellu, R., Giunti, P., Globas, C., Kang, J.-S., Kremer, B., Mariotti, C., Melegh, B., Rakowicz, M., Rola, R., Romano, S., Schöls, L., Szymanski, S., van de Warrenburg, B. P. C., Zdzienicka, E., … Klockgether, T. (2006). Reliability and validity of the International Cooperative Ataxia Rating Scale: A study in 156 spinocerebellar ataxia patients. *Movement Disorders*, *21*(5), 699–704. https://doi.org/10.1002/mds.20781

Schwarz, A., Kanzler, C. M., Lambercy, O., Luft, A. R., & Veerbeek, J. M. (2019). Systematic Review on Kinematic Assessments of Upper Limb Movements After Stroke. *Stroke*, *50*(3), 718–727. https://doi.org/10.1161/STROKEAHA.118.023531

Scott, S. H. (2016). A Functional Taxonomy of Bottom-Up Sensory Feedback Processing for Motor Actions. *Trends in Neurosciences*, *39*(8), 512–526. https://doi.org/10.1016/j.tins.2016.06.001

Scott, S. H., & Dukelow, S. P. (2011). Potential of robots as next-generation technology for clinical assessment of neurological disorders and upper-limb therapy. *The Journal of Rehabilitation Research and Development*, *48*(4), 335. https://doi.org/10.1682/JRRD.2010.04.0057

Seal, J., Gross, C., & Bioulac, B. (1982). Activity of neurons in area 5 during a simple arm movement in monkeys before and after deafferentation of the trained limb. *Brain Research*, *250*(2), 229–243. https://doi.org/10.1016/0006-8993(82)90417-6

Sebastjan, A., Skrzek, A., Ignasiak, Z., & Sławińska, T. (2017). Age-related changes in hand dominance and functional asymmetry in older adults. *Plos One*, *12*(5), e0177845.

Seijas-Macìas, A., & Oliveira, A. (2012). An Approach to Distribution of the Product of Two Normal Variables. *Discussiones Mathematicae Probability and Statistics*, *32*, 87–99.

Seki, K., Perlmutter, S. I., & Fetz, E. E. (2003). Sensory input to primate spinal cord is presynaptically inhibited during voluntary movement. *Nature Neuroscience*, *6*(12), 1309–1316. https://doi.org/10.1038/nn1154

Serrien, D. J., Cassidy, M. J., & Brown, P. (2003). The importance of the dominant hemisphere in the organization of bimanual movements. *Human Brain Mapping*, *18*(4), 296–305.

Serrien, D. J., & Wiesendanger, M. (2001). Dissociation of grip/load-force coupling during a bimanual manipulative assignment. *Experimental Brain Research*, *136*(3), 417–420.

Shadmehr, R., & Mussa-Ivaldi, F. (1994). Adaptive representation of dynamics during learning of a motor task. *The Journal of Neuroscience*, *14*(5), 3208–3224. https://doi.org/10.1523/JNEUROSCI.14-05-03208.1994

Shergill, S. S., Bays, P. H., Frith, C. D., & Wotpert, D. M. (2003). Two eyes for an eye: The neuroscience of force escalation. *Science*, *301*(5630), 187. https://doi.org/10.1126/science.1085327

Shergill, S. S., Samson, G., Bays, P. M., Frith, C. D., & Wolpert, D. M. (2005). Evidence for sensory prediction deficits in schizophrenia. *American Journal of Psychiatry*, *162*(12). https://doi.org/10.1176/appi.ajp.162.12.2384

Shergill, S. S., White, T. P., Joyce, D. W., Bays, P. M., Wolpert, D. M., & Frith, C. D. (2013). Modulation of somatosensory processing by action. *NeuroImage*, *70*, 356–362. https://doi.org/10.1016/j.neuroimage.2012.12.043

Shergill, S. S., White, T. P., Joyce, D. W., Bays, P. M., Wolpert, D. M., & Frith, C. D. (2014). Functional magnetic resonance imaging of impaired sensory prediction in schizophrenia. *JAMA Psychiatry*, *71*(1), 28–35. https://doi.org/10.1001/jamapsychiatry.2013.2974

Shi, Y. X., Tian, J. H., Yang, K. H., & Zhao, Y. (2011). Modified Constraint-Induced Movement Therapy Versus Traditional Rehabilitation in Patients With Upper-Extremity Dysfunction After Stroke: A Systematic Review and Meta-Analysis. *Archives of Physical Medicine and Rehabilitation*, *92*(6), 972–982. https://doi.org/10.1016/j.apmr.2010.12.036

Simon, T., Joo, H., Matthews, I., & Sheikh, Y. (2017). Hand Keypoint Detection in Single Images Using Multiview Bootstrapping. *2017 IEEE Conference on Computer Vision and Pattern Recognition (CVPR)*, 4645–4653. https://doi.org/10.1109/CVPR.2017.494

Smith, M. A., & Shadmehr, R. (2005). Intact Ability to Learn Internal Models of Arm Dynamics in Huntington's Disease But Not Cerebellar Degeneration. *Journal of Neurophysiology*, *93*(5), 2809–2821. https://doi.org/10.1152/jn.00943.2004

Snyder, L. H., Batista, A. P., & Andersen, R. A. (1997). Coding of intention in the posterior parietal cortex. *Nature*, *386*(6621), 167–170. https://doi.org/10.1038/386167a0

Soechting, J. F., & Flanders, M. (1989a). Errors in pointing are due to approximations in sensorimotor transformations. *Journal of Neurophysiology*, *62*(2), 595–608. https://doi.org/10.1152/jn.1989.62.2.595

Soechting, J. F., & Flanders, M. (1989b). Sensorimotor representations for pointing to targets in three-dimensional space. *Journal of Neurophysiology*, *62*(2), 582–594. https://doi.org/10.1152/jn.1989.62.2.582

Sosnoff, J. J., & Newell, K. M. (2006). Are age-related increases in force variability due to decrements in strength? *Experimental Brain Research*, *174*(1), 86.

Sperry, R. W. (1950). Neural basis of the spontaneous optokinetic response produced by visual inversion. *Journal of Comparative and Physiological Psychology*, *43*(6), 482–489. https://doi.org/10.1037/h0055479

Stinear, C. M., Lang, C. E., Zeiler, S., & Byblow, W. D. (2020). Advances and challenges in stroke rehabilitation. *The Lancet Neurology*, *19*(4), 348–360. https://doi.org/10.1016/S1474-4422(19)30415-6

Stolk-Hornsveld, F., Crow, J. L., Hendriks, E. P., van der Baan, R., & Harmeling-van der Wel, B. C. (2006). The Erasmus MC modifications to the (revised) Nottingham Sensory Assessment: a reliable somatosensory assessment measure for patients with intracranial disorders. *Clinical Rehabilitation*, *20*(2), 160–172. https://doi.org/10.1191/0269215506cr932oa

Swinnen, S. P. (2002). Intermanual coordination: from behavioural principles to neural-network interactions. *Nature Reviews Neuroscience*, *3*(5), 348–359.

Swinnen, S. P., & Wenderoth, N. (2004). Two hands, one brain: cognitive neuroscience of bimanual skill. *Trends in Cognitive Sciences*, *8*(1), 18–25.

Takagi, A., Maxwell, S., Melendez-Calderon, A., & Burdet, E. (2020). The dominant limb preferentially stabilizes posture in a bimanual task with physical coupling. *Journal of Neurophysiology*, *123*(6), 2154–2160.

Tanaka, H., Ishikawa, T., & Kakei, S. (2019). Neural Evidence of the Cerebellum as a State Predictor. *The Cerebellum*, *18*(3), 349–371. https://doi.org/10.1007/s12311-018-0996-4

Tanaka, H., Ishikawa, T., Lee, J., & Kakei, S. (2020). The Cerebro-Cerebellum as a Locus of Forward Model: A Review. In *Frontiers in Systems Neuroscience* (Vol. 14). Frontiers Media S.A. https://doi.org/10.3389/fnsys.2020.00019

Tassinari, H., Hudson, T. E., & Landy, M. S. (2006). Combining priors and noisy visual cues in a rapid pointing task. *The Journal of Neuroscience : The Official Journal of the Society for Neuroscience*, *26*(40), 10154–10163. https://doi.org/10.1523/JNEUROSCI.2779-06.2006

Teixeira, L. A. (2008). Categories of manual asymmetry and their variation with advancing age. *Cortex*, *44*(6), 707–716. https://doi.org/https://doi.org/10.1016/j.cortex.2006.10.002

Thomas, E., Yon, D., de Lange, F., & Press, C. (2020). Action enhances predicted touch. *BioRxiv*. https://doi.org/10.1177/09567976211017505

Thoroughman, K. A., & Shadmehr, R. (2000). Learning of action through adaptive combination of motor primitives. *Nature*, *407*(6805), 742–747. https://doi.org/10.1038/35037588

Thrane, G., Thrane, G., Sunnerhagen, K. S., & Murphy, M. A. (2020). Upper limb kinematics during the first year after stroke: The stroke arm longitudinal study at the University of Gothenburg (SALGOT). *Journal of NeuroEngineering and Rehabilitation*, *17*(1). https://doi.org/10.1186/s12984-020-00705-2

Todorov, E., & Jordan, M. I. (2002). Optimal feedback control as a theory of motor coordination. *Nature Neuroscience*, *5*(11), 1226–1235. https://doi.org/10.1038/nn963

Tseng, Y., Diedrichsen, J., Krakauer, J. W., Shadmehr, R., & Bastian, A. J. (2007). Sensory Prediction Errors Drive Cerebellum-Dependent Adaptation of Reaching. *Journal of Neurophysiology*, *98*(1), 54–62. https://doi.org/10.1152/jn.00266.2007

Vaillancourt, D. E., Larsson, L., & Newell, K. M. (2003). Effects of aging on force variability, single motor unit discharge patterns, and the structure of 10, 20, and 40 Hz EMG activity. *Neurobiology of Aging*, *24*(1), 25–35.

Vaillancourt, D. E., & Newell, K. M. (2003). Aging and the time and frequency structure of force output variability. *Journal of Applied Physiology*, *94*(3), 903–912.

Vieluf, S., Godde, B., Reuter, E.-M., Temprado, J.-J., & Voelcker-Rehage, C. (2015). Practice effects in bimanual force control: Does age matter? *Journal of Motor Behavior*, *47*(1), 57–72.

Vieluf, S., Mora, K., Gölz, C., Reuter, E.-M., Godde, B., Dellnitz, M., Reinsberger, C., & Voelcker-Rehage, C. (2018). Age-and expertise-related differences of sensorimotor network dynamics during force control. *Neuroscience*, *388*, 203–213.

Voelcker-Rehage, C., & Alberts, J. L. (2005). Age-related changes in grasping force modulation. *Experimental Brain Research*, *166*(1), 61–70. https://doi.org/10.1007/s00221-005-2342-6

von Holst, E., & Mittelstaedt, H. (1950). Das Reafferenzprinzip. *Naturwissenschaften*, *37*(20), 464–476. https://doi.org/10.1007/BF00622503

Voogd, J., & Koehler, P. J. (2018). *Historic notes on anatomic, physiologic, and clinical research on the cerebellum* (pp. 3–26). https://doi.org/10.1016/B978-0-444-63956-1.00001-1

Voss, M., Ingram, J. N., Haggard, P., & Wolpert, D. M. (2006). Sensorimotor attenuation by central motor command signals in the absence of movement. *Nature Neuroscience*, *9*(1), 26–27. https://doi.org/10.1038/nn1592

Wagner, J. M., Lang, C. E., Sahrmann, S. A., Edwards, D. F., & Dromerick, A. W. (2007). *Sensorimotor Impairments and Reaching Performance in Subjects With Poststroke Hemiparesis During the First Few Months of Recovery Background and Purpose*. www.ptjournal.org

Wagner, J. M., Lang, C. E., Sahrmann, S. A., Hu, Q., Bastian, A. J., Edwards, D. F., & Dromerick, A. W. (2006). Relationships between Sensorimotor Impairments and Reaching Deficits in Acute Hemiparesis. *Neurorehabilitation and Neural Repair*, *20*(3), 406–416. https://doi.org/10.1177/1545968306286957

Wagner, J. M., Rhodes, J. A., & Patten, C. (2008). Reproducibility and Minimal Detectable Change of Three-Dimensional Kinematic Analysis of Reaching Tasks in People With Hemiparesis After Stroke. *Physical Therapy*, *88*(5), 652–663. https://doi.org/10.2522/ptj.20070255

Wang, J., & Sainburg, R. L. (2007). The dominant and nondominant arms are specialized for stabilizing different features of task performance. *Experimental Brain Research*, *178*(4), 565–570.

Wei, G., Lan, C., Zeng, W., & Chen, Z. (2020). View Invariant 3D Human Pose Estimation. *IEEE Transactions on Circuits and Systems for Video Technology*, *30*(12), 4601–4610. https://doi.org/10.1109/TCSVT.2019.2928813

Weller, M. P. I., & Latimer-Sayer, D. T. (1985). Increasing right hand dominance with age on a motor skill task. *Psychological Medicine*, *15*(4), 867–872.

Welniarz, Q., Worbe, Y., & Gallea, C. (2021). The Forward Model: A Unifying Theory for the Role of the Cerebellum in Motor Control and Sense of Agency. *Frontiers in Systems Neuroscience*, *15*. https://doi.org/10.3389/fnsys.2021.644059

Wolpe, N., Ingram, J. N., Tsvetanov, K. A., Geerligs, L., Kievit, R. A., Henson, R. N., Wolpert, D. M., Rowe, J. B., Tyler, L. K., Brayne, C., Bullmore, E., Calder, A., Cusack, R., Dalgleish, T., Duncan, J., Matthews, F. E., Marslen-Wilson, W., Shafto, M. A., Campbell, K., … Villis, L. (2016). Ageing increases reliance on sensorimotor prediction through structural and functional differences in frontostriatal circuits. *Nature Communications*, *7*. https://doi.org/10.1038/ncomms13034

Wolpe, N., Zhang, J., Nombela, C., Ingram, J. N., Wolpert, D. M., Rowe, J. B., Tyler, L. K., Brayne, C., Bullmore, E. T., Calder, A. C., Cusack, R., Dalgleish, T., Duncan, J., Matthews, F. E., Marslen-Wilson, W. D., Shafto, M. A., Cheung, T., Geerligs, L., McCarrey, A., … Villis, L. (2018). Sensory

attenuation in Parkinson's disease is related to disease severity and dopamine dose. *Scientific Reports*, *8*(1). https://doi.org/10.1038/s41598-018-33678-3

Wolpert, D. M., & Flanagan, J. R. (2001). Motor prediction. *Current Biology*, *11*(18), R729–R732.

Wolpert, D. M., & Ghahramani, Z. (2000). Computational principles of movement neuroscience. *Nature Neuroscience*, *3*(S11), 1212–1217. https://doi.org/10.1038/81497

Wolpert, D. M., Miall, R. C., & Kawato, M. (1998). Internal models in the cerebellum. *Trends in Cognitive Sciences*, *2*(9), 338–347. https://doi.org/10.1016/S1364-6613(98)01221-2

Woytowicz, E. J., Westlake, K. P., Whitall, J., & Sainburg, R. L. (2018). Handedness results from complementary hemispheric dominance, not global hemispheric dominance: evidence from mechanically coupled bilateral movements. *Journal of Neurophysiology*, *120*(2), 729–740.

Wu, C., Chen, C., Tang, S. F., Lin, K., & Huang, Y. (2007a). Kinematic and Clinical Analyses of Upper-Extremity Movements After Constraint-Induced Movement Therapy in Patients With Stroke: A Randomized Controlled Trial. *Archives of Physical Medicine and Rehabilitation*, *88*(8), 964–970. https://doi.org/10.1016/j.apmr.2007.05.012

Wu, C. yi, Chen, C. ling, Tang, S. F., Lin, K. chung, & Huang, Y. ying. (2007b). Kinematic and Clinical Analyses of Upper-Extremity Movements After Constraint-Induced Movement Therapy in Patients With Stroke: A Randomized Controlled Trial. *Archives of Physical Medicine and Rehabilitation*, *88*(8), 964–970. https://doi.org/10.1016/j.apmr.2007.05.012

Yan, L., Wu, Y., Zeng, X., & Gao, L. (2015). Dysfunctional putamen modulation during bimanual finger-to-thumb movement in patients with Parkinson's disease. *Frontiers in Human Neuroscience*, *9*, 516.

Yeterian, E. H., & Pandya, D. N. (1993). Striatal connections of the parietal association cortices in rhesus monkeys. *The Journal of Comparative Neurology*, *332*(2), 175–197. https://doi.org/10.1002/cne.903320204

Yon, D., Gilbert, S. J., de Lange, F. P., & Press, C. (2018). Action sharpens sensory representations of expected outcomes. *Nature Communications*, *9*(1). https://doi.org/10.1038/s41467-018-06752-7

Yon, D., Zainzinger, V., de Lange, F. P., Eimer, M., & Press, C. (2020). Action biases perceptual decisions toward expected outcomes. *Journal of Experimental Psychology: General*. https://doi.org/10.1037/xge0000826

Zimmermann, C., Welschehold, T., Dornhege, C., Burgard, W., & Brox, T. (2018). 3D Human Pose Estimation in RGBD Images for Robotic Task Learning. *2018 IEEE International Conference on Robotics and Automation (ICRA)*, 1986–1992. https://doi.org/10.1109/ICRA.2018.8462833

Zollo, L., Rossini, L., Bravi, M., Magrone, G., Sterzi, S., & Guglielmelli, E. (2011). Quantitative evaluation of upper-limb motor control in robot-aided rehabilitation. *Medical & Biological Engineering & Computing*, *49*(10), 1131–1144. https://doi.org/10.1007/s11517-011-0808-1